Correlating laboratory tests with service life performance of marine coating systems

Msc. Materials Science and Engineering
Hemchandran Coimbatore Govindarajan

TU Delft

Correlating laboratory tests with service life performance of marine coating systems

Msc. Materials Science and Engineering

by

Hemchandran Coimbatore Govindarajan

Student number:	5124891	
Supervisor:	Prof. dr. ir. J.M.C. Mol,	TU Delft
Thesis Committee :	Dr. Y. Gonzalez-Garcia	TU Delft
	Dr. L. Pahlavan (MTT)	TU Delft
Daily Supervisor:	Ir. Martijn van Ruiten	

Abstract

Accelerated tests have been commonly used by the marine coating industry to evaluate the performance of a coating in a short duration of time. Replicating natural exposure in an artificially simulated manner is a challenging task due to the various factors that induce corrosion in the natural environment. Continuous salt spray testing is a popular accelerated test, but it does not replicate the actual exposure scenario as intensifying the factors inducing corrosion does not produce the same result as natural exposure. However, it was found that alternating between wetting and drying of the coating correlates well with natural exposure. ISO 12944-9, a standardized accelerated test for corrosion protection in the marine environment, is one such test which alternates between different exposure conditions. This is performed in order to replicate the exposure conditions that a marine structure experiences. This ultimately aids in understanding the performance and durability of the coating within a shorter period. Besides, accelerated tests can be used to correlate with the natural exposure, in order to circumvent the issue of testing coatings in the natural environment for years to understand the coatings performance and durability.

This thesis aims to correlate the performance of a marine vinylester coating reinforced with glass platelets, when exposed in a natural service life environment versus that when tested in an accelerated environment. For accelerated ageing, the standard ISO 12944-9 was used, which is the standard exposure conditions for coating systems undergoing extreme conditions in the marine environment. For the natural exposure, two in-service vessels coated with this marine coating were selected to test its performance. Both vessels were coated for 10 and 15 years without any reapplication.

The coating's performance is evaluated using electrochemical impedance spectroscopy (EIS) in both the natural and accelerated environments. EIS measurements were performed at periodic intervals of 1000 hours until 3000 hours for the accelerated exposure. EIS measurements were obtained on the 10 and 15 years old ship at multiple locations on the hull. This was done to check the uniformity of corrosion protection and variation of coating performance across the ship.

Considering the impedance values for both the accelerated and natural exposure, it can be said that the impedance of the vinylester coating reinforced with glass platelets is atleast 2 orders of magnitude higher than the minimum industry standard requirement even after 15 years of natural exposure. The accelerated results of 1000 hours had good correlation with the impedance measurements performed on the ship that was coated 10 years ago. The magnitude of impedance of ship that was coated for 15 years was lower than the magnitude of impedance obtained from 2000 and 3000 hours of accelerated exposure. This means further exposure in the accelerated environment is needed to correlate with the coating system that is applied for more than 15 years.

Acknowledgments

It would be impossible for this thesis to reach its successful end without the assistance and collaboration of many people to whom I would like to express my sincere gratitude.

I would like to express my deep gratitude to Prof. Arjan Mol for his patient guidance and constant support throughout the entire thesis. Your support and adaptability made this experience an adventure and thank you for that.

I would also like to thank Ir. Martijn van Ruiten for giving me the opportunity to work on this thesis. It has been a very enjoyable journey and I would be forever grateful for this opportunity.

I would also like to extend my gratitude to C-cube without whom this thesis would not have been possible. I would like to thank Guus, Rudy, Gerben, Sebastian and Tjewei from c-cube for their unconditional support throughout this thesis.

I would also like to thank Agnieszka Kooijman for her valuable support in the electrochemical laboratory.

Finally, I would like to thank my parents for their constant support throughout my studies. I wouldn’t be here without you.

Contents

List of Figures

List of Tables

1

Background

1.1. Corrosion

The term corrode is derived from the Latin word corrodere, which means ”to gnaw to pieces”. The term corrode is generally defined as to wear away gradually or to eat into. Like the natural flow of water to its lowest level, all natural processes to attain stability tend to return to the lowest energy state possible. Iron and steel also return to the lowest energy states by combining with water and oxygen to form hydrated iron oxides, which has a similar chemical composition to their original iron ore. The life cycle of steel from iron ore to a finished steel product and then back to iron oxide is shown in figure 1.1 [26].

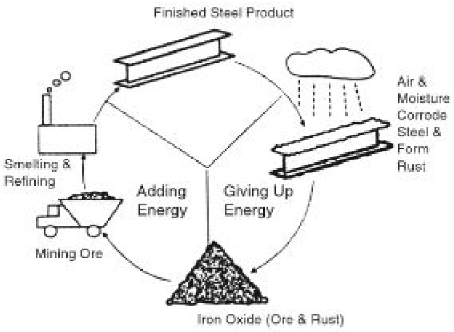

Figure 1.1: Life cycle of steel [26]

Corrosion is defined in multiple ways, either by defining a specific form of corrosion or comprehensively covering all forms of corrosion. Broadly, it can be defined as the electrochemical reaction between a metal and its environment. Which leads to degradation of the properties of the metal [26].

1.1.1. Corrosion and its importance

Corrosion has a huge impact on industries that use metals that are susceptible to corrosion. Three major aspects that can be affected by corrosion are economics, conservation and safety. Due to the toll it takes on these factors, it is very important to be proactive in every stage of the product. Right from material selection, design to manufacturing of the product. If the corrosion aspect is not under consideration in every aspect of making a product that is prone to corrosion, then the safety of the product is a major question mark. This is due to the fact that corrosion can cause failures that have catastrophic consequences. Some examples where corrosion failures occur include pressure vessels, metallic containers for toxic chemicals, boilers, turbine blades and many more.

Corrosion causes material loss in the product in question. This material loss can be attributed to the losses in terms of money, energy and the human input that was used in building the product. Additionally, the product has to be replaced, which in turn adds to the overall cost. It can be seen that the energy, time and human effort that was needed for the initial product is required twice and which is not sustainable.

Replacing a tube that is corroded in an oil refinery may cost a few hundred dollars but such an operation will lead to a shutdown of the plant. Costs of shutting down a plant of a huge scale may cost up to $50,000 per hour or even more [15].

1.1.2. Marine Corrosion

There are various factors that affect corrosion in a marine environment. It includes the corrosion protection used, the material used for the structure and the atmospheric parameters that include temperature, humidity, oxygen, water and its velocity [78]. Corrosion is a slow and gradual process. In atmospheric conditions, uniform corrosion rate is approximately 0.001 mm/year. Marine corrosion is considered to be more aggressive than atmospheric corrosion and the mean corrosion rate is estimated to be 0.05 mm/year. The most aggressive environment considered is the splash zone with a corrosion rate of approximately 0.11 mm/year.This can be attributed to the continuous alteration between atmospheric air and sea water in the splash zone. The splash zone is defined as the area just above the water line, which undergoes periodic wetting and drying. [35].

This loss in material occurs due to certain types of corrosion such as pitting, uniform, groove and the weld metal corrosion. Corrosion control is a tedious job and when doing so both localised and general corrosion must be taken care of [78].

Melchers et al [78] did some extensive work in corrosion of marine structures, which helped in determining the pitting depth, water velocity, dissolved oxygen, water pollution and surface finish. It was also found that certain locations are more prone to corrosion than others. This includes the cargo hold areas which are more prone to general corrosion when corrosion protection is not provided. In case of pitting, it was most observed where paint coatings were used and the shapes of these pits differed depending on the corrosion environment around these pits.[72].

1.1.3. Corrosion Mechanism

To be more specific, the fundamental mechanism of atmospheric corrosion of carbon steel is taken into consideration. It is an electrochemical process, which is an accumulation of individual processes that is explained below. The main factor is the presence of moisture. The moisture level can vary from just being a thin film of moisture or the metal exposed can be thoroughly wet. In case of marine corrosion, the parts of a ship or an offshore structure is either completely wet in case of submerged regions or it undergoes a cycle of wetting and drying depending on various factors. Therefore, it is very important to consider the period for which the part is completely wet. Along with the wetness, factors such as relative humidity, rain, temperature, atmospheric pollution, exposure conditions, properties of the formed oxide, composition of the metal are also taken into consideration. With the contribution of the mentioned factors, the individual processes in the electrochemical process includes the simultaneous oxidation and reduction and the participation of corrosion products [70]. The anodic and the cathodic reactions can be seen below respectively:

$$Fe- > Fe^2 + +2e^- \tag{1.1}$$

$$O2 + H2O + 4e^- - > 4OH^- \tag{1.2}$$

$$2H^+ + 2e^- - > H2 \tag{1.3}$$

Oxidation of Fe and reduction of oxygen can be seen in equation 1.1 and 1.2 respectively. Oxygen is highly soluble in the aqueous medium, therefore it is an acceptor of electrons and reduction of oxygen occurs. During the cases of high pollution with acid products, a cathodic reaction involving the discharge of hydrogen ions is of high importance and the reaction is seen in equation 1.3. As a result of the reaction between the metal and the environment, atmospheric corrosion products of iron and its alloys are formed, commonly known as rust [70].

To understand the mechanism of corrosion in a coated steel system, the example of polybutadiene coated steel is considered, which is exposed to aerated NaCl solution. Polybutadiene is a synthetic rubber which is formed by the polymerization of monomer 1,3-butadiene. Firstly it is the penetration of water, ions and oxygen through the low-resistance conductive pathways that have developed in the coating. Simultaneous anodic and cathodic reaction occur as in equation 1.1 and 1.2 at the metal surface which lead to delamination in cathodic area. This leads to increase in ion concentration at the base area of the least resistance pathway and formation of corrosion product at the metal surface [50].

1.2. Types of marine corrosion

There are various types of corrosion that can occur when exposed to a corrosive environment. The following can be considered as an exhaustive list [83].

- Pitting corrosion
- Crevice corrosion
- Filiform corrosion
- Erosion corrosion
- Cavitation

1.2.1. Pitting

It is a localized form of corrosion which leads to the formation of cavities or holes in the material. Corrosion resistance of a metal or an alloy solely by an oxide film does provide good protection, but after a certain threshold pertaining to the metal or the alloy, the protective film deteriorates at certain areas due to a concentrated chemical attack [30]. This does however lead to destruction of structures, caused by high stresses in critical areas or holes which are created in the structure. However, there is an acceptable level of pitting which is the shallow pitting on the surface which does not lead to through holes. There may be two reasons as to why this can be considered acceptable. One is the economical aspect, which causes huge impact if the structure that undergoes corrosion has to be changed. The second reason can be that the structural integrity is still maintained and the performance of the structure is not compromised. [83].

1.2.2. Crevice Corrosion

Crevice corrosion is a a localized attack on metals that occurs due to the stagnation of solution in crevices. Some examples of the metals that undergo this type of corrosion is the aluminium alloys and stainless steel. This type of corrosion can be considered as a type of localised corrosion (pitting). It occurs at localised areas where the surface is either shielded and a stagnant solution is present [11]. Crevice areas can be found in a number of places. It can be seen in an interface between metal and metal or an interface between metal and non-metal. Some of the examples of crevice surfaces are interface between metal and bolts, rivets, valve seats and gaskets. In the marine environment, this type of corrosion can be seen in the case of fouling, especially under hard-shell fouling. The mechanism relating to the crevice corrosion can be better explained using sequence of events that involve oxygen depletion, chloride-ion concentration, metal-ion build up, local acidification by hydrolysis of metal ions, breakdown of protective film and lateral coalescence of attacked sites [83].

1.2.3. Filiform corrosion

This is a form of corrosion that occurs in environments that are usually wet and it is aided by the presence of soluble ionic species and surface defects in the coatings. It is defined as a degradation process that gives rise to the formation of a filamentous appearance under the coating.

1.2.4. Erosion

This type of corrosion occurs due to the high velocity of abrasive fluid flow. As a result of the high velocity of abrasive species, it causes wear or erosion on the walls of these structures [76]. Erosion results in scraping of the provided protective films or as a result of high velocity and abrasion, the metal itself can be chipped off. There are other factors that accelerate erosion corrosion, which include sharp elbows in piping and turbulent flow. This can be rectified with changes in design, eliminating suspended fluids, cathodic protection and more resistant alloys. In cases where remedial measures are not suitable, weld overlays of corrosion resistant materials are used [83].

1.2.5. Cavitation

It is a form of attack that occurs due to the high difference in relative velocity between the solid and the liquid. When a liquid experiences rotation, flow divergence, it creates areas of low pressure which in turn gives rise to bubbles or cavities. These cavities have a tendency to collapse and form very rapidly, thus creating shock waves. When the cavities collapse on a solid surface, it tends to pull out some material. This phenomenon is very common on rudders of ships [49]. In cases where there is mild cavitation damage, a corrosion attack could take place, thereby aggravating the situation. Therefore, to avoid cavitation damage all together it is advised to design the components in such a way that the liquid flow is improvised limiting the creation of low pressure areas.

1.3. Current issues in the shipping industry

1.3.1. Economical impact of corrosion

Drydocking is an expensive process in terms of time and cost. This can be attributed to the earning capacity of the ships if it were to operate under normal circumstances instead of dry-docking. The total amount of money spent on protective coatings was an estimated $108.6 billion [23]. In regard to the US shipping industry, it was an estimated $ 2.2 billion. This can be classified further into maintenance downtime as $1.6 billion and for the construction of new ships it was estimated to be $1.1 billion. In the oil & gas industry, which accounts for its exploration and production, it was estimated to be around $1.4 billion. The US military has said that corrosion is on top of the list of the life-cycle costs. Their annual direct costs relating to corrosion of systems and infrastructure was an estimated $20 billion. On the other hand, the overall annual direct cost of corrosion for the US economy was $276 billion, which is approximately 3.1 percent of US GDP. If we include the annual indirect cost of corrosion, it is another $276 billion. This adds up to $552 billion dollars, which is an estimated 6% of US GDP. These figures may not be accurate to the point, but they do provide insights into the cost of corrosion and how expensive it can be. Some of these costs are related to preventive measures, and some of them are measures for damage limitation. A report by NACE (National Association of Corrosion Engineers) around the same time as the US reports above, estimated the corrosion protection for the new ships would be $7.5 billion dollars annually, which accounts for about 7 to 10 % of the total cost of the vessel. In the case of chemical tankers, the average cost for corrosion protection accounts for about 30 % of the total cost of the tanker. According to the NACE, the repair, maintenance and downtime costs were estimated to be $10.6 billion dollars [48]. The expenses related to repair of offshore coatings is 15 times higher than that of coating for a new construction. These costs were estimated in the early 2000s and it is practical to assume these costs have climbed up considerably since then [94]. On the other hand, the costs related to corrosion wastage can be reduced by approximately 33%, if an application specific corrosion protection is used [90].

The operating cost of a ship is increased if a vessel's coating roughness is increased over time. The increase in coating roughness leads to increase in frictional resistance during its service life. The coating roughness is a contribution of corrosion, physical damage to the underlying coating system or the additional friction can be due to heavy biofouling. The increase in roughness over the age of the ship can be seen in figure 1.2. On the other axis of figure 1.2, the increase in power usage with increase in hull roughness can also be seen. This leads to increase in operational cost of the ship [93].

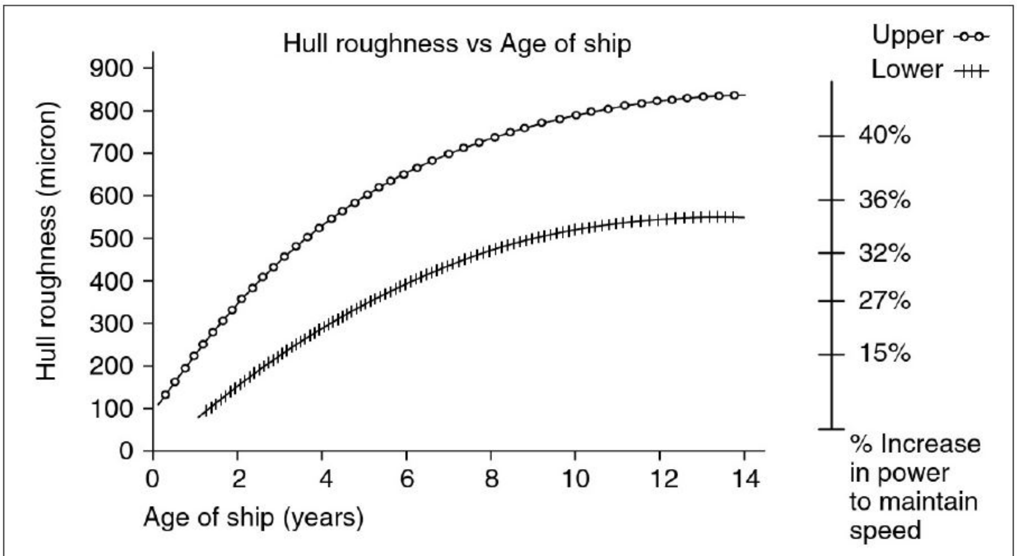

7.9 Increased average hull roughness with ship age and effect on powering.

Figure 1.2: Increase in hull roughness and power usage with increase in age of the ship [93]

1.3.2. Impact of corrosion in the shipping and offshore industry

The corrosion issues faced by the shipping and the offshore industry comes with a lot of contributing factors and complexity. A series of steps have to be taken to protect these structures from corrosive effects of various microbes, saltwater as well as the cargoes that are transported in the ships. This includes the transport of petroleum products that are highly corrosive. Different parts of the ship are prone to corrosion in different ways, such as the double-hulled tanks, the splash zone, the rigs, and the superstructure, which are subjected to various types of conditions such as extreme heat, salt spray, condensation, and so on. All these factors contribute to the deterioration of the tankers functionality due to corrosion. From the years between 1995 and 2001, around 408 tankers collapsed or were on the verge of facing its end [66]. The demise of a lot of these tankers were due to collision but an equal numbers were due to extreme levels of corrosion. If a contractor has very few hours of downtime a month, then it provides very little time to remedy any corrosion related issues, and it becomes even more complicated if the issues are concentrated in certain inaccessible areas of the ships or offshore structures. Increasing the downtime to do some major work on the issues, causes drastic economical impact. Ships that are dry docked for periodic maintenance can be inspected for its corrosion protection, however, the offshore vessels on the other hand do not have the same luxury of periodic maintenance and has to stay years on end up to 20-40 years with its complete functionality.

In the 1990, the US mandated double hulls for all new tankers that were operated in US waters, after the 1989 Exxon oil spill. It was initially expected to have similar or lower corrosion rates, but the corrosion rates rose to new heights. The steel replacement and repairs that were usually done after 15 years for the single hull, was done after 5 years for the double hull. This accelerated corrosion was attributed to the fact that higher strength steels were used, which permits the use of thin plates that are more flexible than carbon plates which were of use in the old tanks. The issue with double hull tanks is that, when hot cargo, such as crude oil, is transported, the cargo heats the ballast tanks. In the case of the single hull, the cargo is cooled by the seawater. In the double hull, the cooling is slowed. Therefore, the temperature of the cargo remains elevated for longer periods of time which increases the rate of corrosion. The corrosion rate doubles for every 10-degree Celsius increase in temperature [88]. There are a variety of factors that calls for a solution to mitigate corrosion. The increasing number of offshore operations, usage of lighter materials taking into consideration the wastage due to corrosion, need for minimum to no maintenance for remote explorations, arctic region explorations and operations under those extreme conditions and also taking into consideration the concerns relating to the effects on the marine life [94]. In ship hulls and ballast tanks, paint cracking is considered a major issue to corrosion. Paint cracking usually occurs as a result of loss of flexibility with aging or due to brittleness. These cracks were found to be in areas of high stress concentrations. They can be fillet welds, weld toes, sharp angles transition between structural details and so on. The issues faced by the shipping and offshore industry can be explained in a sequence as actions that occur. First is the damage that causes the coating to break, due to various reasons. Once the coating is damaged, the underlying substrate is exposed to the harsh environments. If any cathodic protection systems are in place, they kick in to protect the bare metal. At some point, the cathodic protection becomes inadequate, which was the obstruction to further corrosion. Since all the protective systems are down, the sources that are responsible for corrosion are compounded and they result in accelerated corrosion. Once this happens, the structural integrity of the metal starts deteriorating. This results in the various types of expensive repairs and replacements [88][94].

Figure 1.3: Coating detoriation after 4 years of service with conventional hull coating like a foul releasing coating or anti fouling coating [93]

1.3.3. Current corrosion prevention methods and their reliability

Since corrosion issues have come up throughout history, a number of methods to reduce or mitigate them altogether tried and tested. Some of the methods or efforts that have been undertaken are the choice of materials, designing the hulls and the tanks in a specific manner in to order to limit corrosion. Once the above two methods are taken care of then, protecting the metal is done with cathodic protection, protective coatings, corrosion inhibitors and cleaning of vessels and structures and in water to eliminate fouling. A combination of cathodic protection and protective coatings is considered to be one of the most efficient and cost-effective methods as can be seen in figure 1.2. Due to this, it is one of the most commonly used techniques in the fight against corrosion. One of the significant things in regard to solving the corrosion issue on ships is the use of a coating that is long lasting and effective is keeping the corrosive elements away from the underlying substrate. It is a simple method, but if such as coating can be found, its application is never ending. The most common approach for a very long time to deal with corrosion was specifying adequate scantlings. In this method the underlying substrate was exposed to the corrosive elements and once the underlying substrate lost its structural integrity, the metal was replaced. Such was the case for a very long time. Then came the use of protective coatings and cathodic protection. Many stakeholders in the shipping and offshore industry opt for a method that is much safer and economically viable. They opt for the following protections, they are the full scantlings, cathodic protection, and protective coatings. This is protecting the underlying steel on various levels, and the stakeholders opt for this method due to the high costs involved in the replacement of steel, drydocking and onboard repairs [94].

The use of corrosion inhibitors is to limit the damage due to corrosion rather than to prevent corrosion in the first place. This is a method that has been used in the internal parts of the system such as pipes, so as to limit the corrosive effects due to the fluids that pass through these pipes. In regard to protection of the ship's hulls and tanks, protective coatings seem to have the answer in all the aspects. They are reliable, economical, and most effective. Protective coatings is approached in three ways. This is described in detail in the following paragraphs. The first approach is the ideal approach, where the coating is a very good barrier between the substrate and the environment. It performs in the ideal manner like being impenetrable, impermeable, blocking the passage of ions, electrons, moisture, or any kinds of vapor or chemicals from the environment. There are a lot of assumptions in this approach like no entrapment of any kind of corrosive agents underneath the coating. In terms of the coating, it is assumed the coating is tough, flexible and durable for it to protect the underlying steel for years to come. It was unrealistic to think the protective layer would be the ultimate protection. So, two other approaches were used to ensure a long lasting and effective protection. One of them is the use of oil-based primers, which are heavily loaded with red lead. This limits the adverse damage done by the corrosive agents that infiltrate the coating. This is achieved by the formation of a protective layer on the surface of the metal. The second approach is more of cathodic protection, but they are infused into the primer in the form of additives. They work by changing the potential of the corrosive elements that infiltrate the coating, so it becomes less cathodic and hence corrodes less. One such primer that has found widespread use is the inorganic zinc-based primer (zinc silicate) [94]. These two methods are more effective in areas such as the topside and the splash zone which is more prone to the damages that can deteriorate the coating which can act as a starting point for the corrosion. All three methods described above can be utilised for a full proof method. The impenetrable coating can be applied on top of the zinc-based primer discussed earlier. This forms a two-layer protection, such that the topcoat tries to keep the corrosive elements away from the metal as much as possible forming a barrier. If the barrier is broken then the primer underneath can inhibit further corrosion. As a replacement for the epoxies as hard coating, polysiloxane hybrid coatings was found to be a good substitute. It aids in the blending of inorganic siloxanes with epoxies. They were found to be very effective for topside paints. Electrochemical corrosion is process of flow of current between anodic and cathodic surfaces. It is plausible to assume that controlling the corrosion current helps in controlling corrosion [94]. Glassflake technology, is a method that was found to be effecting and long lasting.

1.3.4. Reliability of coating methods

As mentioned earlier, the choice of materials is an important step in the design of the product. This can majorly impact the corrosion levels the product may undergo. The mild structural steel is the one that is most used due to its strength and low cost. But more recently, the corrosion resistance steels are brought into the market for its use in the cargo oil tanks. These corrosion resistance steels are very much similar to the mild steel when they are used in the ballast tanks or the hull. But the use of these steels in cargo oil tanks does corrode much lesser than mild steel. The cathodic and inhibiting approaches that were explained above, work only in certain environments and they act differently in others. For example, these two approaches were found to be ineffective in the ballast tanks and underwater hulls as they are continuously immersed in seawater. The use of hard coatings is of use in creating a strong barrier against the corrosive elements. The type of hard coating widely used is a type of epoxy and they satisfy all the requirements like resistance to liquids, ions, vapours, alkalis and salts. But in the long run they do not weather well. These top coats are affected by factors such as the ultraviolet light in the top side and the splash zone. There are several coatings which are much better to the ones discussed above, but they are not yet in practical use due to several reasons. The coatings and the application methods are seen to be ineffective. This issue is then compensated by the cathodic protection systems to limit the damages by the corrosive elements [94].

1.3.5. Accelerated corrosion tests and their limitations

Accelerated salt spray tests are done in a closed environment, usually in a closed cabinet and it is regarded as one of the most used tests for accessing corrosion. In the salt spray tests, the salt solution is brought in contact with the product being tested in the form of a droplet. This is achieved with the aid of a nozzle in which the salt solution is pumped into. When the salt solution enters the nozzle, it meets a jet of humidified compressed air, that helps in forming a fine droplet spray [9].

For a general assessment or a quality control test of the surface treatments or the coatings, a continuous neutral spray test is used. ASTM B117, BS3900 parts F4, F13 and ISO 7253 are the testing standards used for the neutral salt spray test [9]. Tests such as the Kesternich type tests inject sulphur dioxide inside the closed cabinet for testing various paints and coatings.

ASTM B117 is performed in specialised chambers where the temperature is maintained at 35 °C with a tolerance of +1.1°C to 1.7°C. The chamber is maintained in a pH range between 6.5 and 7.5 pH. 5% salt solution is used with 5 parts soldium chloride and 95 parts ASTMD1193 Type IV water [89]. This type of water is prepared by combination of distillation, continuous electrodeionization, ion exchange, electrodialysis and reverse osmosis [42]. The duration of exposure is not indicated in this standard, but it is done is blocks of 24 hours. Therefore the general practice is 96, 240 and 600 hours of exposure. This test is considered to evaluate the corrosion performance of metals or coated surfaces. This also includes the determination of corrosion tendency after a scratch is made. The results expected form this test includes the evaluation of adhesion of the coating to the underlying metal and how far corrosion has crept from a scratch through the coating to the metal underneath. Correlation of the results from this test with the results from natural exposure is not included as part of this test standard [89].

The parts of BS3900 discussed here are part F4 and part F12. BS3900 part F12 or the ISO 7253 [2] is commonly referred as the neutral salt spray test. It is used to test the corrosion resistance of paints and varnishes. This is done by exposing the paint system in a closed chamber to salt spray at high temperatures of 35°C and also to continuous neutral salt solution at a rate of 1 - 2.5 ml/80cm^2/hour. The test duration is variable and chamber used for this test should be larger than 400 litres [6]. In the case of part F4, it is referred to as the cold salt spray test as this test exposes the paint samples to a salt spray environment at a temperature of 20°C. The synthetic sea water solution is sprayed on to the specimen at a rate of 1 - 1.5 litres/hour of salt solution. The test duration is not fixed [29].

According to Baldwin et al [9], many of the accelerated tests are being conducted on coatings and materials but their analysis is done prematurely. A lot of these tests are being conducted worldwide, but the unrealistic simulation to replicate the external environment is a serious limitation according to Baldwin et al [9]. A huge difference was seen in the corrosion performance between the continuous salt spray test and the outdoor exposure in the case of metallic coatings. One such example is the case of the sacrificial coatings. When an electrodeposited zinc-nickel alloy was tested according to ASTM B117, the resistance to corrosion of this alloy was high in the salt spray test. But when it was exposed to the natural marine environment it did not match the results it showed in the salt spray test. In figure 1.4, the sample example of a Zn-Ni alloy coated on a steel can be seen.

Based on the results obtained by Baldwin et al [9] from the figure 1.4, 10-14 wt% of Ni content was chosen as the ideal concentration of the alloy for optimum performance. From the figure 1.4, it is evident that there is good protection until 14 wt% and above that percentage, the coatings performance degrades. More than the above mentioned percentage of the Ni content in the alloy, it lead to a reduction in the corrosion resistance and this was evident both in the laboratory experiment as well as in the field exposure. The Ni-Zn alloy was exposed to different kinds of environments in Japan, USA and many European countries. With all the limitations, the neutral salt spray test is still the most used for the estimating the corrosion resistance for Al alloys. This is done by exposing the alloy for a long duration of time and estimating the weight loss due to the exposure [9].

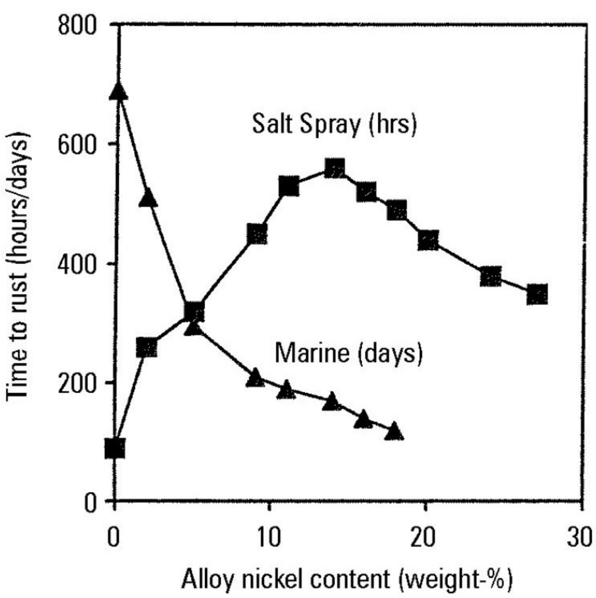

Figure 1.4: Salt spray test vs marine exposure [9]

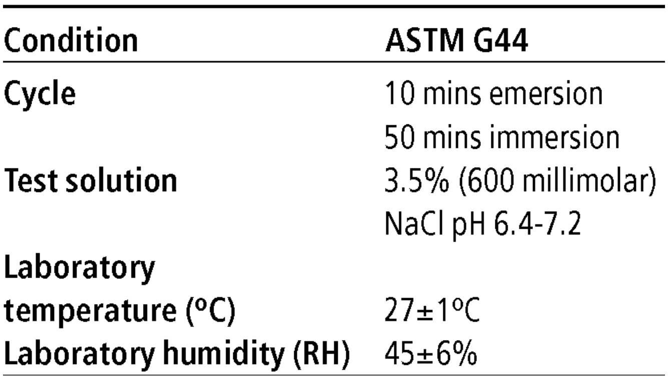

Condition	ASTM G44
Cycle	10 mins emersion 50 mins immersion
Test solution	3.5% (600 millimolar) NaCl pH 6.4-7.2
Laboratory temperature (°C)	27±1°C
Laboratory humidity (RH)	45±6%

Figure 1.5: ASTM G44 test standards [9]

In the figure 1.6, the ranking of the Al alloys was based on the exposure of the Al alloys in the natural environment for time duration of 1 year and for the case of the neutral salt spray test, the Al alloys were exposed to the test for a time duration of 42 days . Baldwin et al [9], also inferred from figure 1.6 that the ranking of the alloys in the alternate immersion column was much similar to the natural marine exposure, unlike the neutral salt spray test. The ASTM G44 was the standards used for the immersion and emersion test as can be seein in figure 1.5. While using the ASTM G44 test on the chromate free primers, Baldwin et al [9], were able to find good differentiation between the chromate free primers but similar results were not found in the case of the chromic acid anodised surfaces. To estimate the corrosion resistance of the anodic films, the neutral salt spray test has been the go to test. According to the Baldwin et al [9], when it comes to correlating the neutral salt spray test with results from the natural environment exposure, there is not much information available. On the other hand, Baldwin et al [9], observed that the anodic film test rankings in the natural conditions do match with certain accelerated tests.

Baldwin et al [9], by using electrochemical probes found that reducing the amount of chloride levels in the ASTM G44 cycle lead to similar mechanisms of corrosion that was usually seen in natural weathering conditions. As can be seen in figure 1.7, it indicates the corrosion resistance of a 8 micrometer Zn-Ni alloy coating. It is subjected to a ASTM G44 test, with different sodium chloride levels as can be seen in figure 1.7. The evaluation factor used to assess the corrosion resistance in this case was the time to first red-rust. From figure 1.7, it can be seen that the time red rust increased when the nickel content was higher in the case of 600mM/L and 6mM/L concentration of sodium chloride. As can be seen this trend is not the same as the one found in the marine conditions in figure 1.4, in fact it is the exact opposite and similar in pattern to the neutral salt spray test. In the case of low (6mM/l) sodium chloride in the solution, the time to red rust reduced with an increase in the nickel content. The trend of the low (6mM/l) sodium chloride level is akin to the behaviour found in the case of the outdoor marine conditions. From the above three cases of sodium chloride solution, the low sodium chloride condition along with the alternate immersion cycle was found to be the closet replication of an accurate corrosion test.

To make sure that the low-chloride cycle is in fact a effective technique. Baldwin et al [9], tested a number of 8 micrometer thick metallic coatings on steel. The coatings tested where the following:

- Electrodeposited zinc-0.8 percent cobalt.
- electrodeposited zinc-14 percent nickel.
- electroplated zinc
- electroplated cadmium
- physical vapour deposited aluminium.

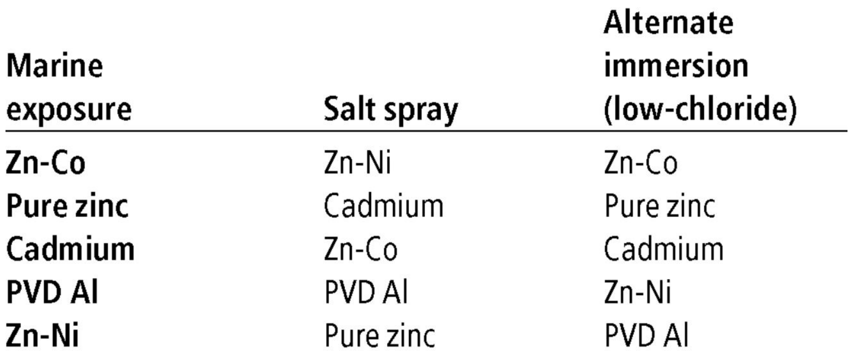

Marine exposure	**Salt spray**	**Alternate immersion (low-chloride)**
Zn-Co	Zn-Ni	Zn-Co
Pure zinc	Cadmium	Pure zinc
Cadmium	Zn-Co	Cadmium
PVD Al	PVD Al	Zn-Ni
Zn-Ni	Pure zinc	PVD Al

Figure 1.6: Comparison between three different exposure [9]

It is very evident for Baldwin et al [9], after comparing the low-chloride cycle with the data from marine exposure and salt spray in figure 1.6. The alternate immersion test was a much better match with the outside marine exposure as compared to the salt spray. In the case of the salt spray, the ranking were completely dissimilar and had only one match with the marine exposure. Although the alternate immersion had high correlation, it was not an accelerated test. Therefore, Baldwin et al [9] suggest that, to improve the accuracy of the cabinet based test, the principles that were used to develop the improved alternate immersion test could be used [9].

Badwin et al [9], found that the alternate immersion-emersion tests was very useful in obtaining very good correlation between the natural exposure and the lab exposure tests.

In 1992, substantial tests were done by Mallon et al [60], in which they found the need to do

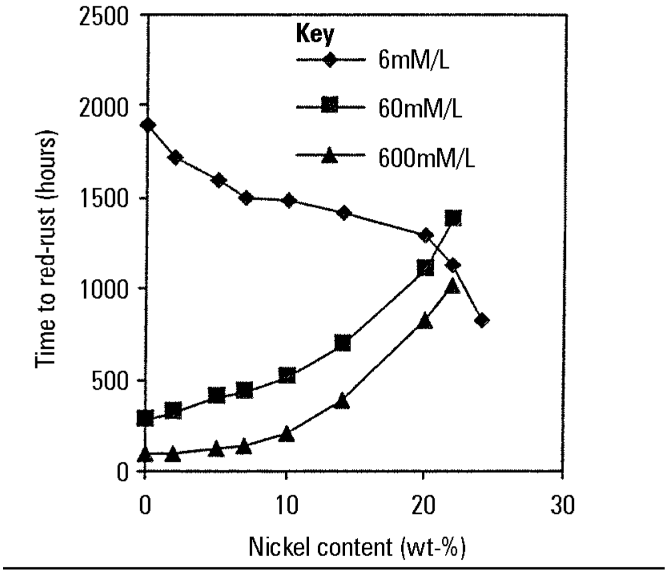

Figure 1.7: Corrosion resistance of ZN-Ni alloy coatings [9]

the field tests alongside the accelerated corrosion tests. Although in recent years, some better correlation was seen due to the alternate immersion tests. Simpson et al [86], report some problems in the neutral spray test and some unacceptable factors that are taken into consideration. It was very difficult for the simple accelerated tests to replicate the real life scenario. In 1992 Garber et al [32], evaluated coatings on galvanised steel culverts using a simple accelerated test to identify the correlation between the accelerated and natural weathering conditions. The accelerated test was not able to reproduce the results obtained in natural weathering and they reported the simple acceleration test unsuccessful in reproducing the results. This claim was supported by Montle et al [69], who found the accelerated tests to have low correlation with field tests. Montle et al [69] found good correlations in this case of field tests which were conducted in the mid-west USA for organic coatings using electrochemical methods to obtain AC impedance. Prohesion tests done on paint films has shown good correlation to the natural outdoor field tests according to Cremer et al [24]. Prohesion test is a cyclic accelerated corrosion testing which is an attempt to simulate long term natural exposure. It is a very relevant test for paints on steel.

In the accelerated corrosion test, certain variables are accelerated so as to simulate artificial ageing. But this might not be case at all times. Meeker et al [67], increased the temperature and lowered the humidity in a simulated accelerated environment. The failure modes in this scenario did not match failures in the field tests. In the field tests, the failures did not occur at high temperatures or at low humidity. There were also cases in which the high variability of the variables in the accelerated corrosion tests have been the cause for hindering the corrosion failure mechanism .

To replicate the exposure an offshore steel component in the splash zone, Gkatzogiannis et al [35], made use of a SSC (Salt Spray Chamber) testing device according to ISO 9227. The specimen was exposed to alternating environments as in the real situation. Inside the chamber, salt fog and atmospheric air was used to expose the specimen in alternate fashion. In an attempt to create a more aggressive environment to the real situation, Gkatzogiannis et al [35], made use of 50g/L of sodium chloride as opposed to 35g/L of sodium chloride in real sea water. This was approximately 43% higher concentration to the real seawater. The SSC tests, in general have been used to evaluate the tolerance of number of coatings. Using these tests, the time for the specimen to corrode is estimated, but correlating the time periods of the tests with the outdoor marine situation is not provided [35].

1.3.6. Environment of Testing

To test a coating to be used in the marine industry, it is exposed to salt water. To simulate such a condition in the laboratory, Sharma et al [84] found 3.5% NaCl to be the standard composition to simulate the marine constituents in the laboratory [3].

On the other hand Liu et al [53] used a slightly different seawater composition as follows : 96.5 wt.% H_2O, 2.73 wt.% NaCl, 0.24 wt.% $MgCl_2$, 0.34 wt.% $MgSO_4$, 0.11 wt.% $CaCl_2$ and 0.08 wt.% KCl.

The seawater in which the product is immersed for its functionality can vary depending on which part of the world it is in [41]. The water to which the product is being exposed can be classified into the following:

- Brackish coastal water
- Polluted sea water
- Clean sea water from open seas

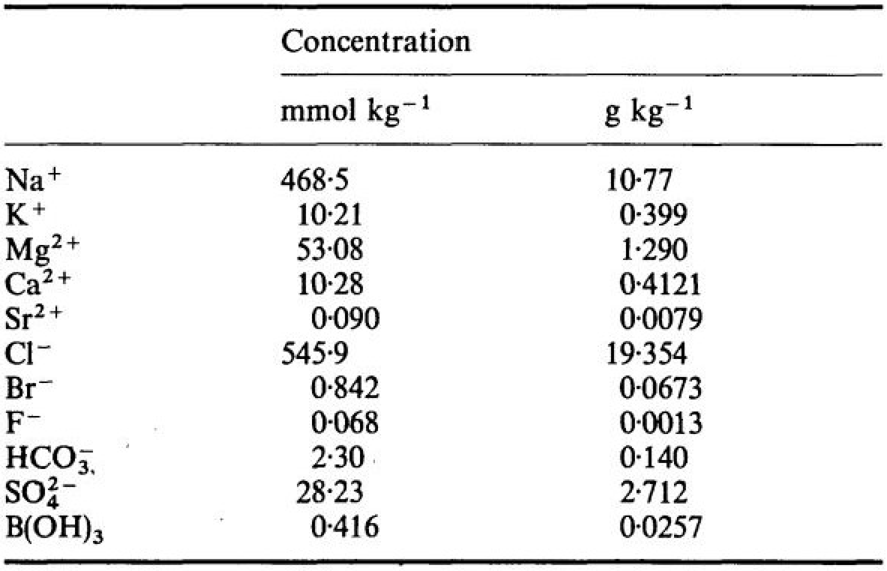

	Concentration	
	mmol kg^{-1}	g kg^{-1}
Na^+	468·5	10·77
K^+	10·21	0·399
Mg^{2+}	53·08	1·290
Ca^{2+}	10·28	0·4121
Sr^{2+}	0·090	0·0079
Cl^-	545·9	19·354
Br^-	0·842	0·0673
F^-	0·068	0·0013
HCO_3^-	2·30	0·140
SO_4^{2-}	28·23	2·712
$B(OH)_3$	0·416	0·0257

Figure 1.8: Concentration of abundant ions and molecules in sea water [41]

Below listed are some of the factors that influence the properties of sea water

- High salt concentration
- Relatively high and constant pH
- High ionic conductivity
- Solubility of gases (in the case of corrosion - oxygen and carbon dioxide is relevant in this case)
- Buffering capacity - ability of the water to maintain a stable pH when any addition to it is made.

- Biological life existence - macrofouling, microfouling and any kind of animals
- Ratio of the major constituents is found to be constant everywhere.

Some of the factors mentioned in list above are interlinked with each other and the variables that cause this interlink can be biological, physical or chemical. These variables include temperature, light intensity, nutrients availability and depth of exposure of the product. In the biological and physical viewpoint, the variations can be daily, seasonal or due to tidal fluctuations. Ionic conductivity of sea water is a major contributor in estimating the salinity of sea water, which is an example of the interlink between the factors in the above mentioned list. It falls anywhere in the range between 32-35 wt-%. Oxygen, pH, temperature, chloride, organic compounds, biological activity, flow velocity, calcium and magnesium are the factors which influence corrosion. The general pH in natural sea water is considered to be high and this further tends to increase with the reduction in oxygen at the metal surface. This increase in pH leads to decrease in solubility of magnesium and calcium oxides, hydroxides and salt. Which in turn aids in the formation of a calcareous layer. It is a layer consisting of calcium carbonate and other salts on the metal surface. This layer aids in preventing the penetration of oxygen to the underlying surface and reducing the current demand. Depending upon their various contributions in the sea water at a particular location, different concentration of sea water can found in different locations and hence the difference in corrosion levels [41].

1.3.7. Natural weathering and artificial weathering

Correlating artificial weathering with natural weathering has been a challenging task for a long period. Although certain overlaps could be found but a convincing correlation between the natural and the artificial weathering is a cause of concern. It is difficult to predict the performance of the coatings in real life with the results obtained from the artificial testing.

There are some reasons for the lack of correspondance between the artificial and natural weathering according to Deflorian et al [28]. The artificial weathering tests are highly simplified for convenience or due to any other factors. They ignore many environmental stresses that are essential in replicating the actual situation. Deflorian et al [28], also report that intensifying the external factors for a long duration does not assure a similar consequence as natural weathering. As the intensity of concentration of the external factors created artificially is not linear.

While evaluating the painted panels, Rosales et al [79], found that the corrosion and blistering were most significant at the incision made in the sample. This was the case in the sample that had undergone accelerated test and the sample that was aged naturally. When Rosales et al [79], further analysed the samples in areas away from the incision. They were able to observe painting defects such as adhesion failure, porosity, low cross-linking density and so on. The reactivity of the substrate metals were also observed in different atmospheric conditions [79].

1.4. Coatings and their significance

1.4.1. Types of coatings used in marine applications

Corrosion resistant materials constitute of pigments, fluid vehicle materials, solvents or thinners and drier additions. Some of the pigments include metal-oxides such as the TiO_2, Fe_2O_3 and $ZnCrO_4$. Pigments used for corrosion protection acts as a colouring component and controls the rate of corrosion. Due to the controlling aspect they are also called as corrosion inhibitors [96]. Fluid vehicle materials indicate the transport of fluid of different essential components that are used for the evolution of certain coating structure and properties. The drier additions act as a catalyst, expedite the oxidation or polymerisation of drying. The solvents on the other hand is a volatile liquid that aides in the coating being easily applied, sufficiently covered and then it quickly evaporates [99].

Classification of commercial coatings materials are listed as follows:

- Oil-based coating
- Alkyd-based coating
- Water based coating
- Urethane based coating
- Chlorinated rubber based coating
- Vinyl- based coating
- Epoxy-based coating
- Zinc-based coating

Out of the above listed 8 coatings, the first 3 coatings are namely the oil-based coating, alkyd based coating and the water based coating, which cannot be used for marine structures. The oil-based coatings are inexpensive and their ease of application is very high as they are natural oils derived from plants and fish. In spite of its pros, it has certain cons that make it impossible for use in harsh environments such as offshore. The cons are its permeability to moisture and less than satisfactory corrosion resistance in acid environments. The alkyd-based coatings (resin obtained from the reaction of glycerin and phthalic anhydride) have relatively superior resistance to corrosion as compared to the oil-based coatings. But they are not advised for use in a chemical containment as is the case of marine tankers. Acrylic coatings and polyvinyl acetates are examples of water based coatings. Water based coatings are known as low volatile organic compounds, they have little odor and they are easy to cleanup and apply. But they are not useful in marine coating systems [99].

Urethane based coatings are formed by the reaction of polyols and isocynates. They are known to have good abrasion resistance and toughness. Their resistance to corrosion is known to be equal to that of epoxy and vinyl systems. Chlorinated rubber based coatings are used in marine applications and are formed by the reaction of aromatic solvents and chlorinated natural rubber. This coating resists inorganic solvents and water, so they do not wet well and drying occurs rapidly. In order to achieve better corrosion resistance, the chlorinated rubber based coating is to be over-coated with a top coat of neoprene coating. However their performance above 65.5°C, is sub-optimal. Vinyl based coating are a result of polymerization of compounds that contain vinyl groups, like vinyl chloride. They are known to be more corrosion resistant than the alkyd-based and oil based coating systems. Below the temperature of 65.5°C in aqueous acid and alkaline environments they have shown notable resistance to corrosion. The cons of this coating is the poor adhesion and wetting. One of the widely used coating is the epoxy-based coating, formed by reaction of polyphenols and epichlorohydrin. Classification of epoxy coating is done based on the hardening method. Amine-hardened epoxy is an example of this classification which comprises of the hardener and the resin and they are mixed right before application. Some of the advanced epoxy-based corrosion resistant coatings provide great options for marine structures. Zinc based coatings comprises of zinc particulates in an inorganic or organic vehicle. They are known to be used in slightly alkaline, neutral and in corrosive atmosphere. The organic based zinc paint is primarily used for primer coating in steel structures as they have less surface preparation, not flammable and it is easier to topcoat. Zinc is also known to have great adhesion to the underlying steel substrate [99].

Glassflake Coating

Glass in itself a great barrier and provides great resistance to alkalies or salts and chemicals. It is also known that glass is an excellent electrical insulator. But glass as a standalone barrier cannot be used, even though glass can be used to cover a metal by fusion. It is due to the fact that, they are very fragile, rigid, brittle and they are less expensive to be used in coatings to act as a barrier between the metal and the external environment. Knowing the advantages that glass posses, it would be wise to look at ways to incorporate glass into coatings. Even though synthetic resins (polyester, epoxy and vinylester) have played a major part in coatings due to their toughness, adhesion and high resistance. As a standalone component of a coating, their lifetime has not been very high and they need constant maintenance. Combining glass with a synthetic resin would help in bridging the gap between the pros and cons of both the synthetic resin and glass. To achieve this, large glass flakes are mixed together with a base resin. Doing so would make the glass flakes adhere firmly to the resin and it would result in a thick coating, that would form a barrier that is impenetrable as can be seen in figure 1.9. In theory this does seem like a pretty straightforward solution, but in reality it is quite difficult to get it right from the time the glassflake coatings where first introduced around 1960. There are many factors that are influencing this coating and they are discussed below [94].

Firstly lets start with the type of glass to be used. Among the wide range of glass available, the C or ECR glass which is known to be the most resistant to chemicals and therefore it is the better suited glass for the glassflake reinforced coating. In spite of the glass variety chosen being expensive, the cost a stakeholder must undergo if a less resistant coating/less expensive coating is used in place of the glassflake coating is very high in comparison. Once the type of glass is chosen, the method to make glassflakes is to be chosen from the two methods available, namely the spun and the bubble method. Each has its own advantages and one needs to look into the cost benefit analysis prior to choosing the type of method to make glassflakes. The spun method is known to be the more expensive one among the two and in spite of it being expensive the spun method is chosen for the flat and straight flakes it produces unlike the bubble method which produces curved flakes from pre-melted glass marbles. It was also seen that the final product was very much controllable in the spun method and to achieve the same the bubble method was quite difficult. The size and aspect ratio of the glass flakes is of keen importance in order for the glass to provide the prefect barrier that is very difficult to penetrate. In order to achieve this, the size and aspect ratio of the glassflake must be relatively large. Aspect ratio of the glass flake equals low thickness to surface area. With a high aspect ratio, the glassflakes tend to overlap each other as the surface area is larger in comparison to the thickness of the flake and this means they block more of the path length for diffusion of corrosive species [18]. An example of the glassflakes with relatively larger size and aspect ratio can be seen in the figure 1.9. If such a scenario is not present with relatively large flakes, but the glassflakes are in the form of a powder then it is analogous to a coating that is porous and permeable. This means that even though the coating has glassflakes, it is similar to a situation where there is no glassflakes in the coating. Such a coating would not be able to provide the necessary resistance in a marine environment. In addition to the glassflakes, the resin used in the coating fills the gaps left by the glassflakes, as the glassflakes are not continuous. Therefore, it is very important to find the balance between the concentration of the resin and glassflakes in the coating. It might be very tempting to include more of the glassflakes in the coating as the impermeability increases with increase in glass content. But if done so, it would bring out the failure mechanisms related to glass when used in fusion with metal. The failures in these coatings would be due to the properties of glass which pose as a weak link in this application as it might not be flexible enough to adhere to the steel and act as a barrier. Bonding or coupling agents are also made use of in an attempt to improve adhesion of the glassflakes. In addition to improving the adhesion, the bonding/coupling agents also improve the flexural and tensile strength which in turn aids in reducing the vapor permeability and water absorption. Therefore,the effectiveness or the ability of the coating to form a strong barrier to the incoming corrosive species is mix of various factors discussed above. Conventionally, coatings reinforced with glassflakes are known to last longer due to their superior protection as compared to any other type of coating. A coating reinforced with glassflakes can be applied to a good surface treated metal, with a thickness of atleast a 1000 μm. This is achieved by spraying of two coats, each with a thickness of 500 μm. The minimum time between each coat should be 3 hours and there is no maximum time. The prerequisite to applying a coating is proper surface treatment. Even though the coating applied is a suitable one and checks all the boxes, the improper surface treatment of steel can be detrimental and can cause premature failure. For the coating to work as per the specification, the coating must adhere completely to entire surface with a profile or sufficient key and a clean surface for the coating to bond firmly. The standard requirement must be 75 μm profile and a cleanliness of SA 2.5 or SP10 which is near white steel [94].

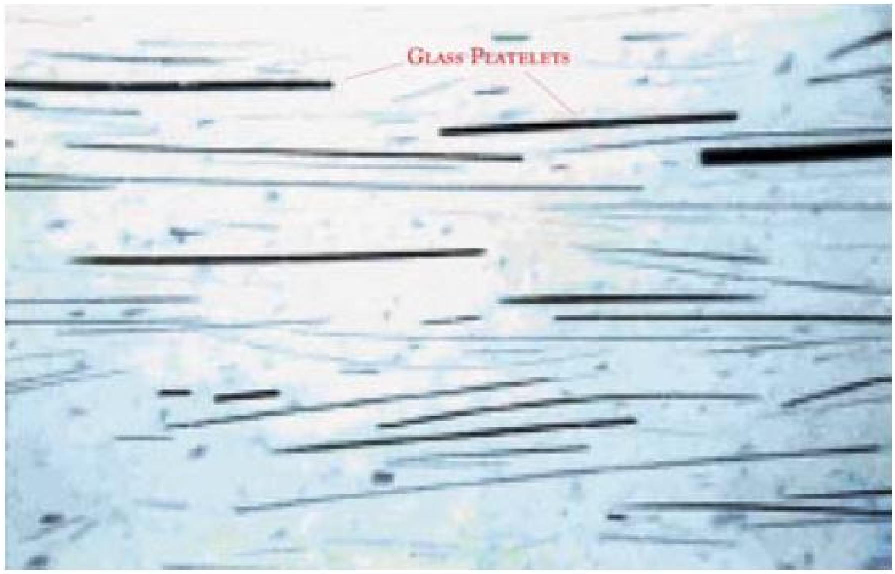

Figure 1.9: Glassflake coating [94][92]

1.4.2. Thickness of coating systems

Thickness of a coating is essential in terms of the time it takes to remove the water or solvent. In surface irregularities or corners, depending on the thickness of the coat, the coating is susceptible to cracking. Hence the thickness of the coatings is a significant aspect. It depends on factors such as the environment it is exposed to and the type of coating used. The coating being too thick or too thin can be fatal during the service life of the product [99].

Optimum coating thickness for different types of coatings can be seen below

- Zinc primer coat : 2-3 mils (50-75 μm) dry film thickness
- Top coat of polyamide epoxy : 4-6 mils (100-150μm)
- urethane acrylic coat : 1.5-2.5 mils(35-60μm) for exterior service

Certain examples of coatings that are resistant to corrosion for ferrous surfaces in sea water are vinly (4-5 coats), Coal Tar Epoxy (2-3 coats), Epoxy polyamide (2-4 coats),Top cover coat (maybe for wear resistance) and Epoxy Zinc-rich primer (2 coats) [99].

1.4.3. Application of coating

The application of a coating on marine structures are usually done by the use of rolling, brushing or spraying [99]. In case of an interior structure of a ship, it is not so easy due to the presence irregularities such as stiffeners and geometrically complex structural components. Therefore the metal surfaces of the ballast tank are pre-treated by grid blasting to provide a clean surface. The clean surface is essential to provide proper interfacial bonding between the coating and the metal. Sufficient care is taken during coating application to mitigate the presence of cavities [37].

There are certain things to take into consideration while coating a marine structure. Condensation of moisture occurs on the steel surface in times of high humidity. During the occurrence of rain, fog, haze or high humidity it is advised not to perform any kind of painting or blast cleaning. It is also advised not to coat a steel surface if its temperature is less than 3°C. Some other factors that needs to be considered while choosing a coating material, method of surface preparation and coating practices is the health and safety of the employee and as well as the environmental implications [99].

The time interval between coatings is a crucial aspect in terms of performance of the coating, hence the overcoating conditions and timing are to be followed as recommended by the paint manufacturer. As the temperature and time dependence of curing condition and coating application is very high, it is essential to maintain the temperature of both air and the substrate. Certain coatings are designed with repairs and maintenance in mind. Due to which, application of brush or roller, surface preparation are suitable for such coatings [99].

1.4.4. Common failures of coatings

There can be various reasons due to which a failure occurs in a coating. Failure occurs prematurely in a lot of coatings due to improper surface preparation, inaccuracy in coating application, curing processes and also due to the external factors influencing the service life of the coating. Pinholes, mud cracking, sagging, holidays and improper thickness are some of the issues that arise due to improper coating application. Another aspect is the discrepancies in surface preparation, it leads to poor adhesion between the coating and the substrate. If so, it can lead to different types of coating failures such as intercoat delamination, blistering, peeling and crawling. Sharp edges, skip welds and crevices occur due to poor design or fabrication of structures which in turn can lead to premature coating failures. Curing is an important process after coating application, if sufficient time is not provided it can lead to failure of the coating. Coating failures that occur due to improper curing include alligatoring, wrinkling and pinholes [99].

1.4.5. Composition of coating system and their configuration

17 different types of coatings are classified based on the composition of each coating as can be seen in figure 1.10. All the coatings that are mentioned in figure 1.10 were coated on a ANSI 1018 flat steel panel of dimensions 10.2 cm x 15.2 cm x 0.32 cm. The other type of steel panel used was a 0.050 cm thick 1008 steel sheet which was supplied by a hot-dip manufacturer and was coated with the paint system D. The paint system A is defined as a Zn phosphate layer which does not have a Al or Zn sacrificial layer. The paint system B has a ZRP (Zinc rich paint) layer. The paint system C has a thermal spray Zn layer as a sacrificial metallic coating.

The paint system D has a sacrificial metallic layer which constitutes of a continuous hot-dip (CHD) Zn or Zn-5Al sacrificial metallic layer and finally the paint system E has a sacrificial metallic layer which constitutes thermal sprayed Al [81].

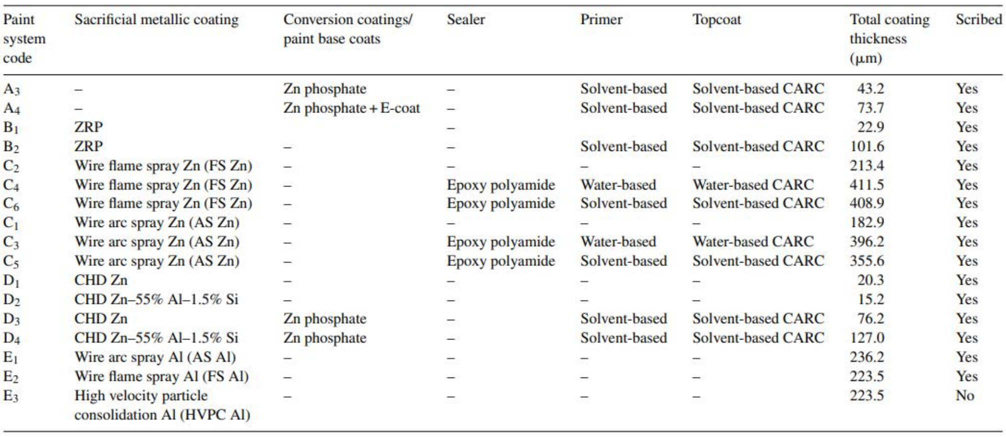

Paint system code	Sacrificial metallic coating	Conversion coatings/ paint base coats	Sealer	Primer	Topcoat	Total coating thickness (µm)	Scribed
A_3	–	Zn phosphate	–	Solvent-based	Solvent-based CARC	43.2	Yes
A_4	–	Zn phosphate + E-coat	–	Solvent-based	Solvent-based CARC	73.7	Yes
B_1	ZRP		–			22.9	Yes
B_2	ZRP	–	–	Solvent-based	Solvent-based CARC	101.6	Yes
C_2	Wire flame spray Zn (FS Zn)	–	–	–	–	213.4	Yes
C_4	Wire flame spray Zn (FS Zn)	–	Epoxy polyamide	Water-based	Water-based CARC	411.5	Yes
C_6	Wire flame spray Zn (FS Zn)	–	Epoxy polyamide	Solvent-based	Solvent-based CARC	408.9	Yes
C_1	Wire arc spray Zn (AS Zn)	–	–	–	–	182.9	Yes
C_3	Wire arc spray Zn (AS Zn)	–	Epoxy polyamide	Water-based	Water-based CARC	396.2	Yes
C_5	Wire arc spray Zn (AS Zn)	–	Epoxy polyamide	Solvent-based	Solvent-based CARC	355.6	Yes
D_1	CHD Zn	–	–	–	–	20.3	Yes
D_2	CHD Zn–55% Al–1.5% Si	–	–	–	–	15.2	Yes
D_3	CHD Zn	Zn phosphate	–	Solvent-based	Solvent-based CARC	76.2	Yes
D_4	CHD Zn–55% Al–1.5% Si	Zn phosphate	–	Solvent-based	Solvent-based CARC	127.0	Yes
E_1	Wire arc spray Al (AS Al)	–	–	–	–	236.2	Yes
E_2	Wire flame spray Al (FS Al)	–	–	–	–	223.5	Yes
E_3	High velocity particle consolidation Al (HVPC Al)	–	–	–	–	223.5	No

Figure 1.10: Composition of the coatings and their configuration [81]

In the figure 1.11, the micrograph of a coating system and its schematic can be seen. In figure 1.11, a sealer (Metcoseal EPS) and a thermal spray coat is made use of and the role of the sealer is to create a barrier between the corrosive environment and the metallic coating by clogging the voids and pores of the spray metal coating. Conversion coating is done so as to provide a good base for durability and paint adhesion. It converts the metal surface into a nonmetallic polycrystalline coating constituting of manganese, nickel, zinc phosphates and iron. As can be seen in the figure 1.11 and figure 1.10, the conversion coatings used for this study was E-coat (electrocoating) and Zn phosphate.

The commercial conversion coatings used in this study for E-coat was Powercron 590 by PPG, it is a cathodic epoxy electrode position primer and the Zn phosphate used was Bonderite B958 by Henkel. Above the conversion coating/sealer, a primer is used so as to provide an essential adhesion between the top coat and the metal. Two types of primer is made use of as can be seen in figure1.10, one is a water based primer (MIL-P-53030) and the other is a solvent-based epoxy primer (MIL-P-53022). Above the primer is the top coat, which in most of the cases in this study was either a water-based (MIL-DTL-64159) or solvent-based (MIL-C-53039) CARC (chemical-agent-resisting-coating). After being exposed to liquid chemical agents, the surface is very effectively and easily decontaminated while also reducing the signature response and increasing the durability of the system. The thickness of different coatings as can be seen in figure 1.10. For each of the coating thickness to be averaged, ten measurements were taken. This includes the four corners, the middle and on either side of the test plate. All the thickness measurements in figure 1.10 is a representation of the coating thickness that differs from one coating to another. Therefore one coating is applied much thicker than the other as can be seen in the difference between the A3 paint system and C4 paint system [81].

1.4.6. Coating degradation mechanism of water ballast tank

To describe the degradation mechanism of a coatings, an epoxy amine-based ballast tank coating is used by Paul et al [40]. Flakes of this coating which was well intact with the steel substrate was chipped off a flat surface from the ballast tank. The coating has been in-service for the past 18 years. The degradation of the 18 year old coating has been has been compared by Paul et al [40] and it is explained further below.

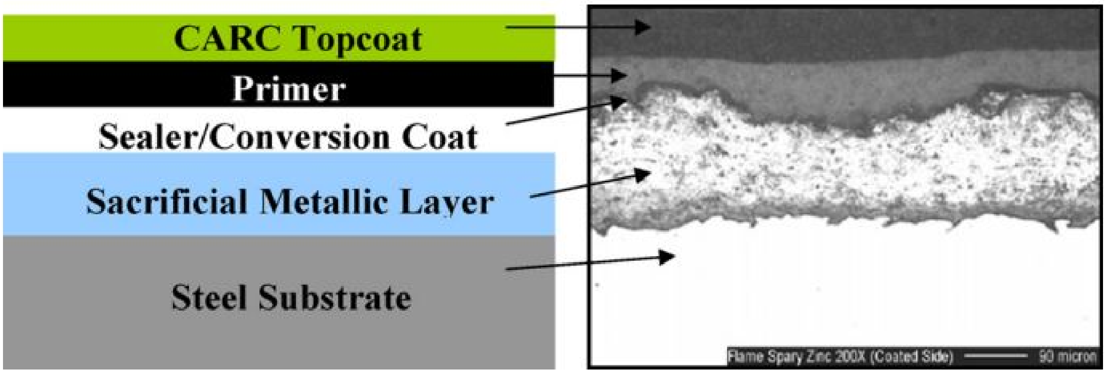

Figure 1.11: Schematic and micrograph of a coating system [81]

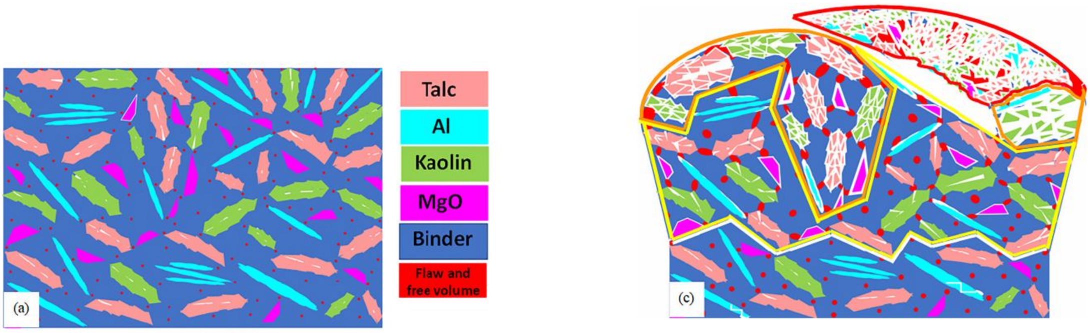

(a) Before Coating degradation (b) Propagating coating degradation

Figure 1.12: Propagation of Coating degradation [40]

When in comparison to the fresh coating, the electrochemical barrier protection provided by the 18 year old coating to the steel substrate was reduced by three orders of magnitude. The reduction in impedance was mainly attributed to the hygrothermal ageing cycles experienced by the coating during its service life. These cycles exert a stress along with temperature variations during filling and discharging of sea water. When such stresses are being applied on the coating, the coating undergoes expansion and contraction. In this case, the coating predominantly underwent expansion rather than contraction. Expansion of the coating was due to the fact that the ballast tanks are filled with sea water, upon which water is being absorbed by the coating, ultimately resulting in swelling and thereby exerting stress by expansion. The coating also underwent contraction, during the process of deballasting, desorption of water had taken place. But this contraction did not last long due to an increase in temperature in the adjacent cargo tank, which was filled with hot crude oils [40].

It was seen that the increase in temperature and volume aided the polymer binder in leaching of small molecules and evaporation of solvents. Due to which there was increase in absorption of free water in the coating as was proved in the corrosion of aluminium. Stress generation and distribution is a key factor in the degradation mechanism, therefore aligning and distributing the pigments play a significant role. Alignment of pigments parallel to the surface was observed to be beneficial in terms of reducing the contraction stress development. In terms of distribution, clustering of pigments parallel to the surface aided in restricting the expansion of coating and thereby slowing the degradation process. In cases where the orientation of the pigment is vertical or near vertical to the surface as can be seen in the figure1.12, it leads to accelerated rates of degradation and the cause for it was attributed to the reduction in lateral restraint [40].

In figure1.12, two images can be seen. On the left side, image of a coating in its initial condition is depicted. The propagation of a coating degradation can be seen on the right side. As the degradation mechanism propagates, fracture occurs in the barrier pigments. This leads to de-bonding of barrier pigments from the polymer binder. This is evident in the right side image (amber zone) of figure 1.12. Once the de-bonding happens, it leads to fragmentation of both the barrier pigments and the polymer binder. At later stages of degradation, the pigments become a bunch of nano-cystals, completely void of any polymer binder (this can be seen in the red zone of the right image of figure 1.12). It was observed that,when pigments become fragmented and form nano-crystals, they tend to leave the surface of the coating. This leads to the surface roughness and gradual thinning of the coating [40].

Local damage of coating, increased free volumes, cavities, widened fractures, loss of bonding between binder and pigment and hydration of polymer binder were causes for the penetration of electrolyte into the coating. This lead to a reduction of impedance value from (fresh coating) $5.7 \times 10^{10}\ \Omega\ cm^2$ to $4.1 \times 10^7\ \Omega\ cm^2$ [25][8]. Which was well within the threshold of meeting the minimum industry standard requirement of less than $10^7\ \Omega\ cm^2$. which indicates the coating is in a poor condition with significant failure of barrier protection properties [40].

1.4.7. Comparison between different coatings

Sharma et al [84], did an experiment to study the corrosion behaviour of Al_20_3-13% TiO_2 and Cr_2O_3 coated ship hull steel in a simulated sea water environment of 3.5% NaCl solution. When observing the microstructure of this coating in the ships, some micro pores were to be found but micro cracks were not present. It was known from previous studies that the presence of pores, cracks, splats and laminar microstructure would lead to material degradation. From observing the microstructure,Sharma et al [84], also found the absence of laminar microstructure and columnar grains.

On further analysis, Sharma et al found a corrrelation between porosity and corrosion resistance. The porosity of the coating Al_2O_3-13%TiO_2 was 2.293% and for the Cr_2O_3 coating it was found to be 1.69%. The corrosion rate for Al_2O_3-13%TiO_2 coating was 0.0133 mm/year and for Cr_2O_3 it was 0.0128 mm/year. From this it can be said that, when the porosity of the coating is less, it is said to be more corrosion resistant .

Liu et al [55], studied the corrosion behaviour of metallic coatings, plasma sprayed ceramic on carbon steel in seawater. They found that potential for all the coatings in their study to be really high during the starting phase of immersion. This was due to the fact that coatings were strong initially, abstaining the solution from reaching the substrate. It was understood that it was the essential time required for the solution to reach the substrate by diffusing through the pores and pinholes on the surface. Once this diffusion occurs, the potential of the coating decreases gradually with increase in immersion time. After a certain point, potential reaches an equilibrium potential [55].

In the figure 1.13, potential of the coatings with respect to the immersion time can be seen. Two metallic coatings and two ceramic coatings are plotted in figure 1.13. It can be seen that the metallic coatings Ni60 and Q235 both have slopes that are much more stable. But the same cannot be said about the two ceramic coatings. The potential of the two ceramic coatings decreases drastically with increase in immersion time. This can be attributed to the presence of pores in the ceramic coatings.

When comparing the corrosion potentials of all four coatings. ZrO2, Al2O3 and Ni60 coating had a noble corrosion potential, when compared to the Q235 coating. In this case the Q235 was less noble and corrosion rate of Q235 coating when coupled with other coatings of positive

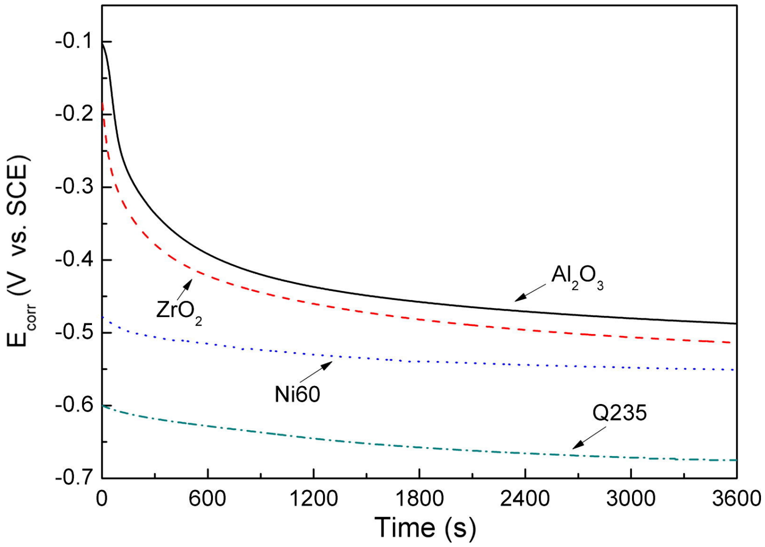

Figure 1.13: Corrosion Potentials of Ceramic and Metallic Coatings [55]

corrosion potentials will also depend on the area of the coating. If the area of the Q235 coating is much smaller than than the other coatings when coupled, then the corrosion of the small area Q235 coating will increase rapidly. The extent to which the coating will undergo corrosion will depend on the pores and pinholes in the coating [55] [54].

The figure 1.14 shows the characteristic impedance spectra and the corresponding equivalent circuit for a metal that is coated in 3.5% NaCl solution. R_s represents the electrolyte resistance and C_1 represents the dielectric capacitance in the equivalent circuit seen in figure 1.14. With increase in exposure time in the marine conditions, oxygen, ionic species and water permeate through and contribute to the increase in paint conductivity. R_1 in a physical sense describes the lower resistance paths that short-circuit the organic coating, C_1 describes the value related to the water uptake. The other terms in the equivalent circuit comes into play when the permeating corrosive species reach the underlying metallic substrate. This is the time when corrosion starts, which brings in a second time constant due to the relaxation of the electrochemical double layer (C_2) and a charge transfer resistance (R_2) and it can be related to the corrosion process as $1/r_2$ [79].

For samples with $R_1 > 10^8\ \Omega\ \mathrm{cm}^2$, corrosion protection is really high and they can be attributed to the capacity of the paint and its ability to slowdown the diffusion of the corrosive species into the paint/metal interface. This type of coating is an addition to an already effective inhibiting action of the underlying base coating pigment. With the above mentioned mechanisms in work, the metal can be assumed to be isolated from both external conditions it was exposed to and also from the 3.5% NaCl solution it was exposed to during the EIS measurements [79].

Rosal et al [79], found that the resistance of the organic coatings were inversely proportional to the average cross section of the conductive pathways through which the electrolyte could pass through. The meeting of the electrolyte with the metal substrate could happen mainly due to two factors. One of the factors is how the paint has been formulated, ie, does the coating delay the diffusion of the electrolyte and accelerate the corrosion or vice versa by altering the conductive pathways. The other factor is the external surroundings that is not controllable and how far it affects the metal depends a lot on the kind of environment and its severity. It was evident from the experiments for Rosal et al [79] that the high conductive pathways were a result of the low R_1 values. The R_1 value also helped in providing further information regarding

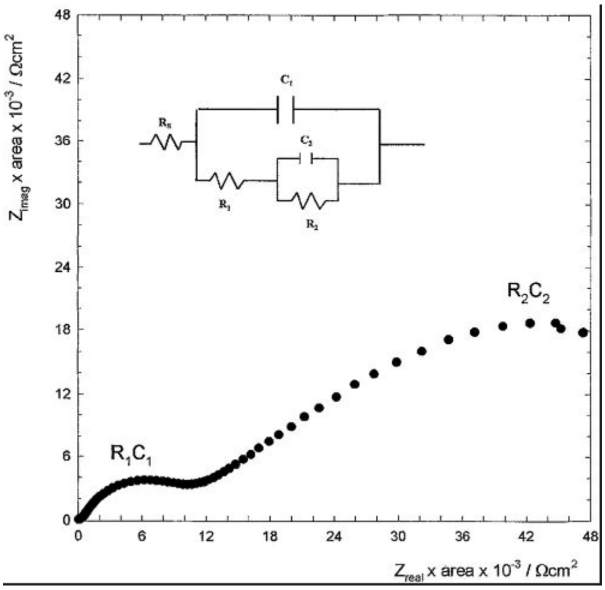

Figure 1.14: Characterization of a corroding coating metal system [79]

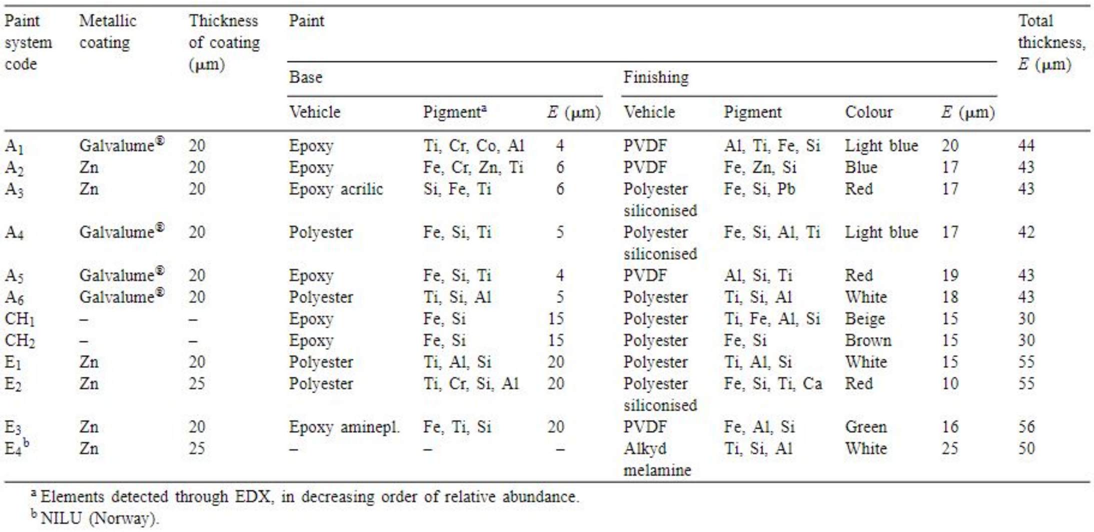

Paint system code	Metallic coating	Thickness of coating (μm)	Paint							Total thickness, E (μm)
			Base			Finishing				
			Vehicle	Pigment[a]	E (μm)	Vehicle	Pigment	Colour	E (μm)	
A_1	Galvalume®	20	Epoxy	Ti, Cr, Co, Al	4	PVDF	Al, Ti, Fe, Si	Light blue	20	44
A_2	Zn	20	Epoxy	Fe, Cr, Zn, Ti	6	PVDF	Fe, Zn, Si	Blue	17	43
A_3	Zn	20	Epoxy acrilic	Si, Fe, Ti	6	Polyester siliconised	Fe, Si, Pb	Red	17	43
A_4	Galvalume®	20	Polyester	Fe, Si, Ti	5	Polyester siliconised	Fe, Si, Al, Ti	Light blue	17	42
A_5	Galvalume®	20	Epoxy	Fe, Si, Ti	4	PVDF	Al, Si, Ti	Red	19	43
A_6	Galvalume®	20	Polyester	Ti, Si, Al	5	Polyester	Ti, Si, Al	White	18	43
CH_1	–	–	Epoxy	Fe, Si	15	Polyester	Ti, Fe, Al, Si	Beige	15	30
CH_2	–	–	Epoxy	Fe, Si	15	Polyester	Fe, Si	Brown	15	30
E_1	Zn	20	Polyester	Ti, Al, Si	20	Polyester	Ti, Al, Si	White	15	55
E_2	Zn	25	Polyester	Ti, Cr, Si, Al	20	Polyester siliconised	Fe, Si, Ti, Ca	Red	10	55
E_3	Zn	20	Epoxy aminepl.	Fe, Ti, Si	20	PVDF	Fe, Al, Si	Green	16	56
E_4[b]	Zn	25	–	–	–	Alkyd melamine	Ti, Si, Al	White	25	50

[a] Elements detected through EDX, in decreasing order of relative abundance.
[b] NILU (Norway).

Figure 1.15: Characteristics of Tested Materials [79]

the barrier properties.

In the experiment done by Rosal et al [79], the different coatings and their composition can be seen in figure 1.15. In the case of A_1 to A_6 coatings in figure 1.15, it was observed that the EIS results of these coatings indicated a reduction in coating resistance with increase in time. These samples have been exposed to three different locations for a 1-year time period. The three stations are namely Punta del Este (Uruguay), La Voz (Venezuela) and Jubany (Argentina). Among the three locations, the La Voz was known to have the most harsh environmental conditions. Even though it was the most aggressive among the three locations, some unusual behaviour was noticed by Rosal et al [79]. After the first year of exposure, the coatings A_1,A_3 and A_6 seemed to get better. This was possible mainly due to the fact that the corrosion products of Zn had obstructed both the intrinsic as well as the extrinsic defects. This was consequence of dissolution of the metallic coating. In the case of the other samples and the same sample as above when exposed to comparatively less harsh

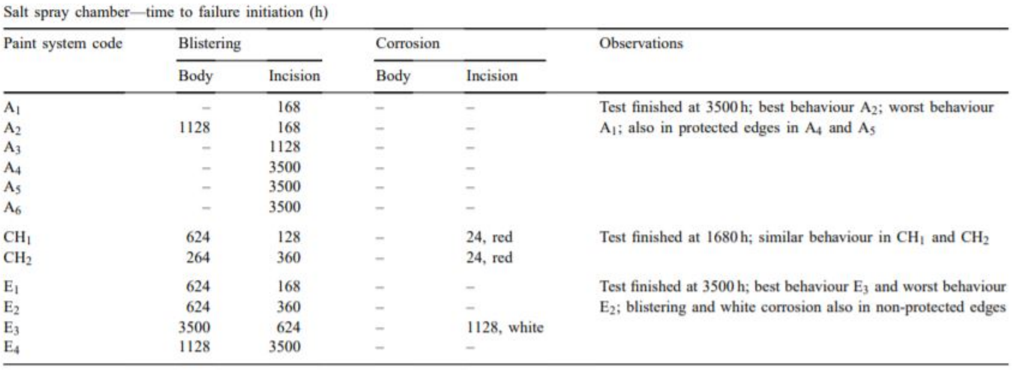

Salt spray chamber—time to failure initiation (h)

Paint system code	Blistering		Corrosion		Observations
	Body	Incision	Body	Incision	
A_1	–	168	–	–	Test finished at 3500 h; best behaviour A_2; worst behaviour A_1; also in protected edges in A_4 and A_5
A_2	1128	168	–	–	
A_3	–	1128	–	–	
A_4	–	3500	–	–	
A_5	–	3500	–	–	
A_6	–	3500	–	–	
CH_1	624	128	–	24, red	Test finished at 1680 h; similar behaviour in CH_1 and CH_2
CH_2	264	360	–	24, red	
E_1	624	168	–	–	Test finished at 3500 h; best behaviour E_3 and worst behaviour E_2; blistering and white corrosion also in non-protected edges
E_2	624	360	–	–	
E_3	3500	624	–	1128, white	
E_4	1128	3500	–	–	

Figure 1.16: Salt spray test - Time to failure initiation [79]

conditions, the performance of the coating was either continuously oscillating or decreasing for large time periods. Rosal et al [79], found that the consequence of this was again the obstruction of the defects by the corrosive products of Zn and the organic film/ coating forming new ionic conductive paths. One of the reasons for failure in all three locations was found to be the paint blistering at the region of incisions. Some of the factors that contributed to the failure of the coatings are the radiation of the sun and penetration of Cl^- ions.

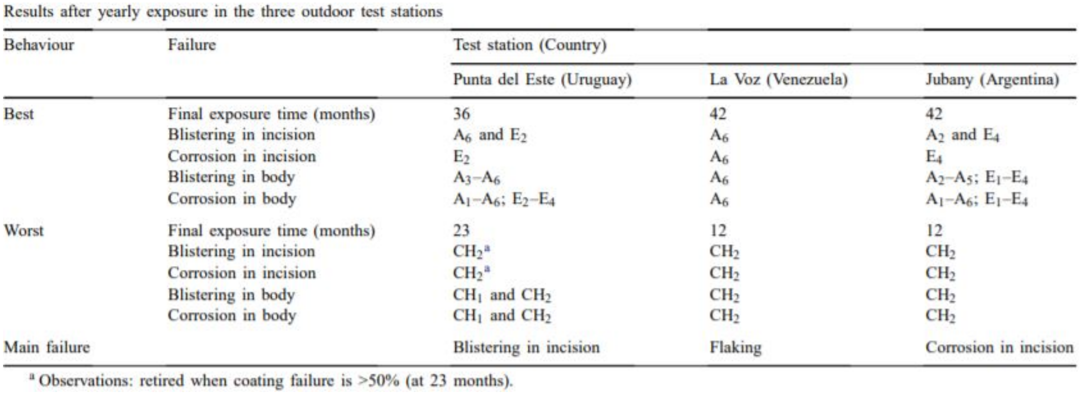

Results after yearly exposure in the three outdoor test stations

Behaviour	Failure	Test station (Country)		
		Punta del Este (Uruguay)	La Voz (Venezuela)	Jubany (Argentina)
Best	Final exposure time (months)	36	42	42
	Blistering in incision	A_6 and E_2	A_6	A_2 and E_4
	Corrosion in incision	E_2	A_6	E_4
	Blistering in body	A_3–A_6	A_6	A_2–A_5; E_1–E_4
	Corrosion in body	A_1–A_6; E_2–E_4	A_6	A_1–A_6; E_1–E_4
Worst	Final exposure time (months)	23	12	12
	Blistering in incision	CH_2[a]	CH_2	CH_2
	Corrosion in incision	CH_2[a]	CH_2	CH_2
	Blistering in body	CH_1 and CH_2	CH_2	CH_2
	Corrosion in body	CH_1 and CH_2	CH_2	CH_2
Main failure		Blistering in incision	Flaking	Corrosion in incision

[a] Observations: retired when coating failure is >50% (at 23 months).

Figure 1.17: Results after yearly exposure to three outdoor test stations [79]

While analysing the results Rosal et al [79], compared the ionic resistance of the samples at all three locations as mentioned above. They found that the A_i samples had oscillating R_1 values and provided better protection for a longer duration (42 months) when compared to the rest of the samples. In comparison to the rest of the coatings the A_i had least gloss depletion and minimum to no colour change as well. The CH_i E_i samples did not even come close to the duration of the A_i samples in terms of offering good protection. E_i lasted for 24 months and CH_i samples lasted a mere 12 months, also their respective R_1 values were less than 10Ω cm^2. When looking into the performance of the coatings when they were exposed the La Voz station (most aggressive of all three locations), all the coatings did not seem to perform differently with respect to each other. They were able to last a mere 24 months and this lead them to a conclusion that all the coatings they tested were only suitable for less severe conditions as opposed to aggressive conditions such the La Voz station. Similarly the R_1 values for A_i and E_i were $< 10^5$ Ω cm^2, but in the case of the non-metallic coated steel (CH_i), $R_1 > 10^7$ Ω cm^2. It was able to achieve these R_1 values due to the accumulation of corrosion products of steel. In the Punta del Este station, which is a less harsh station compared to the

La Voz station. The samples were able to last longer in comparison (36 months) and and their R_1 values were greater than 10^6 Ω cm^2. On the other hand the CH_i samples had lower R_1 ($<10^6$ Ω cm^2), due to which it was able to last a mere 24 months.

Rosal et al [79], found that the most failures were noticed when blistering and corrosion both occured in the incision. In the case of the Zn based coatings, the time for the appearance of the red corrosion products increased at the incision and the edges. These coatings also helped in pore blockages.

1.5. External factors influencing the coating

1.5.1. Role of chloride concentration

Chloride concentration is one of the main factors due to which corrosion occurs. To initiate corrosion, the chloride concentration should exceed a certain amount known as the chloride threshold level (CTL) [74].

To understand the relationship between pit depth and chlroide concentration, a AISI 316L specimen was used. The specimen was immersed in Cl^- containing aqueous solution of various pH for a duration of 4 months under static and dynamic conditions. The pit depths were measured microscopically. The depth of the pit increases with increase in Cl^- concentration as can be seen in figure [59].

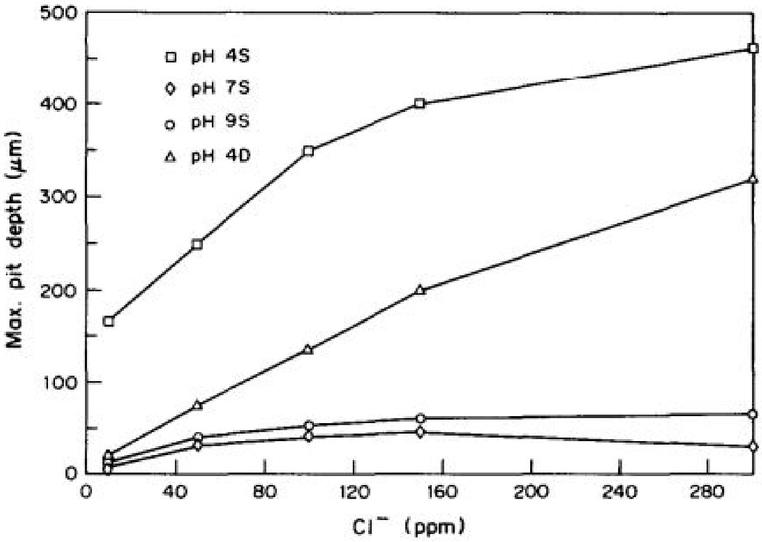

Figure 1.18: Maximum pit depth of AISI 316L when exposed to Cl^- containing aqueous solution for a duration of 4 month in various pH values

1.5.2. Significance of surface treatments

Rajput et al [77], conducted an experiment on three test specimens with varying surface roughness and coated with an epoxy coating. The test plates were submerged in sea water for a period of eight months in laboratory conditions. Rajput et al [77], found the performance of the coating to be dependent on the surface roughness of the steel plates. Johnson et al [44], in 1990 observed that almost 90% of the coating failures are either due to improper surface preparation or due to faults in applying the coating on the surface.

Before the coating is applied, preparation of the surface is an extremely significant process. It is this process that determines the roughness of the surface and it is achieved by abrasive blast cleaning.

There are several contaminants that can interfere with the coatings ability to achieve a good level of wetting and adhesion. These contaminants include salt residues, hydrocarbons, loosely bound corrosion products of oxides and rust, natural deposits of dirt and water. Surface preparation practices that are used, needs to be able to eradicate any contaminants on the surface. Surface preparation techniques can either be solely chemical or mechanical or a combination of both. Chemical surface preparation techniques include the acid pickling, flame cleaning and solvent cleaning. Wet abrasive blasting, shot or grit blasting, power tools and water jetting are some of the mechanical surface preparation techniques [99].

1.5.3. Submerged zone

Underwater hull, propeller, rudder, bilge keel, shaft brackets and so on are some of the parts that are completely underwater. To protect such parts, a combination of protection measures are taken. A suitable coating that can widthstand the adverse conditions and cathodic protection. The suitable coating applied would consist of both anti-fouling and anti-corrosive properties. While the cathodic protection is either provided by impressed current cathodic protection system or by means of a sacrificial anode system. The cathodic protection is considered as a back up option in cases when the coating has been damaged due to certain unforeseen circumstances or the performance of the coating has deteriorated sufficiently due to long service life.

In terms of corrosion, ballast tanks pose the highest threat. As they are exposed to seawater at varying levels inside the tank, cyclic changes in temperature, repeating wetting and drying cycles similar to the splash zone, hydrostatic pressure, insufficient drainage, difficult access and so on. In addition to this, sand particles present in the water inside the ballast is a major threat and local erosion is caused by the high flow rates near the inlets and the outlets. Babu et al [7], say that for submerged parts of the tank, both cathodic protection and a suitable coating is essential. It was known by babu et al [7], that sacrificial anode was a better choice in the case of ballast tanks than impressed current cathodic protection because of the possibility of hydrogen evolution.

1.5.4. Need for Corrosion Monitoring

Corrosion occurs due to the combination of various factors. This includes the following [65]:

- Salt laden air
- Condensation
- Localized high temperature
- Saline water
- Rain dew
- Naturally occurring substances that cause corrosion

The hull is a part of the ship that when exposed to aggressive corrosive environment undergoes different types of corrosion. General, galvanic, pitting and so on are the types of corrosion that are possible to occur. Different types of corrosion occurs due to different reasons. Stray current corrosion occurs due to improper earthing of the weld equipment. If the hull is exposed to slow or stagnant water, then pitting corrosion is possible. This type of stagnant water is usually found in dockyard basins. If galvanic corrosion is to occur,it occurs between a noble material and the hull. Other types of corrosion that occurs in ship structures are micro-

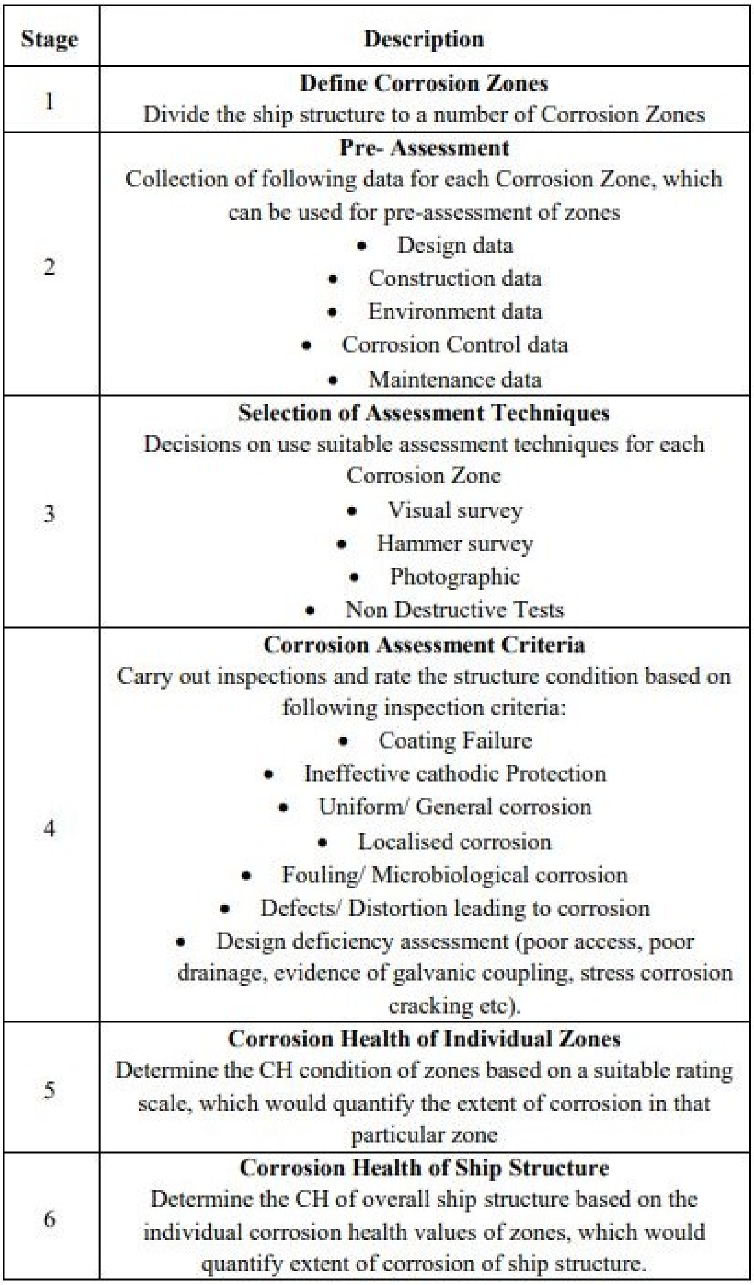

Stage	Description
1	**Define Corrosion Zones** Divide the ship structure to a number of Corrosion Zones
2	**Pre- Assessment** Collection of following data for each Corrosion Zone, which can be used for pre-assessment of zones • Design data • Construction data • Environment data • Corrosion Control data • Maintenance data
3	**Selection of Assessment Techniques** Decisions on use suitable assessment techniques for each Corrosion Zone • Visual survey • Hammer survey • Photographic • Non Destructive Tests
4	**Corrosion Assessment Criteria** Carry out inspections and rate the structure condition based on following inspection criteria: • Coating Failure • Ineffective cathodic Protection • Uniform/ General corrosion • Localised corrosion • Fouling/ Microbiological corrosion • Defects/ Distortion leading to corrosion • Design deficiency assessment (poor access, poor drainage, evidence of galvanic coupling, stress corrosion cracking etc).
5	**Corrosion Health of Individual Zones** Determine the CH condition of zones based on a suitable rating scale, which would quantify the extent of corrosion in that particular zone
6	**Corrosion Health of Ship Structure** Determine the CH of overall ship structure based on the individual corrosion health values of zones, which would quantify extent of corrosion of ship structure.

Figure 1.19: Table for corrosion assessment [7]

biological corrosion, erosion corrosion, crevice corrosion, heat exchanger corrosion and high temperature corrosion [7].

Due to the above discussed types of corrosion, various factors of the ship are affected. Corrosion increases the deterioration rate of the ship, drag of the ship is increased and it increases the loading stress. When the deterioration rate of the ship is increased, the ship is under high risk of premature failure. This leads to huge economical impact and safety of goods and personnel. On the other hand if the ship undergoes various corrosion prevention measures and checks, then a lot of catastrophic events can be avoided in the first place. A good to excellent coating applied to a ship, can help preventing a lot of planned as well as unplanned maintenance and the costs that come with it [7].

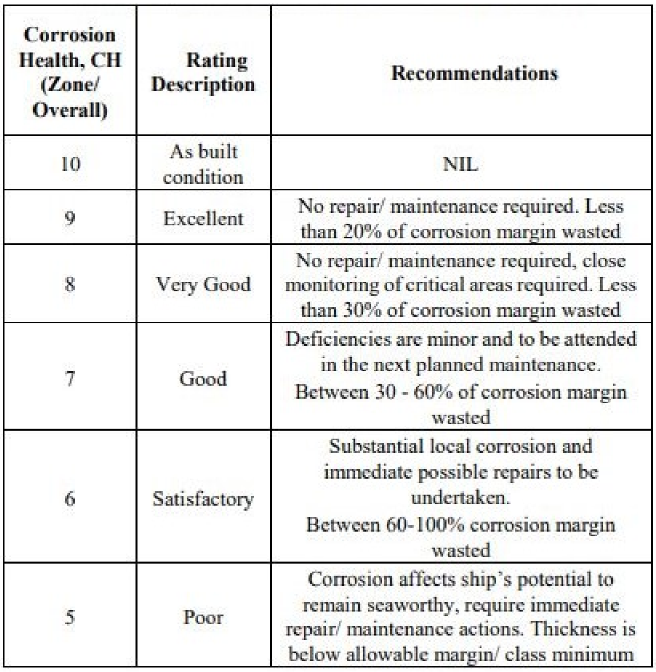

Corrosion Health, CH (Zone/ Overall)	Rating Description	Recommendations
10	As built condition	NIL
9	Excellent	No repair/ maintenance required. Less than 20% of corrosion margin wasted
8	Very Good	No repair/ maintenance required, close monitoring of critical areas required. Less than 30% of corrosion margin wasted
7	Good	Deficiencies are minor and to be attended in the next planned maintenance. Between 30 - 60% of corrosion margin wasted
6	Satisfactory	Substantial local corrosion and immediate possible repairs to be undertaken. Between 60-100% corrosion margin wasted
5	Poor	Corrosion affects ship's potential to remain seaworthy, require immediate repair/ maintenance actions. Thickness is below allowable margin/ class minimum

Figure 1.20: Corrosion health rating and description [7]

Such measures for prevention of corrosion starts right from the design and selection of materials. The measures include protective coatings , fabrication methods, vapour phase inhibitors, humidification, use of cathodic protection which include impressed current cathodic protection or sacrificial anodes [7].

Inspection of ships to mitigate the effects of corrosion involve:

- Assessing corrosion
- Assessing coating
- Assessing cathodic protection
- Looking for possible strucutural defects
- Cleanliness of compartments
- Assessing the remaining thickness of the plate under inspection

Monitoring of corrosion is a complex matter and it involves various factors. If a ship is considered, different areas of the ship are susceptible to different types and levels of corrosion. The level corrosion might differ from one area of the ship to another. Different areas of the ship undergo different rates of corrosion. Due to the various factors involved, there is not one specific measurement technique that aids in analysing the condition of the product being inspected. A corrosion technique which has a high success rate in predicting the conditions of product in terms of corrosion, has the ability to reduce downtime, costs of maintenance, increase safety, pollution reduction, provide a warning before major damage and helps in extending the functional life of the product [7].

1.5.5. Guidelines for inspecting corrosion damage

Corrosion initiation occurs due to coating damage that occurs either due to improper application of the coating or the coating damage might happen due to some heavy contact with an external object. Edges, weld seams, heat affected zones, notches are some of the areas where the coating quality can be poor. So while inspecting for corrosion, these are some of the areas to look into. Looking into the other aspect where coating damage is caused by external factors such as stress and strain due to certain overloads, vibrations, wear, dents repair work and so on is also needed. These factors cause corrosion and thereby reducing the thickness of the steel plate under the coating. Poor quality of the coating may also be caused by improper surface treatment and if welding is done on a coated specimen and not repaired properly [7].

Corrosion can be a major issue in the complex shaped structures. One way to look at it is in the case of inspecting the product in those complex shaped areas, where visible access is limited and if some damage can be detected, it would be very difficult to repair them. On the other hand, due to limited access, if a damage cannot be detected, then the product might undergo significant corrosion in an undetected manner. It is very important to design a product with corrosion in mind. Even though corrosion resistance materials are chosen, a design that aids in keeping the corrosive elements away is very essential. Inadequate drainages, horizontal surfaces in some of the designs that aids in aggravating corrosion [7].

1.6. EIS Measurements

To analyse a coating in an immersed state takes 1000's of hours. With the help of EIS measurements valuable insights can be gained about the coating in a short span of time. Since the corrosion process is an electrochemical process, it would be a good estimate to measure the electrochemical resistance to understand the coatings ability to withstand intrusions of the corrosive agents and prevent them from reaching the underlying substrate [80][79].

Significant effort has been made to develop a method to get more insights into the organic coatings that can reproducible, accurate and numerical. EIS is seen as a very useful tool in this regard. It not only provides results in a short duration, but also provides insights into the corrosion mechanism involved. This type of method helps in identifying coating damages before any visual inspection is done. The sensitivity of the EIS test aids in lowering the total test time taken [95][4].

1.6.1. History of EIS

Impedance as concept was first introduced by Heaviside between the period 1880-87. During this time he coined the term impedance, reactance and admittance. Heaviside also developed the concept of operational calculus, which was seen as a way to solve the differential equations by converting them to algebraic equations. Which in-turn would aid in flow description of current through the circuits which contains capacitors, inductors and resistors. But this method was not mathematically proven and hence was criticized heavily [56].

During the period 1939-1942, to analyse the corrosion protection properties of coatings, J.K. Wirth [45][71] made use of the electrical resistance measurements (DC). Very soon in the year 1948, Bacon et al [8], published their work which consisted of more than 300 coating systems that were extensively tested with DC resistance to form a classification for the coating systems. If the resistance value is $> 10^8$ Ω cm^2, then it is considered a good coating system, but if it is $< 10^6\Omega$ cm^2 then it is considered a poor coating system. In addition to measuring the resistance values of the coatings, the water uptake by polymer coatings was also measured using the capacitance at a single frequency or multiple frequency around the 1000Hz range [45][27].

One of the first applications of EIS was done in the year 1973 by Menges and Schneider. Once these applications were introduced, it was uphill in terms of the publications on EIS. It was also aided by the speedy development of automated data acquisition, accurate instruments and the development of quantitative data analysis [64]. Though EIS has been established as a powerful tool for analysing the corrosion protection of coatings, it still has its own practical limitations and it requires the use of skilled workers to analyse data [95][4].

1.6.2. Principle of EIS

Derived from the latin word impedire (means to hinder) [4], Impedance is the electrical equivalent of electrical resistance and it aids in measuring the widthstanding capacity of the coating system. The widthstanding capacity of the coating system is evaluated by disturbing it from its steady state by introducing a perturbation. The perturbation is usually introduced into the system in the form of an alternating voltage and the current response of the coating system is measured [27]. The perturbation applied on the coating system consists of a DC bias potential over which a sinusoidal perturbation(E_t) is superimposed with E_t= E_0 sin(wt). In the case of a linear time-invariant(LTI) system, a sinusoidal current response is expected, where I_t = I_0 sin(wt+ϕ). E_0 and I_0 are the amplitudes of the perturbation and the current response respectively and ϕ is the phase shift in the current response w.r.t to the applied potential and it can be seen in figure 1.21.

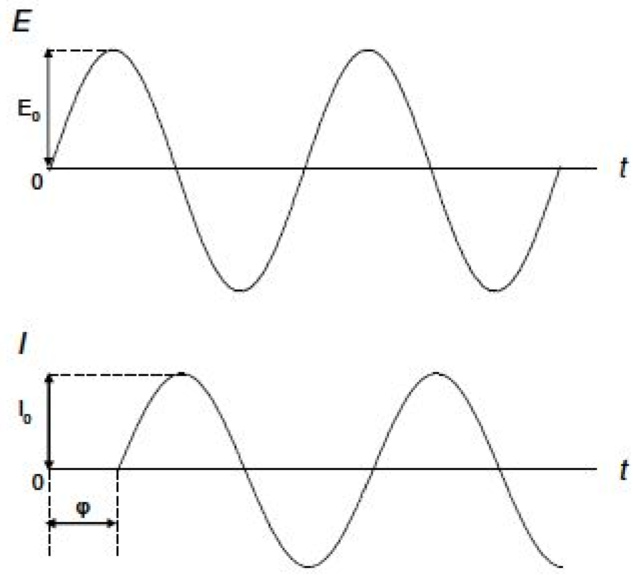

Figure 1.21: Perturbance and current response

Electrochemical systems are neither time-invariant nor linear in reality. In an ideal situation, a system is considered linear if input signals x1(t) and x2(t) leads to output of y1(t) and y2(t) respectively [27] [4]. On the other hand a system is considered time-invariant if the system reacts in a similar manner to a given input at point in time. In a situation where there are well defined conditions, it is observed that the systems behave in a linear time invariant manner. One condition where the system is considered as LTI is when the system variations are marginal in comparison to the measured time. Another condition is when both the input and the output signal have marginal variations around a certain setpoint and the relation is assumed to be linear and can be seen in figure 1.22.

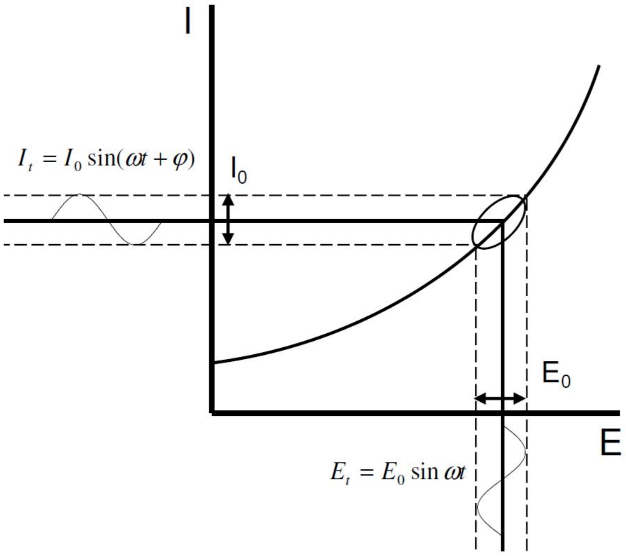

Figure 1.22: Input and output around a certain setpoint [95]

1.6.3. Analysis of Data

There are two types of approaches which are used for data analysis, namely the phenomenological approach and the fundamental approach.

1.6.4. Fundamental Approach

In the fundamental approach, a physical model is considered that accounts for the occurring process in the measured system in terms of the physio-electrochemically valid concepts. The physical model aids in formulating a transfer function which represents a mathematical relation between both the input and the output signal of the system. The transfer function contains all the parameters of the physical model and is fitted to the measurement data. By this method, significant insights on the reaction mechanism is obtained by the use of data from EIS. As there are positives, there are limitations to this method. To provide a reliable transfer function, it is essential to almost completely understand the reaction mechanism. Also, it is very difficult to come to a conclusion in obtaining a useful transfer function due to the complexity of the electrochemical systems.

1.6.5. Phenomenological Approach

Due to the complexities of the fundamental approach, the phenomenological approach is used for analysing the impedance data. Unlike the use of well-founded physical models, electrical equivalent circuits are used for the interpretation of the EIS data. The electrical equivalent circuits comprises of capacitors and resistors and they are designed such that they have similar impedance characteristics as the measured impedance data [51]. To construct the most probable equivalent circuit (MPEC), there are certain guidelines to be followed.

It usually starts with researching previous results and obtaining qualitative circuits. In the case of simple systems, information is obtained by analysing graphs of Nyquist and Bode plot. A characteristic shape is seen in the plots and it is attributed to the combination of capacitors, resistors and other electrical elements. Further analysing the plot shape gives an estimate of each of the individual component values and also the relation between the electrical components and how they are linked together. The hierarchical model of the elements used in the circuit should be in line with a meaningful theoretical model [57][87][34]. The elements in the circuit is kept as low as possible to avoid the unresolved issues the comes up with the additional elements [52][100]. It is often tempting to increase the number of elements which allows for the better fitting of the results. When an equivalent circuit is used for fitting the measurement data, the error distribution is done over the full frequency range and it should not follow a recognisable sine wave rather it should be done in a random manner. It is when the error distribution is not done in a random manner that the circuit is extended and there is a presence of time constant. Hence a desirable model is one that finds good balance between an acceptable error and one that has physical meaning [52]. To access the validity of the impedance data, Kramers-Kronig is used, with its own limitations [13].

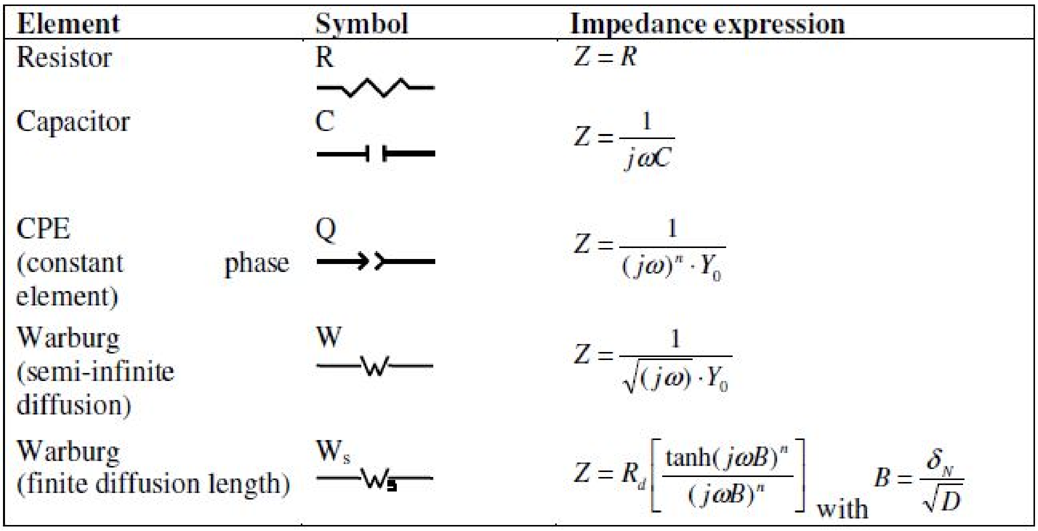

Element	Symbol	Impedance expression
Resistor	R	$Z = R$
Capacitor	C	$Z = \frac{1}{j\omega C}$
CPE (constant phase element)	Q	$Z = \frac{1}{(j\omega)^n \cdot Y_0}$
Warburg (semi-infinite diffusion)	W	$Z = \frac{1}{\sqrt{(j\omega)} \cdot Y_0}$
Warburg (finite diffusion length)	W_s	$Z = R_d\left[\frac{\tanh(j\omega B)^n}{(j\omega B)^n}\right]$ with $B = \frac{\delta_N}{\sqrt{D}}$

Figure 1.23: Impedance elements[101]

In the figure 1.23, you can see an overview of impedance elements. The resistor indicates the resistance faced by the charge carriers and the accumulation of charges is indicated by the capacitor. A constant phase element is a universal element, which indicates real elements such as the resistor(n=0), capacitor(n=1), inductor(n=-1) or even non-ideal di-electric behaviour for which the n equals non-integer values which range between -1 and 1. To model linear semi-infinite behaviour diffusion (occurs if diffusion layer thickness is infinite), the Warburg element is used(W). The same element can be represented with a constant phase element with n = 0.5. When the diffusion layer is said to have finite dimensions and the diffusing species are permeable through the boundary, W_s element is used [95][101].

1.6.6. Impedance Spectra of Protective Coatings

The plot shape of an impedance spectra changes from time to time depending upon the exposure the coating has undergone. During the initial periods, the coating is expected to show largely capacitive behaviour [97][4]. Two types of plots are used for the analysis of the impedance spectra, they are the Nyquist plots and the Bode plot. There is a steep rise of the capacitive arc along the imaginary axis and a straight line with a slope (m = -1) was seen in the Nyquist plot and the Bode Magnitude plot respectively. The figure 1.24 shows a setup to measuring an typical impedance spectra.

When the coating is immersed for long durations of time, the shape of the plot changes and it means the electrolyte has penetrated through the coating. It is indicated in the plot shape change, with the diameter of the semi-circle decreasing with time and the capacitive arc becoming a semi-circle with dashed lines in the Nyquist plot. In the case of the Bode magnitude

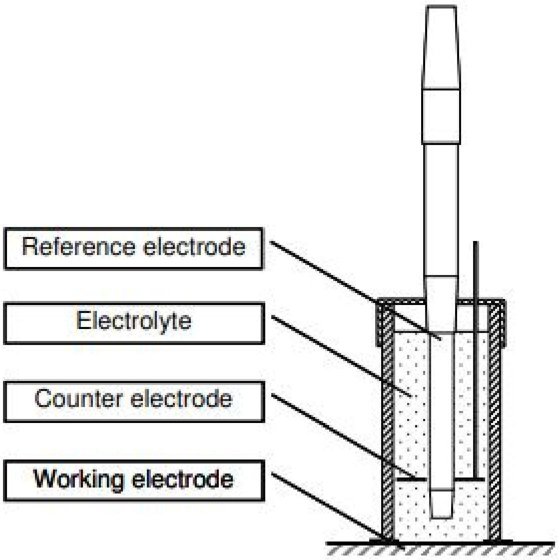

Figure 1.24: Typical Impedance Spectra

plot, corresponding to the Nyquist plot, there is a reduction in the intercept of the log$|Z|$ axis. Both of the above mentioned changes in the shape of the plot indicates a decrease in coating resistance. The shapes changes as an effect of the increasing immersion times and the penetration of the electrolyte through the coating as can be seen in the figure 1.25.

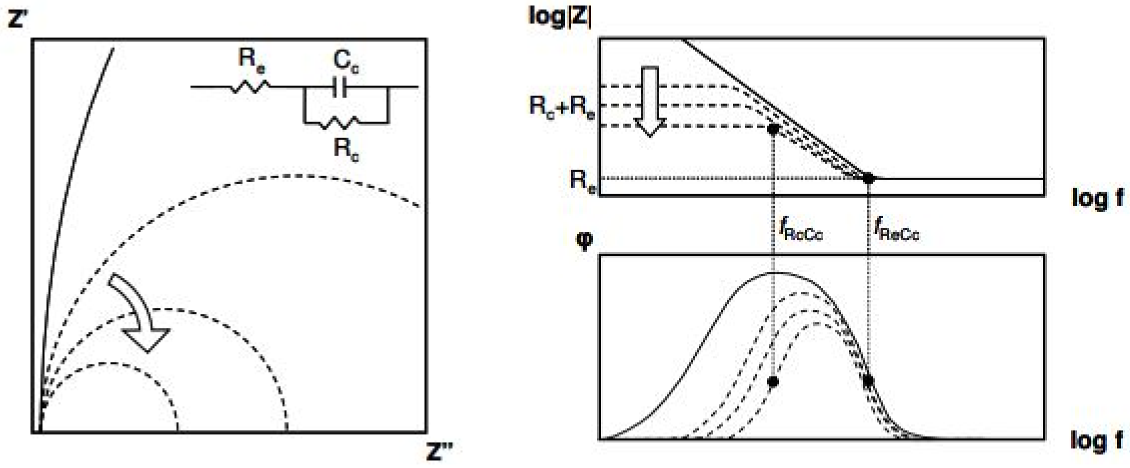

Figure 1.25: Nyquist and Bode Plot for coating degradation

In the figure 1.25, an equivalent circuit can be seen with the coating capacitance(C_c), coating resistance(R_c) and the electrolyte resistance(R_e). In the figure 1.25, there are two breakpoint frequencies f_{RcCc} and f_{ReCc}, which help in characterising the shape of the Bode magnitude plot. The breakpoint frequencies, as can be seen in the equation below is known to be inversely proportional to their related time constants. With the time constant τ =$R_x.C_y$

$$f_{RxCy} = \frac{1}{2\pi.R_x.C_y} \tag{1.4}$$

The occurrence of the breakpoint frequencies in a certain position is due to a particular magnitude of the component. Up until f_{RcCc}, the current passes through the two resisters in series and the capacitor is blocked. In this case the circuit behaves as a resistor with the impedance $|Z|$ = R$_e$ + R$_c$. Between f=0 and f=f$_{RcCc}$, the R$_c$ (resistance due to coating) is observed to be much greater than R$_e$ (electrolyte resistance). During this frequency range, the impeding capacity of the resistor does not change with frequency, so it is known to be independent of frequency in this particular range. Due to this,a straight line parallel to the log-f axis is seen in the Bode magnitude plot and in the case of the Bode phase plot, zero phase angle can be seen in the above mentioned frequency range. The same cannot be said about the frequency range between f$_{RcCc}$ and f$_{ReCc}$. In this frequency range, the impedance is dominated by C$_c$ and it has an impedance $|z|$=1/2π f C$_c$. When C$_c$ dominates the impedance, the Bode magnitude and the Bode phase plot both behave in a slightly different manner. The Bode phase plot rises towards -90° w.r.t to the capacitive behaviour of C$_c$ and the Bode magnitude plot indicates a straight line with a slope(m) = -1. After the f$_{ReCc}$ frequency range, the Bode phase plot approaches a phase angle of zero and the Bode magnitude plot becomes a straight line parallel to the log-f axis. This indicates that the impedance is due to $|z|$=R$_e$ and the impedance due to the C$_c$ has become negligible. All of the above mentioned mechanisms can be better understood with figure 1.25.

The above mentioned Nyquist and Bode plots are specific for a coating in the first stage of degradation. A mechanism associated with a defective coating under activation control can be seen in the following lines and in figure 1.26. In the case of continuing coating degradation, another semi-circle is seen in the Nyquist plot. As can be seen in the figure 1.26, there are two semi-circles that can be seen in the Nyquist plot. The semi-circle in the low frequency range helps in gaining insights about the reactions occurring at the electrode surface, while the semi-circle in the high frequency range aids in gaining insights about the coating properties. In addition to the two semi-circles, two additional elements can be seen, which represents a double layer capacitance (C$_{dl}$) and charge transfer resistance (R$_{ct}$). As it was stated above, the relative magnitude of the components help in determining the positions of the breakpoint frequencies. With the relative magnitude of the components as C$_{dl}$>C$_c$ and R$_{ct}$>R$_c$>R$_e$, the breakpoint frequencies are as follows f$_{RctCdl}$<f$_{RcCdl}$<f$_{RcCc}$<f$_{ReCc}$. In the high frequency range, the circumstances are similar to the one seen in the previous scenario where it was explained for a coating in the first stage of degradation. In the frequency range between f=0 and f=f$_{RctCdl}$, the current passes through the resistors in series with $|z|$=R$_e$+R$_c$+R$_{ct}$. Out of the three resistors in the series the R$_{ct}$ has the highest impedance in the specified frequency range. In the next frequency range as can be seen in the figure below, the impedance is dominated by largest capacitor C$_{dl}$. In the consecutive frequency range, the between f$_{RcCdl}$ and f$_{RcCc}$, the impedance C$_{dl}$ becomes negligible and in the higher frequency range the impedance is only determined by the electrolyte $|Z|$=R$_e$ and the bode magnitude and Bode phase plot indicate a horizontal line and a phase angle approaching zero respectively.

In the case of diffusion control, the rate at which the corrosive species diffuses through the pores is at a slower rate than the charge transfer process. Due to this there is an appearance of a low frequency diffusion tail in the Nyquist plot inclined at the typical angle 45°. This scenario is depicted in figure 1.26, in such a case an additional element known as the Warburg element (W) is included in series with R$_{ct}$ in the equivalent circuit. In the low frequency range, the Bode phase plot approaches 45° and the Bode magnitude plot has a slope of -1/2.

1.6.7. ISO 12944 and its importance

The ISO 12944 is the standard for paints and varnishes for corrosion protection of steel structures. The intention of all the parts of the ISO 12944 is to provide a serious of instructions. The ISO 12944-1 provides information about the overall scope of the ISO standard. In the ISO

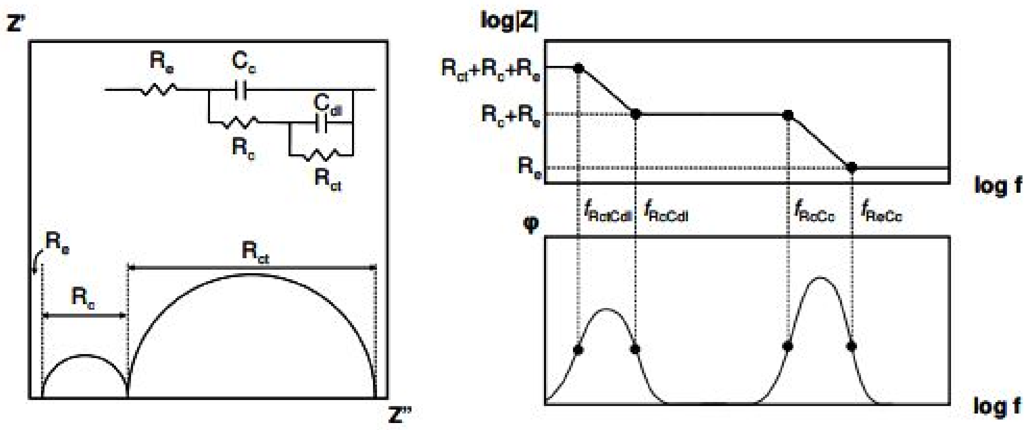

Figure 1.26: Nyquist and Bode plot of a defective coating

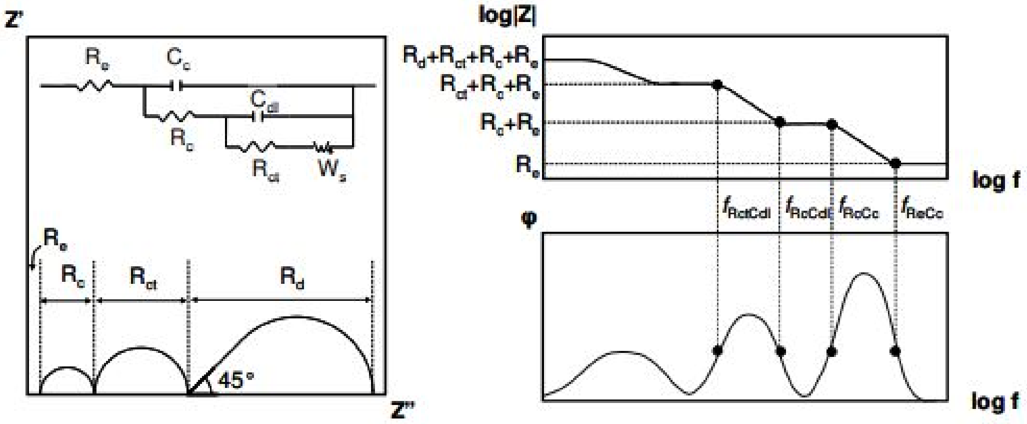

Figure 1.27: Diffusion control in Nyquist and Bode plot

12944-1, there are some basic terminologies and their definitions and it provides a general introduction to the rest of the parts of the ISO 12944 standard. Offshore structures are exposed to harsh environments, and in order for them to withstand the extreme conditions and function as intended, it needs sufficient corrosion protection. It is also of significant importance to avoid any health, safety and environmental issues. In order to do the intended tasks of these structures, they are required to meet certain requirements and undergo certain laboratory tests to evaluate their durability. The structures are exposed to environments of corrosion category CX (offshore) and immersion category Im4.

This ISO test is only suitable for carbon steel structures and also for the paint systems that are designed to operate in the temperature range between -20° and +80°. In the immersion category (Im4) the paint system should be intended to operate in the ambient temperature of upto a maximum of 50°. Finally, the test intends to provide insights into the composition of the components that comprise the coating system, the testing methods to determine the durability of the coating and the criteria to be used to analyse the results of the test [1]

1.7. Correlation of accelerated test with outdoor exposure

1.7.1. Acceleration Factor

Acceleration tests are being done on samples to estimate the performance of the sample in real life for many years to come. The amount to which a sample can be accelerated is an essential aspect to gain insights into the lifetime of the coating. The acceleration provided by a particular lab test can be found by relating an outdoor exposure test with the test results obtained from the accelerated lab result. To aid in this correlation, the below equation is used [47][10][46].

$$A = \frac{x_{test}}{x_{field}} . \frac{t_{field}}{t_{test}} \tag{1.5}$$

A is the acceleration factor, x_{test} and x_{field} are the response (eg:creep(mm)) due to accelerated and field test respectively, t_{field} and t_{test} are the duration (in hours) of field and accelerated exposure respectively.

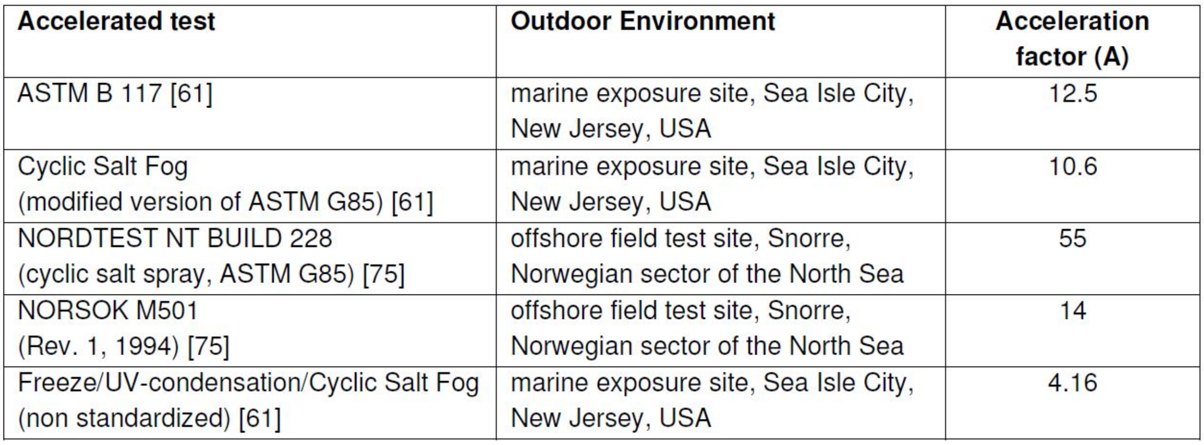

Accelerated test	Outdoor Environment	Acceleration factor (A)
ASTM B 117 [61]	marine exposure site, Sea Isle City, New Jersey, USA	12.5
Cyclic Salt Fog (modified version of ASTM G85) [61]	marine exposure site, Sea Isle City, New Jersey, USA	10.6
NORDTEST NT BUILD 228 (cyclic salt spray, ASTM G85) [75]	offshore field test site, Snorre, Norwegian sector of the North Sea	55
NORSOK M501 (Rev. 1, 1994) [75]	offshore field test site, Snorre, Norwegian sector of the North Sea	14
Freeze/UV-condensation/Cyclic Salt Fog (non standardized) [61]	marine exposure site, Sea Isle City, New Jersey, USA	4.16

Figure 1.28: Acceleration factors of the accelerated exposure is compared with the field exposure and the acceleration factors are derived for the average scribe creep [17]

Materials exposed to the outside environment are expected to undergo degradation. But the rate at which a material undergoes degradation depends on two factors. One is the material involved and the other is the varying rates of the corrosive environment with time. Tiemends et al [91] found that the acceleration factors used in the laboratory was dependent on the material exposed and inherently meant the materials capacity to withstand without detrimental change. Therefore, the acceleration factors has a wide range, as can be seen in figure 1.28. Due to the constantly changing rates of degradation in the outside environment, varying accelerating factors are also seen over time [10].

To expose the material to extreme condition in a short duration of time, laboratory test was seen as way to replicate the years of exposure in a short duration in the laboratory. To achieve this, acceleration factors were increased by intensifying the lab conditions. The anticipated result, however, had no correlation, in fact it was an unrealistic comparison between the two conditions [75][43][36][61]. Chong [20] and Knudsen et al [46] found an interesting relation between the correlation of accelerated tests with natural exposure and acceleration factor. They observed a decrease in correlation with an increase in the acceleration factor.

1.7.2. Correlation coefficient

The correlation of accelerated tests with field tests has been a challenging task [21]. To aid with it, correlation coefficients are used to indicate an uniformity of acceleration within a batch of samples [47]. The following equation can be used in calculating the correlation coefficient [20][38].

$$r = \frac{\sum(x_i - \bar{X})(y_i - \bar{y})}{\sqrt{\sum(x_i - \bar{x})^2 \sum(y_i - \bar{y})^2}} \tag{1.6}$$

In the above mentioned equation, r represents the correlation coefficient, x_i and y_i represent the single response values (eg.creep(mm)) from the two tests that are being correlated. The parameters $\bar{x}$ and $\bar{y}$ are the average response values (eg.creep(mm)) from the two tests being correlated. The correlation coefficient represents a linear relationship between the two tests that are being correlated [47]. In a case when r = 1 or r = -1, it indicates a strong linear relationship between the two correlated tests. On the other hand if r= 0, then it can be said that no linear relationship is present between the two correlated tests. Apart from this, there are a lot of variations that are present in calculating the linear correlation coefficient. This includes the weight factors and the overall performance indices like the sum of the individual ratings such as rusting, blistering, delamination and so on [33][91].

For the correlation coefficient, one other correlation coefficient is used known as the Spearman rank [19][82][33]. It does not use the linear relationship for analysis. The analysis is done on the ranks of the performance and not on the values of physical properties. The calculation of the spearman rank is done using equation [85].

$$r_s = 1 - \frac{6\sum d_i^2}{n(n^2 - 1)} \tag{1.7}$$

The parameter r_s represents the Spearman rank correlation coefficient, whereas the d_i and n indicate the difference in statistical rank of two corresponding systems and number of pair of values respectively. In the figure 1.29, an example for calculating the spearman coefficient is shown. It can be seen that data from both the outdoor exposure test and the accelerated test are translated into a performance rank.

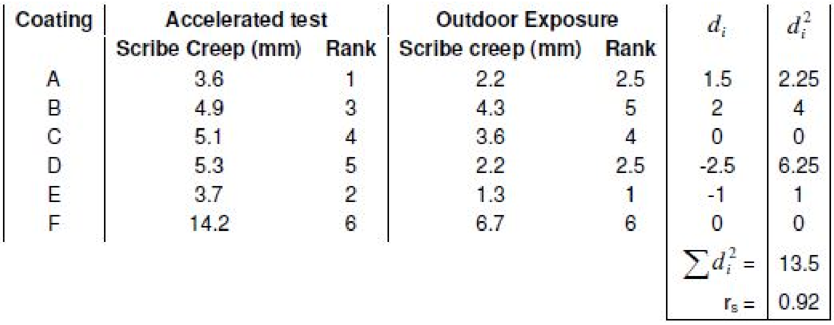

Coating	Accelerated test		Outdoor Exposure		d_i	d_i^2
	Scribe Creep (mm)	Rank	Scribe creep (mm)	Rank		
A	3.6	1	2.2	2.5	1.5	2.25
B	4.9	3	4.3	5	2	4
C	5.1	4	3.6	4	0	0
D	5.3	5	2.2	2.5	-2.5	6.25
E	3.7	2	1.3	1	-1	1
F	14.2	6	6.7	6	0	0
					$\sum d_i^2 =$	13.5
					$r_s =$	0.92

Figure 1.29: An example for calculating the spearman rank correlation coefficient between the outdoor and accelerated exposure.

The differences in d_i of the corresponding ranks are calculated and squared and the squared d_i is summed and used in the equation 1.7 to calculate r_s.

1.7.3. Case studies of previous correlation studies

The number of extensive long-term correlation studies in itself is a handful. There are some studies that worth mentioning. A program was introduced by SSPC/ASTM to analyse the procedure to test industrial maintenance coatings [14]. One of them is the study done by CSCT (Cleveland Society for Coatings Technology). CSCT [19] undertook a study to investigate some compliant coatings as opposed to some coatings containing ingredients that are either legally banned or might have some negative impacts on the environment. CSCT [5] conducted a common accelerated test, and compared the data from the accelerated test with 9 different field tests that the samples were exposed to. In figure 1.30 it can be seen that different standardized evaluation methods were made use of to get the averaged correlation of the test with that of the field test.

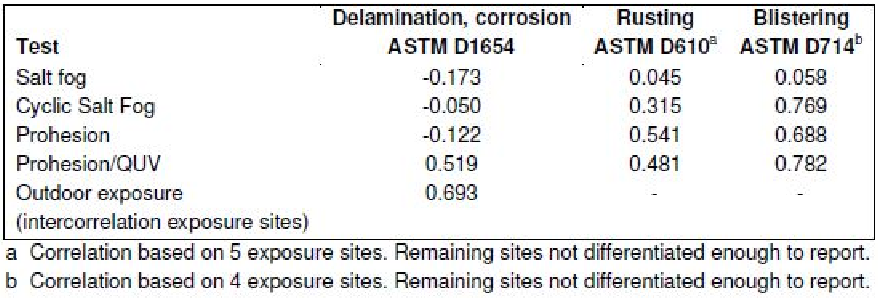

Test	Delamination, corrosion ASTM D1654	Rusting ASTM D610[a]	Blistering ASTM D714[b]
Salt fog	-0.173	0.045	0.058
Cyclic Salt Fog	-0.050	0.315	0.769
Prohesion	-0.122	0.541	0.688
Prohesion/QUV	0.519	0.481	0.782
Outdoor exposure (intercorrelation exposure sites)	0.693	-	-

a Correlation based on 5 exposure sites. Remaining sites not differentiated enough to report.

b Correlation based on 4 exposure sites. Remaining sites not differentiated enough to report.

Figure 1.30: Correlation with 9 different exposures [5]

As can be seen from figure 1.30, the highest correlation for rust creepage (ASTM D1654), when inter correlating 9 different exposure sites was found to be r_s=0.69. Among the accelerated tests, the prohesion/QUV had the highest correlation for rust creeepage, which was r_s=0.52 [5].

To access the performance of a coated panel, an artificial scribe was made as a relatively quick method to differentiate between high performance coating systems. Doing so, it would be easier to access the damage protection properties of the coating system but not its barrier properties [12][16]. Also, this is not the usual way in which a coating breakdown occurs, it is more of a gradual process and it so happens with general rusting, cracking, blistering and so on. In the study done by CSCT, the field exposure in the 9 different sites did not show much blistering and rusting. But in the acceleration tests, some of the results seen in figure 1.30 in ASTM D714 (blistering) and ASTM D610 (rusting) show a clear discrepancy between the accelerated test and the field exposure test and it was due to the unnatural conditions the samples were exposed to.

To find out which acceleration test could best replicate the actual corrosion performance in marine conditions, Knudsen et al [46], exposed a scribed test panel to an offshore field for a duration of 5 years. Similar specimens to the one placed in a offshore field were exposed to 4 different acceleration tests. The parameter used to assess the performance of the coating was the average and maximum scribe creep. The overall correlation factor (r) was used in this study and for the case of the average scribe creep for the cyclic salt spray test and the standard salt spray test the correlation factor r was 0.34. In the case of the Volvo test (Volvo corporate Standard 1027,1375 procedure 2A) the r values was 0.76. For the NORSOK test, the correlation was determined for two test series and it was 0.62 and 0.76 respectively. On the contrary to the previously mentioned study, in this study it was observed that some of the coatings had large scribe creep from the samples that was exposed to the field tests. But the same scenario was not be observed during any one of the 4 different accelerated tests. This is completely opposite to what was observed in the previous study done by CSCT. In their case, the scenario observed in the accelerated test was not observed in the field test and in the case study by Knudsen et al, none of the accelerated tests were able to predict the large scribe creep in the actual field test, which was exposed for a duration of 5 years.

One other study was done by TNO and ECCA (European Coil Coating Association) in 1999, to evaluate the reliability of the various acceleration tests and how they correlate with a sample that has undergone 10 years of field exposure. The whole study was done with 6 European sites, 9 laboratory tests and 49 different systems [91]. Correlation was done based on the use of weight factors and the amount of attack in mm^2 per m^2 or mm^2 per m along the scribes and the edges. The correlation coefficient exceeded 0.9 for certain permutations of tests,exposure sites, substrates and the coefficient variation is rather large. So the study done by ECCA and the TNO concluded that the none of the accelerated tests in the study were reliable enough to predict the durability in the medium and long-term in the case of the coil-coated materials. Hubrecht et al [39], had undertaken a similar test as the above mentioned and the test was conducted by 4 different laboratories. The observed scribe creep on many occasions was significantly different and hence it affected the performance rank of the system.

It is known that the most reliable method to analyse a coating is by exposing the coated substrate to the environment to which the application of the product will be exposed to. But doing so would require a huge amount of time,hence the accelerated test have become the go to test to evaluate the coating in a short duration of time [73]. There are various acceleration tests, but only a some of them have come close to reproduce the coating performance ranking as could be seen in the field tests. The cyclic test and the combined UV and cyclic salt fog test are some of the examples of the tests that are able to come close to reproducing the coating performance ranking as seen in the outdoor exposures. On the other hand the standard salt spray test cannot be used for estimating the performance ranking and also for predicting the service life of the coating systems.

A single testing method that suits all environments and all types of coatings is currently not enough to be a representative test method. This is due to the fact that certain coatings tend to perform better in one environment but the same coating is not able to replicate the same performance in an another environment. The difference in external environment causes the coating to perform differently in different environments.

2

Experimental Procedure

In order to analyse the performance of the coating, the following tests were planned.

- CQM (EIS) measurement at reference(before exposure), 1000 hours, 2000 hours and 3000 hours of accelerated exposure.
- CQM (EIS) measurement on ships coated with a vinylester glassflake coating and which were exposed to 10 years and 15 years of field exposure.
- Traditional EIS measurement prior to exposure and after 2000 hours of accelerated exposure.

2.1. Coating Thickness

The the glass flake vinyl ester coating coating was applied on grade A steel test panels. A total of 5 test panels were used, and a vinylester glassflake coating was coated onto the steel plate after Sa 2 1/2 grit blasting. The dimensions of the test panel are 200 x 120 x 3 mm, and the corners of the panel were rounded with r = 3mm. Two coats of the glass flake vinyl ester coating was applied on both sides of the panel, with each coat consisting of 500 μm thickness.

Prior to the test plates being exposed to an aggressive environment, data was collected which included the dry film thickness, pull-off adhesion strength and zero impedance measurements. The dry film thickness of the plates ranged from 978 μm - 1743 μm, and it was tested using a Defelsko positector F-6000. A total of 8 measurements were taken on each of the five test panels.

Test Panel	DFT avg (μm)	DFT min (μm)	DFT max (μm)	Std.dev (μm)
Panel 1	1390	1139	1628	142
Panel 2	1290	978	1652	187
Panel 3	1435	1153	1649	145
Panel 4	1353	1194	1414	64
Panel 5	1531	1336	1743	128

2.2. ISO 12944

ISO 12944 was first published in the year 1998 and has been the industry standard for prevention of corrosion in steel by the use of protective paint systems. Once the above mentioned test plates are placed inside the cabinets, they undergo a seven day cycle for a duration of 3000 hours. The seven day cycle can be categorised in three different sections. Three different sections are namely UV/condensation ISO 16474-3, salt spray ISO 9227 and low temperature of -20°. In the first 3/7 days, the plates are exposed to UV/condensation ISO 16474-3, followed by three days of salt spray ISO 9227 and finally on the last day of the seven day cycle, the test plates are exposed to a low temperature of -20° as can be seen in figure 2.1. One full week (168 hours) of exposure constitutes of 72 hours of exposure to UV and condensation. In these 72 hours of exposure,it alternates between four hours of exposure to UVA-340 lamps at (60 ±3)°C and four hours of exposure to condensation at (50 ±3)°C. After the first 72 hours, it is followed by another 72 hours of salt spray exposure and finally followed 24 hours of exposure to low temperature at (-20 ±2)°C. To reach this particular low temperature of (-20 ±2)°C , it takes the cabinet a duration of 30 minutes. The ISO 12944-9 cyclic ageing resistance test is generally done for a duration of 4200 hours, which is equivalent to 25 cycles of 168 hours (1 week) of exposure. Due to time constraints, this study is done for duration of 3000 hours, which is equivalent to 18 cycles.

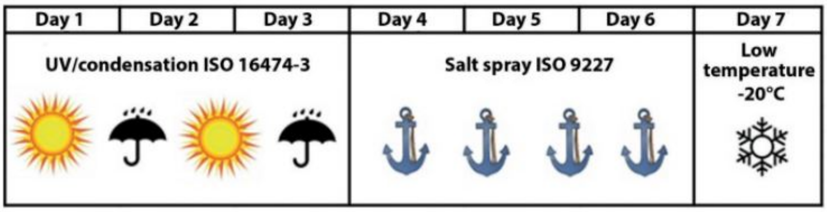

Figure 2.1: ISO 12944 7 day cycle

2.2.1. Preparation for ISO 12944-9

A total of 4 test plates were planned to be used for the purpose of accelerated cycling ageing resistance test. Prior to exposing the 4 test plates inside the ISO 12944-9 cabinet, the 4 test plates were conditioned using the conditioning pads from C-cube. The conditioning was done with the help of conditioning pads, 0.5 % NaCl and conditioning magnets. The conditioning pads are to be saturated with 0.5 % NaCl and it is to be placed on the backside of the conditioning magnet. For each test plate two conditioning magnets were placed on them. Before placing each magnet, the same procedure was followed as mentioned above. The conditioning magnets were placed around 5 cm from each other. For protective coatings, it is advised by C-cube to condition the test plate for a duration of a week. This conditioning was done to trap moisture in the area of the conditioning magnet. It is expected that the moisture trapped inside the magnet penetrates the coating during this time.

Since one out of the five test plates was used for a destructive adhesion pull-off test, the other four test plates were placed inside the cabinet for accelerated exposure after the initial CQM measurements were conducted. Prior to placing them in the cabinets, in addition to the CQM measurement, a scribe was made horizontally down to the bare metal at the lower end of the test plate as can be seen in figure ??. The specification of the scribe is 50 mm long and 2 mm wide. The purpose of the scribe made is to check for the occurrence of under-film creep. After the scribe was made on all four test plates, they were placed in the cabinet for the ISO 12944 test.

2.3. CQM - Coating Quality Measurement

ISO 16773-2

ISO 16773-2 focuses on providing guidelines to optimize the collection of EIS data on systems that have an impedance greater than 10^9 Ω cm^2. This does not exclude the measurement of systems with low impedance. The electrochemical cell is defined as follows : The most commonly used measurement cell is the two and three electrode setup in an aqueous solution. It is essential for the cell to be constructed from materials that do not deteriorate or corrode to prevent any contamination of the solution. The cell is designed keeping in mind the placement of the working electrode, reference electrode, counter electrode, thermometer, the gas inlet and outlet tubes inside electrolyte chamber. An example of the electrochemical cell can be seen in figure 2.2. In figure 2.2 the items are labelled as:

- 1 : Reference electrode
- 2 : Counter electrode
- 3 : Electrolyte
- 4 : O - ring
- 5 : Coating
- 6 : Working electrode

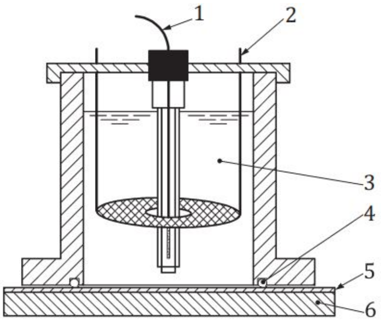

Figure 2.2: Example of an electrochemical cell in ISO 16773-2

2.3.1. Accelerated CQM Measurement

After a duration of 1 week, the CQM measurement was conducted using the following steps. To conduct the CQM measurement, the essentials include the CQM handheld device, sensor cable and a Faraday's cage, measurement liquid and extension cable. First with the use of the measurement liquid which is 0.5% NaCl, wet the two sensors by gently pouring some measurement liquid onto measuring side of the sensor.Then the sensor cables are connected to the CQM handheld. Now the conditioning magnets are removed and one test plate is placed inside the Faraday's cage along with the handheld CQM device. Once the conditioning magnets are removed, two wet spots will be visible in the exact area where the conditioning magnets are placed. The two wet sensors are to be placed in the exact location of the two wet spots. Once the sensors are placed onto the wet areas of the test plate, the CQM measurement can be started with a press of a button. The start time on the CQM handheld device is noted down at the start of each measurement to identify the measurement data on each test plate. Each measurement takes approximately a duration of 2 minutes. While the device is measuring it indicates by displaying 'SWEEP' on its screen. After a duration of 2 minutes, once the measurement is completed, it displays it by indicating a 'DONE' message. This procedure is followed for all the test plates and for each test plate the measurements were taken more than once. Each measurement data is stored in the device and can be seen only when the handheld device is connected to a computer after the measurement is conducted. Therefore, all the measurements were taken all at once and then the handheld device was connected to the computer. Once the handheld device is connected to a computer, it is run through a software developed by C-cube. This procedure was followed at various stages of the exposure time. The point of each measurement include the zero hour measurement (before exposure), 1000, 2000 and 3000 hours of exposure inside the cabinet of ISO 12944-9.

To measure the impedance of the coating after 1000 hours of exposure, the panels were taken out of the cabinet and were conditioned with conditioning pads on two different locations on the test plate for a duration of 48 hours. After the said period of 48 hours, the conditioning pads were removed and they were placed inside a Faraday cage to prevent any vibrations or background noise. To measure the impedance of the system, a CQM device was used. It consists of sensors, one works as the working electrode and the other sensor works as the reference and the counter electrode, completing the circuit. The two sensors were placed on the exact location the test plates were conditioned, after removing the conditioning pads. The measurement area for experiments done using CQM handheld device is 10 m^2. After which the CQM device starts to collect electrochemical measurements by the press of a button on the device. After pressing the button, the Faraday cage is closed to prevent any outside disturbances. Each of the 4 test plates exposed to the extreme conditions were tested at each point of measurement.

2.3.2. Field Measurement

Paivi - 15 years

For the field measurements, two different ships were selected based on the number of years it has been exposed to the external environment. The ships included in this study are namely Paivi and Botalo I. These two ships were coated with the glass flake vinyl ester coating for 15 and 10 years respectively.

The first ship chosen was a general cargo ship named Paivi - 15 years (Ice going vessel). The the glass flake vinyl ester coating coating was applied on the ship in the year 2007. The the glass flake vinyl ester coating coating was applied on this ship from just above the water line to the bottom of the ship. It is a ice going vessel and has been in operation for 15 years after the glass flake vinyl ester coating coating was applied on the vessel. Electrochemcial measurements were taken by using the CQM device on different parts of the ship where the glass flake vinyl ester coating was coated. The measurements were taken on the submerged parts of the ship as the ship was docked during the time of measurement. The same procedure was followed as with above mentioned test panels using the two sensors of the CQM device. Due to the limited time available with the ship, the conditioning done on the test panels prior to the CQM measurement were not possible for long duration of time. But it was still performed for a very short duration in comparison. Also, the ship was docked only two days prior to the test was conducted. Due to this reason, additional conditioning was not necessary for the ship being tested. The conditioning was done in several areas of the hull prior to measurement. After 30 minutes of conditioning, the CQM sensors were used to obtain EIS measurements. The same procedure was followed on various parts of the ship hull and this can be seen in figure 2.4. Obtaining EIS measurements on various areas of the ship makes for an exhaustive list of measurements. Which contributes to the mean impedance and mean phase angle of the coating after 15 years of field exposure.

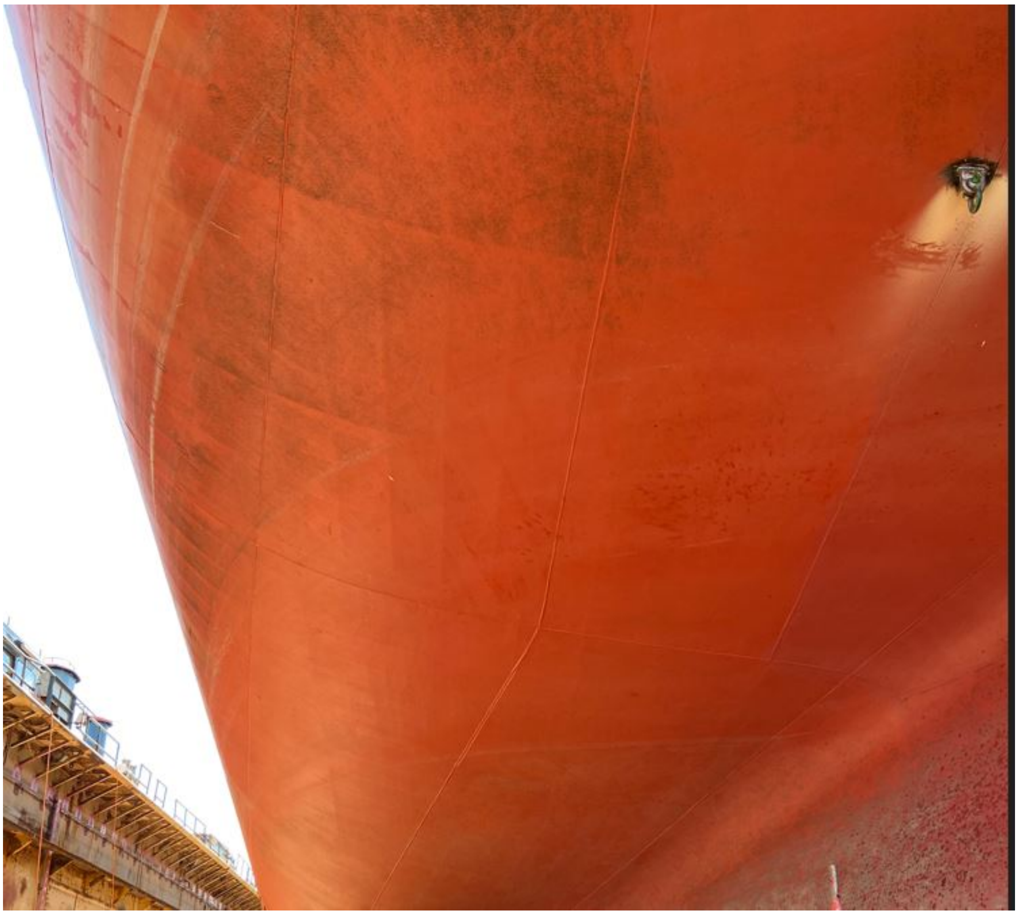

Figure 2.3: The glass flake vinyl ester coating 15 years after application on the Paivi

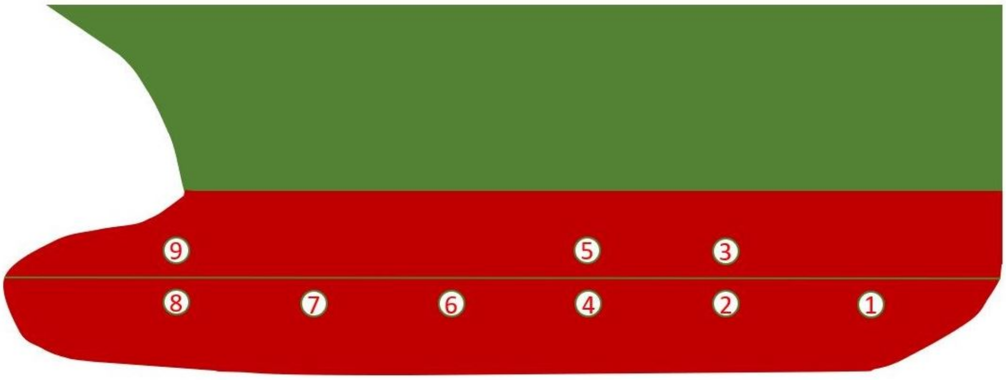

Figure 2.4: Schematic of measurement points on Paivi

Botalo I - 10 years

The second ship chosen was Botalo I 7 (10 years old), which was coated with the glass flake vinyl ester coating in 2012. For this ship, the measurements were done just above the waterline, as the ship was in water. To acquire accurate measurement of the coating system, there shouldn't be any moisture or liquid in between the two sensors. If so, the current passes through the water in between and the impedance of the coating is not measured. Due to which, it was not possible to do any measurements underwater. Therefore, the measurements needed to be done carefully by placing the sensors in places where there was no water in between them. By using the CQM device, measurements were taken on the water line in different parts of the ship as seen in figure ??. This was done so as to check if the impedance of the coating was same throughout the ship or did one part of the ship undergo more degradation than the other. Conditioning was not done for the measurements of this ship as all the measurements were done just above the water line which is more prone to contact with water. Therefore conditioning was not necessary for this measurement.

Figure 2.5: Schematic of measurement points on Botalo I

2.4. Traditional Electrochemical Impedance Spectroscopy

A three-electrode setup was used for this experiment to conduct an electrochemical experiment. The three-electrode setup consisted of the working electrode, the reference electrode and the counter electrode. To establish contact between the working electrode and the metal underneath the coating, the test panel used for the initial and after exposure pull-off adhesion test was used, which exposed the metal underneath. A copper tape was used to establish contact between the metal and the working electrode. The reference and the counter electrode were immersed in the electrolyte consisting of 3.5% NaCl solution. Ag/AgCl was the reference electrode, and platinum was used as the counter electrode. Each electrode was connected to a Biologic potentiostat to acquire electrochemical measurements. The three-electrode setup was done on panel no : 4 and panel no : 5. As mentioned earlier, one side of panel no : 4 was used for the destructive pull-off adhesion test. So the other side of the panel no : 4 was used as zero measurements for the three-electrode setup. The panel no : 5 was used to acquire electrochemical measurements at the 2000 hours checkpoint. A total of three setups were used, as can be seen in figures 2.6, 2.7 and 2.8. The setup in 2.6 depicts the traditional three-electrode setup. The setup in figure 2.7 uses the CQM device to conduct the experiment instead of the Biologic potentiostat. With the working electrode sensor in contact with the bare metal and the other cable acts as a reference and counter wire connecting to the CQM device. A platinum mesh is immersed in the 3.5% solution and is connected to the reference and counter cable. In figure 2.8, the EIS measurements are taken using the Biologic potentiostat. The working electrode has a connection similar to the traditional three-electrode setup. For the case of the reference and counter, the CQM sensor was used and connected to both the reference and counter electrode cables. This was done to establish the differences in the working mechanism between the CQM handheld device and the traditional three-electrode setup.

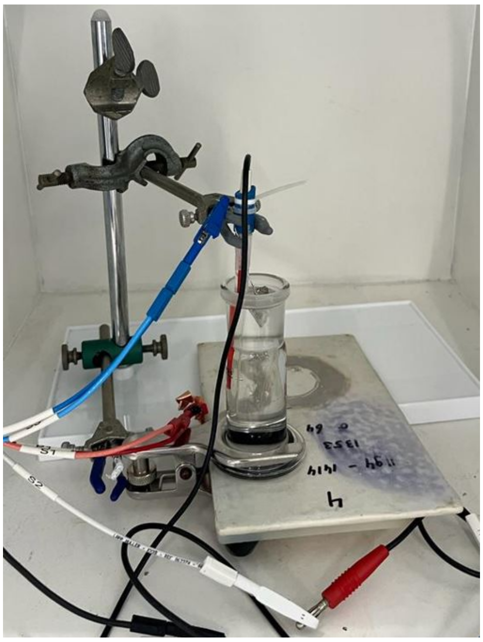

Figure 2.6: Traditional three electrode setup with red cable connected to the copper tape which is in contact with the bare metal, Ag/AgCl and platinum mesh as the reference and counter electrode connected to the white and blue cables respectively and immersed in 3.5% NaCl solution.

Figure 2.7: Performing EIS measurements using the CQM device. The working electrode sensor is in contact with the bare metal and the other cable with connections of the reference and the counter electrode is connected with the platinum mesh which is immersed in the 3.5% NaCl solution.

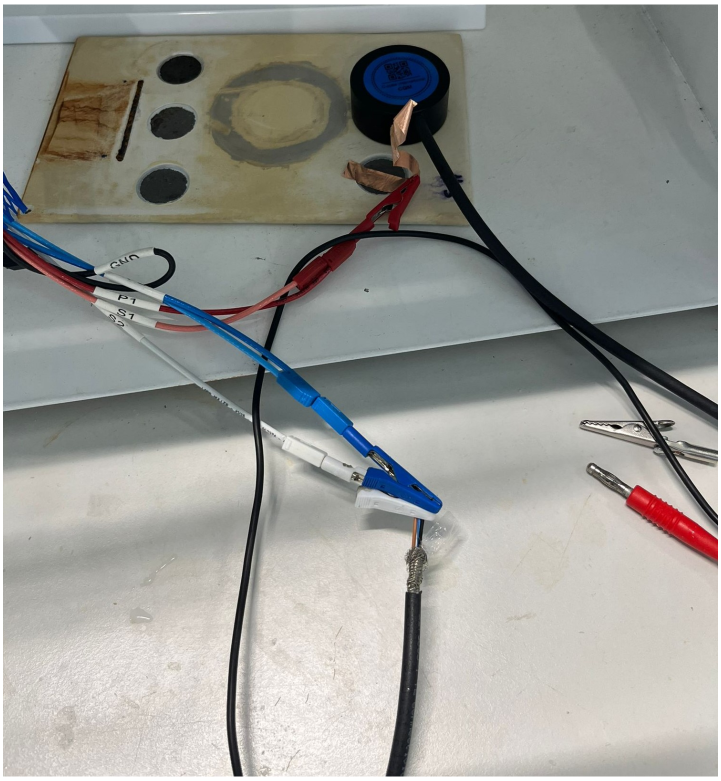

Figure 2.8: EIS measurements using biologic connections. The working electrode cable is connected with the copper tape which is in contact with the bare metal and the reference and counter electrode of the CQM sensor is connected to the reference and counter cables of biologic.

3

Results and Discussion

Results generated from experimental investigations are presented in this section. The experimental results include the pull-off adhesion test, undercreep observation, EIS measurements done using the handheld CQM device, EIS measurements using the three electrode setup and finally it includes the fitting of equivalent circuit parameters with the EIS results. EIS measurements using the CQM handheld device were obtained before exposure to ISO 12944-9 and after 1000, 2000 and 3000 hours of exposure to the test panels according to ISO12944-9. It also includes CQM EIS of an ice-going ship that was painted with the glass flake vinyl ester coating 15 years ago named Paivi and another ship that was coated with the glass flake vinyl ester coating 10 years ago named Botalo I. The environment in which the above mentioned test plates are exposed to are discussed above in the section ISO 12944. The aim of performing these experiments is to correlate the accelerated laboratory tests with the performance of in-service coatings on marine structures. This aids in understanding the effect of the accelerated tests on the coating tested and if it is able to replicate the results of the in-service performance of marine structures.

3.1. CQM - Coating Quality Measurement

3.1.1. CQM before exposure

EIS data is represented in terms of bode plots, which includes the impedance magnitude |Z| at each tested frequency. The impedance spectrum of the Bode plot can be seen in the figure 3.1. It indicates the mean impedance spectrum which is obtained by measuring the 5 different test panels. This is done prior to exposing them to accelerated environment of ISO 12944-9.

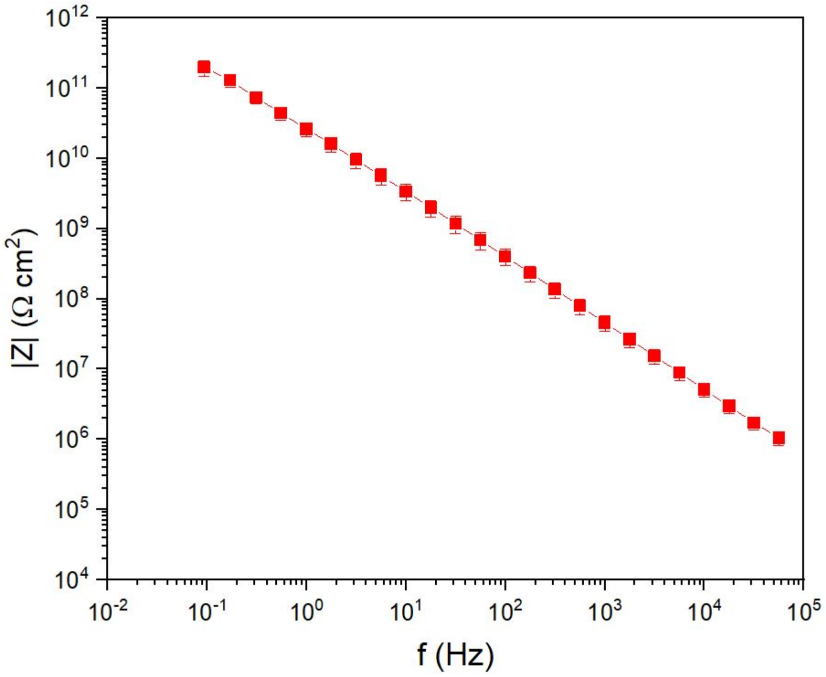

Figure 3.1: CQM : Mean impedance before any exposure

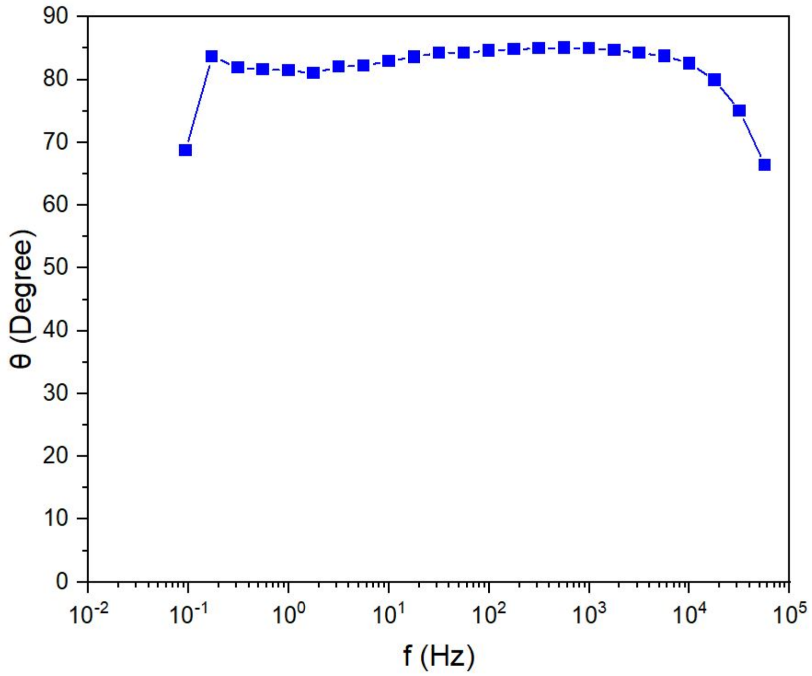

Figure 3.2: CQM : Phase angle before any exposure

The mean impedance |Z| for all the test panels is 1.97x10^{11} Ω cm^2 at 10^{-1} Hz. This is obtained after multiplying the surface area exposed with the impedance value obtained. To determine the deterioration of a coating, the magnitude of impedance at a low frequency of 10^{-1} Hz at different exposure time is used. Depending upon the magnitudes obtained at this frequency at consecutive exposure times, comparisons are made with the initial magnitudes of impedance to determine the performance of the coating. The phase angle measured at each frequency has been plotted below. In the case of before exposure, the phase angle is almost a horizontal line close to -90°. This indicates the coating is maintaining a purely capacitive behaviour. The impedance curve is a straight line and phase angles are close to -90° as can be seen in figure 3.2. This indicates the high barrier property of the coating [31].

3.1.2. CQM after 1000 hours of exposure

The magnitude of impedance after 1000 hours of exposure has decreased to 7.61x10 ^{10} Ω cm^2, as compared to the magnitude of impedance at 0 hours which is 1.97x10^{11} Ω cm^2 in the low frequency region of 10^{-1} Hz. The magnitude of impedance is higher than the minimum industry standard requirement of 10^7 Ω cm^2. Therefore, the coating provides good corrosion protection to the underlying substrate according the minimum industry standard.

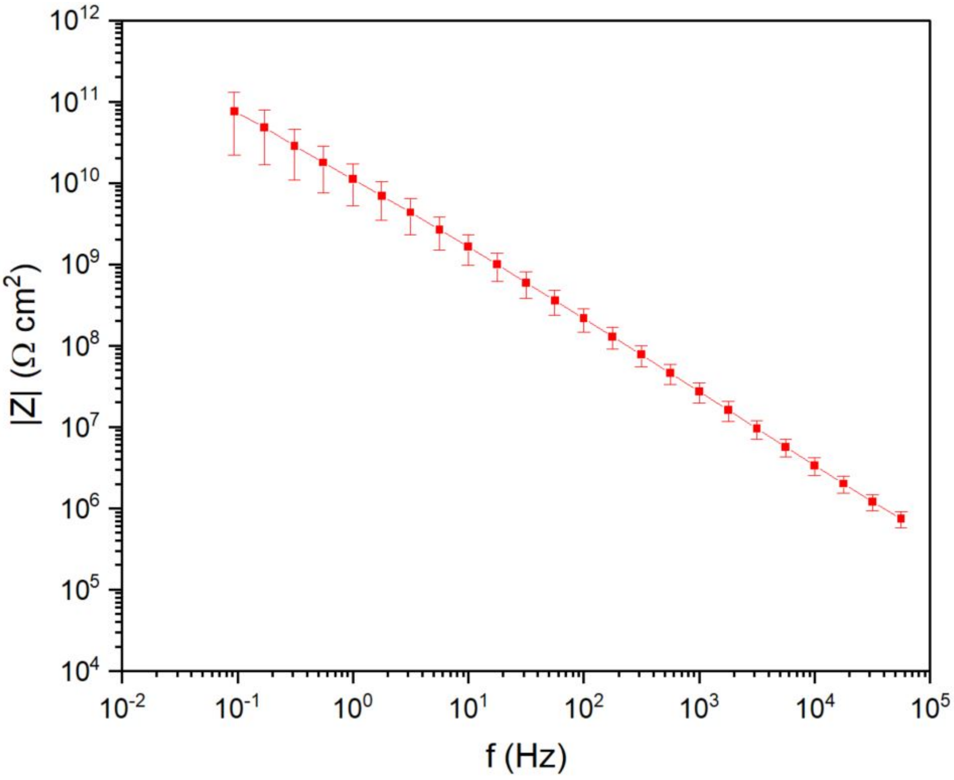

Figure 3.3: CQM : Mean impedance after 1000 hours of accelerated exposure

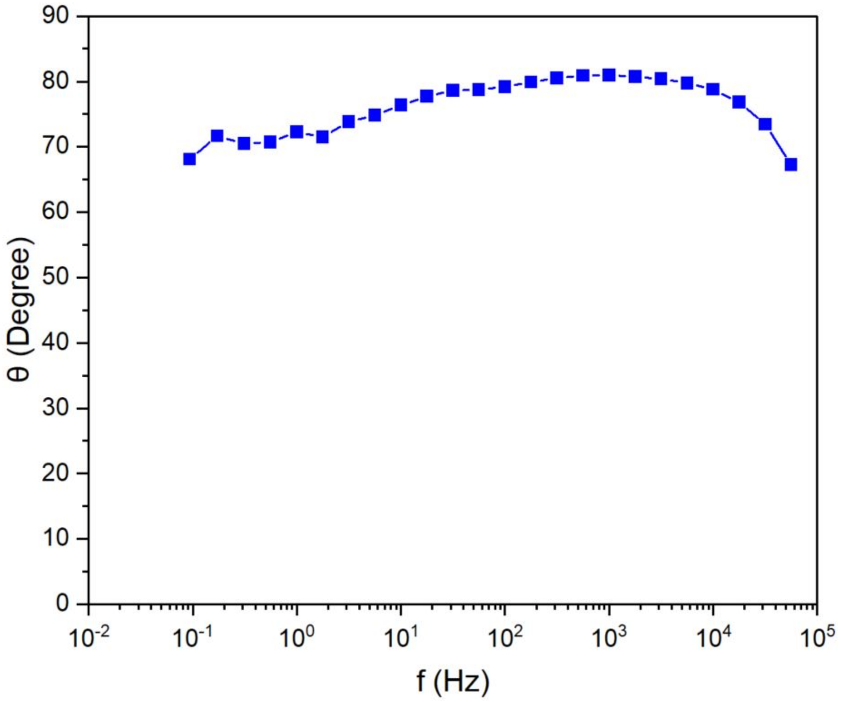

Figure 3.4: CQM : Phase angle after 1000 hours of accelerated exposure

3.1.3. CQM after 2000 hours of exposure

The magnitude of impedance after 2000 hours of exposure is equal to 3.88x10^{10} Ω cm^2 as compared to the magnitude of impedance at 0 hours which is 1.97x10^{11} Ω cm^2 in the low frequency region of 10^{-1}Hz. The magnitude of impedance is higher than the minimum industry standard requirement of 10^7 Ω cm^2.

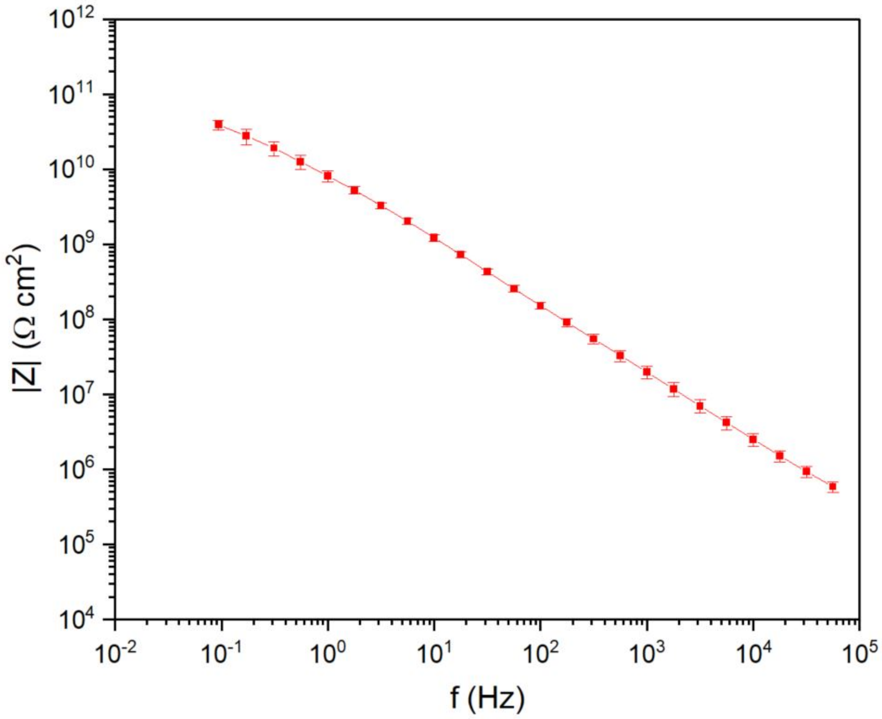

Figure 3.5: CQM : Mean impedance after 2000 hours of accelerated exposure

All the exposure times and their phase angles have been plotted in figure 3.16.

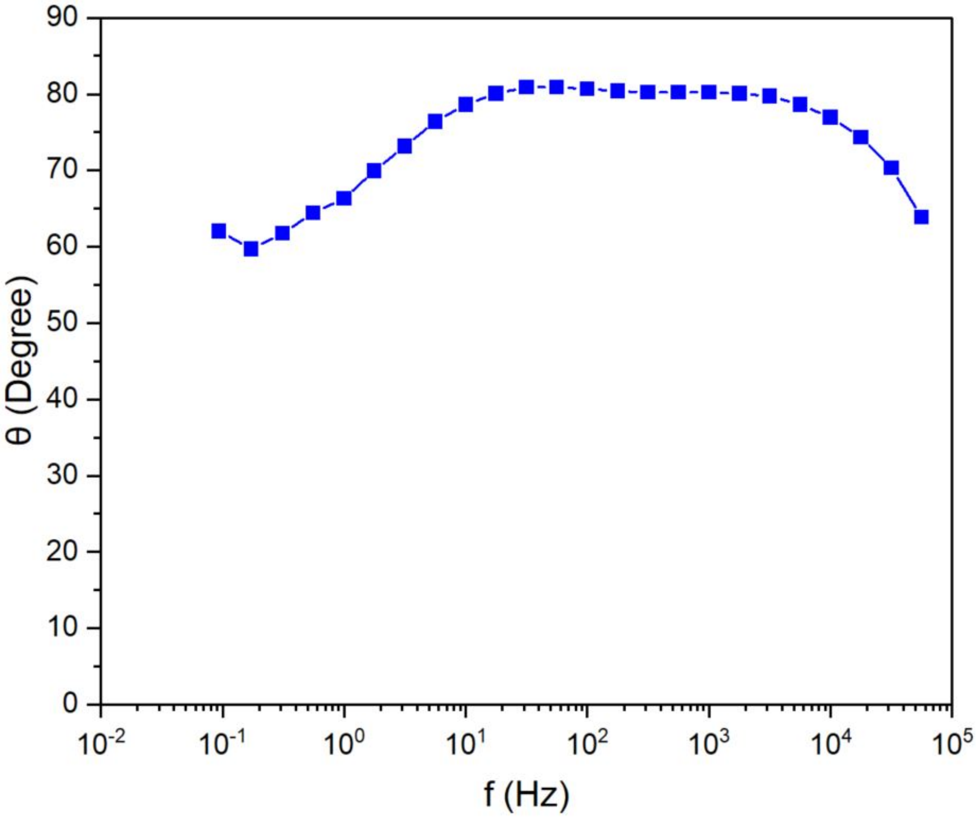

Figure 3.6: CQM : Phase angle after 2000 hours of accelerated exposure

3.1.4. CQM after 3000 hours of exposure

The EIS measurements were conducted again after 3000 hours of exposure. The magnitude of impedance at 10^{-1} Hz is 4.23x 10^{10} Ω cm^2 and at the same frequency the magnitude of impedance after 2000 hours of exposure is 3.88x10^{10} Ω cm^2. As can be seen in figure 3.7, the magnitude of impedance at the lowest frequency is marginally higher than the magnitude of impedance after 2000 hours of exposure. Seeing the marginal difference, it can be said that the coating has similar protective properties as seen in the 2000 hours of exposure. By looking at the impedance curve at 2000 hours and comparing it with 3000 hours, it can be said that there is no siginificant change in the performance of the coating, which means that the coating retains its barrier properties after 3000 hours of accelerated exposure.

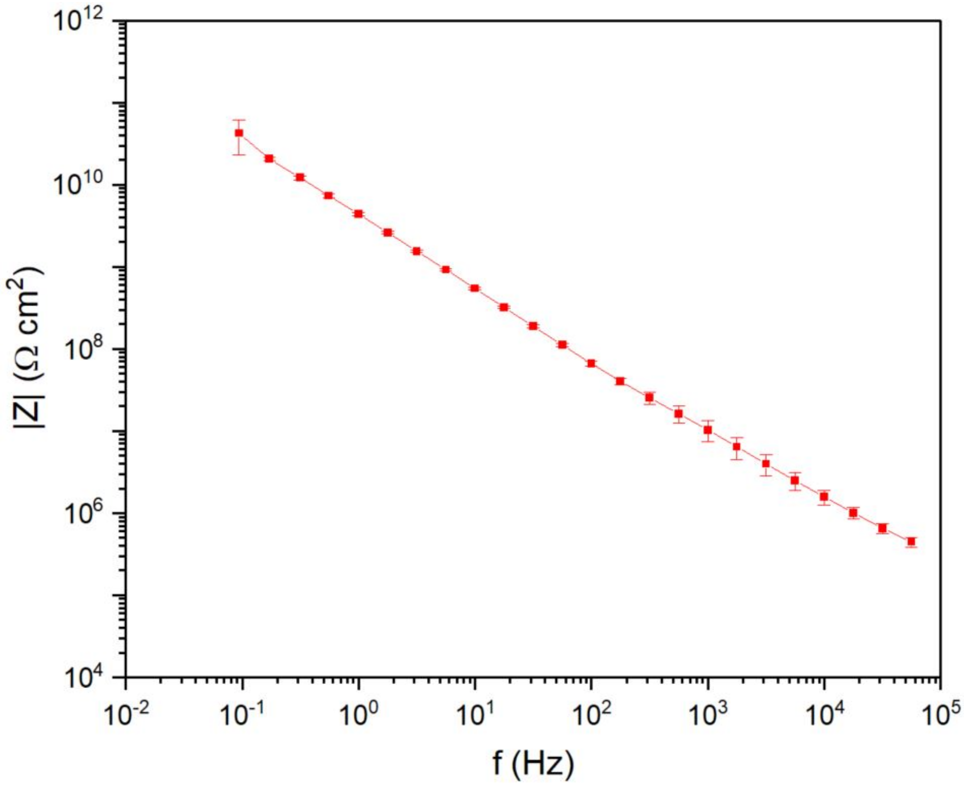

Figure 3.7: CQM : Mean impedance after 3000 hours of accelerated exposure

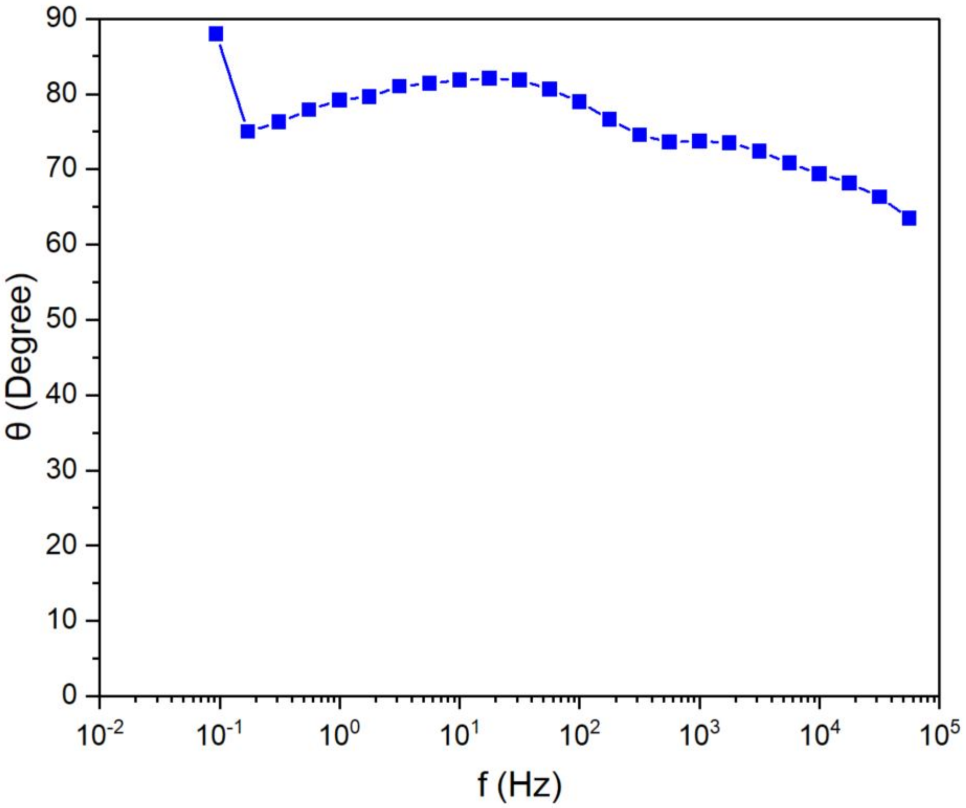

Figure 3.8: CQM : Phase angle after 3000 hours of accelerated exposure

As you can see from the phase angle comparison graph in figure 3.16, there is a decrease in phase angles with exposure time until 2000 hours of exposure. But for the case of 3000 hours, the phase angle are approaching -90° at the low frequencies and towards the high frequencies there is a downward trend [68]. This can be attributed to the material property of the coating, where the corrosion inhibitors present in the coating are blocking the pathways. This can be interpreted that the phase angles are increasing with exposure time in the low frequency region. This can indicate the coating is still in good condition as the phase angles are increasing in the low frequency range and decreasing in the high frequency range.

In figure 3.9, the impedance curves with increase in exposure time can be seen. All these test samples were exposed to the accelerated cyclic ageing resistance test according to ISO 12944-9. Even after 3000 hours of exposure, the impedance value at the lowest frequency still remains at a very high value of 4.23x10^{10} Ω cm^2.

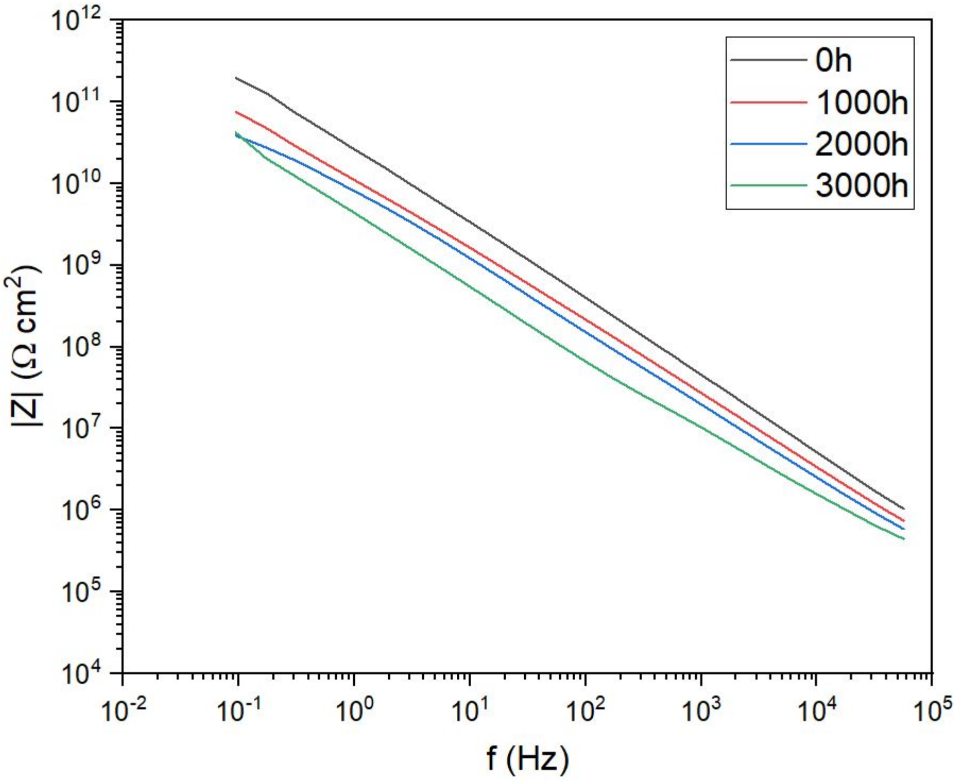

Figure 3.9: Impedance 0 vs 1000 vs 2000 vs 3000 hours of accelerated exposure in ISO 12944-9

Figure 3.10, represents the impedance at each frequency for the accelerated exposure. It has four data points, each represent the before exposure, 1000 hours, 2000 hours and 3000 hours respectively. Each curve in figure 3.10 represents each frequency.

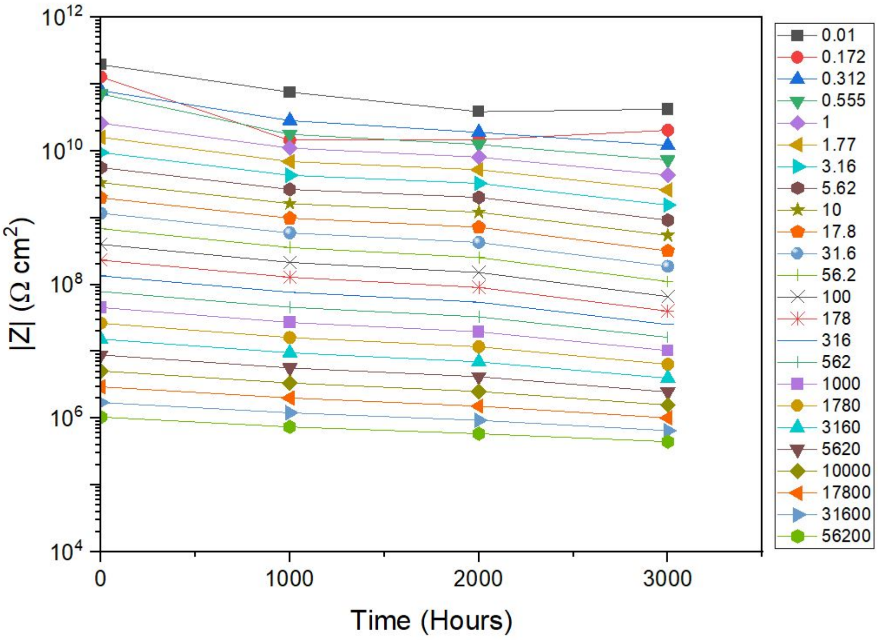

Figure 3.10: Magnitude of impedance is plotted at each measured frequency with increase in exposure time.

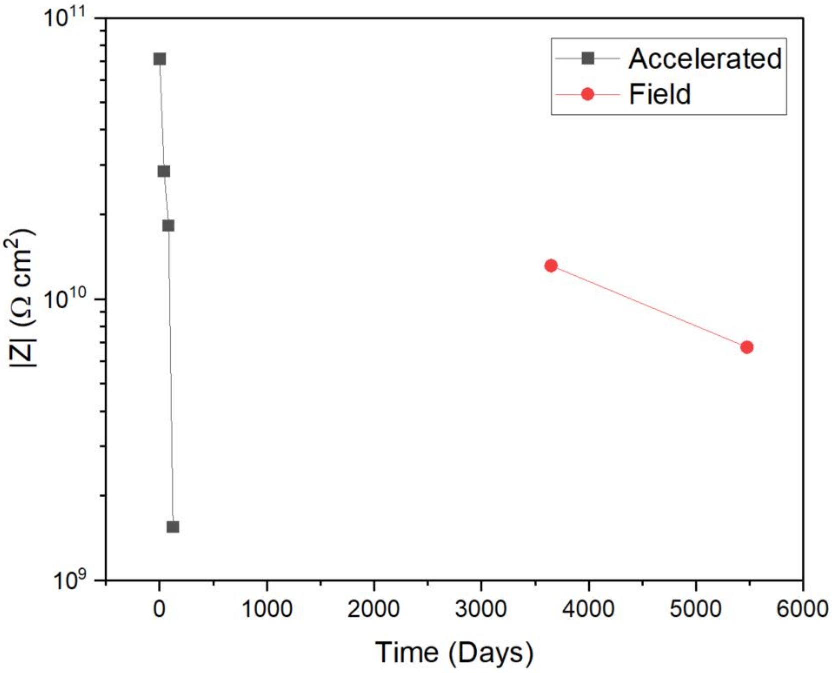

Figure 3.11: Real Impedance at 0.01 Hz for both the accelerated and field exposure as a function of exposure time

Impedance data points in each of the frequency curves has a decreasing trend with increase in exposure time as can be seen in the phase angle comparison as well in figure 3.16. According to Mansfeld et al [64], the real part of impedance undergoes a decreasing trend with increase in exposure time. This can be seen in the case of the glass flake vinyl ester coating as well in the case of the accelerated and field tests in figure 3.11. This can be correlated to the reduction in impedance curves in figure 3.9 and can be attributed to the increase in coating capacitance with increase in exposure time. As can be seen in figure 3.11, the real impedance of 10 years and 15 years is very much comparable to the 1000 and 2000 hours of accelerated exposure respectively.

3.1.5. CQM 10 years Botalo I Ship

A total of 8 measurements were taken at different parts of the Botalo I ship. As The magnitude of impedance bode plot is plotted as mean of the 8 different measurements. As the measurements were taken without the use of a Faraday cage in an outdoor environment, this gives rise to some scatter in the measurements. The magnitude of impedance at 10^{-1} Hz is 1.52x10^{10} Ω cm^2.

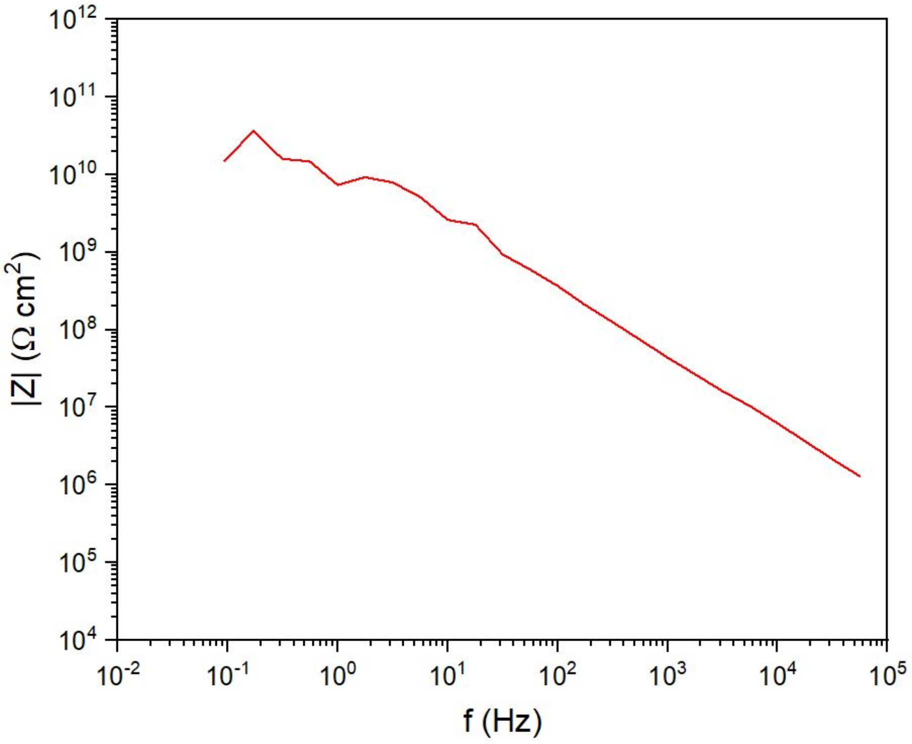

Figure 3.12: CQM : Impedance after 10 years (Botalo I) of natural exposure

3.1.6. CQM 15 years - Paivi

A total of 29 measurements were taken at different parts of the Paivi ship hull. The impedance magnitude of the bode plot is plotted as mean of the 18 different measurements only. It was informed that certain parts of the ship had been re-coated with another coating due to certain mechanical damages the ship had undergone. To eliminate measurements of another coating, only 18 out of 29 measurements were taken into consideration. As the measurements were taken without the use of a Faraday cage in an outdoor environment, this gave rise to some scatter in the measurements. The magnitude of impedance at 10^{-1} Hz is 4.27x 10^9 Ω cm^2.

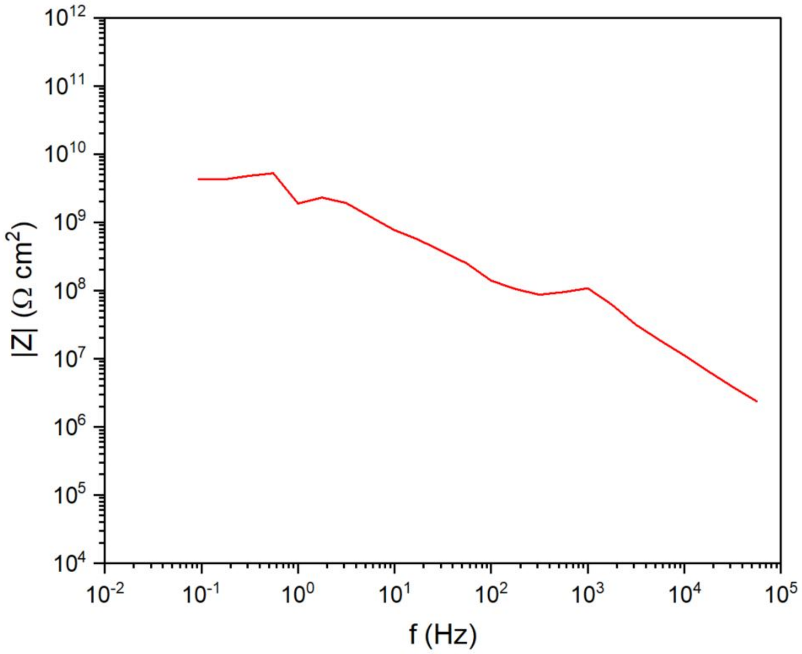

Figure 3.13: CQM : Impedance after 15 years (Paivi) of natural exposure

3.2. Comparison between accelerated and field test

3.2.1. CQM 1000 hours vs 10 years

The impedance curve of 1000 hours of accelerated exposure and 10 years of real time exposure has been plotted in the same graph in figure 3.14. It can be seen from the graph that the 10 years impedance curve matches with 1000 hours of exposure. From this comparison graph it can interpreted that the degradation that the glass flake vinyl ester coating undergoes in 10 years can be replicated with 1000 hours of accelerated exposure.

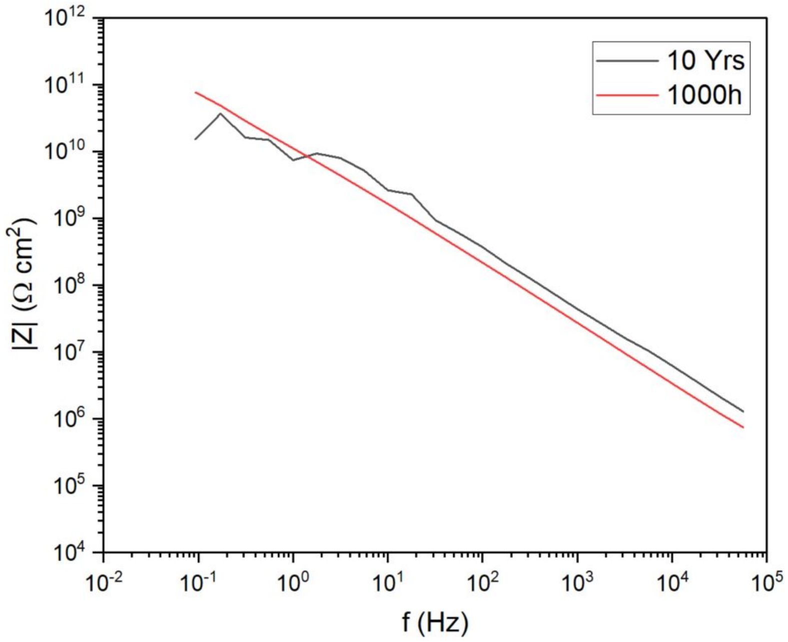

Figure 3.14: CQM : 10 years vs 1000 hours - Impedance comparison

3.2.2. CQM 3000 hours vs 2000 hours vs 15 years

The impedance curve of 2000 hours and 3000 hours of accelerated exposure and 10 years of real time exposure has been plotted in the same graph in figure 3.15. It was an attempt to check if the 15 year impedance curve matches with the impedance curve of accelerated 2000 hours measurement. The magnitude of impedance at 10^{-1} Hz of 15 years of outdoor exposure and the 2000 hours of accelerated exposure were not as close as the case of 1000 hours and 10 years. In an attempt to see how many hours of accelerated exposure is equivalent to 15 years of outdoor exposure, another set of measurements was taken at 3000 hours of accelerated exposure as well. It was expected that the degradation in the 3000 hours exposure would be similar but the 3000 hours of exposure had very little degradation. In fact the magnitude of impedance at the lowest frequency measured after 3000 hours of exposure was very close to the 2000 hours of exposure than the impedance curve of 15 years of exposure as can be seen in figure 3.15. It can be inferred from figure 3.15 that it is still not clear as to how many hours of exposure is still required in the accelerated cabin to have a similar degradation in terms of impedance in comparison to the 15 years of exposure.

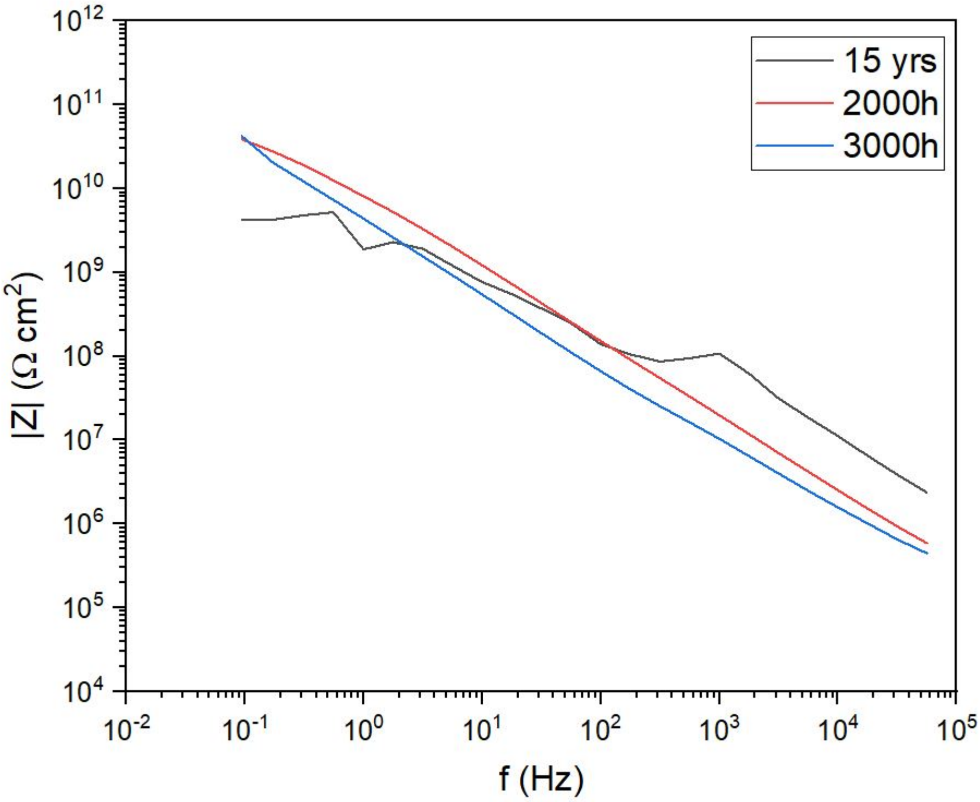

Figure 3.15: CQM : 15years vs 2000 hours vs 3000 hours - Impedance comparison

$$\phi = \omega C_c R_c [102] \tag{3.1}$$

In equation 3.1, it indicates that the measured phase angle is dependant on the applied current frequency, coating resistance and capacitance. In the early stages of a coating before any exposure, the resistance of coating (R$_c$) has a very high value in comparison to the coating capacitance (C$_c$). Due to which in EIS measurements most of the current passes through the capacitance. This leads to the phase angle of a metal coating system to be close to 90°

in the middle to high frequency range as can be seen in figure 3.2. As the coating undergoes deterioration, the electrolyte penetrates through the coating. This is a consequence of reduction in coating resistance and increase in coating capacitance. This further leads to increase in current flow through the resistance and the reduction in phase angle at a given current frequency.

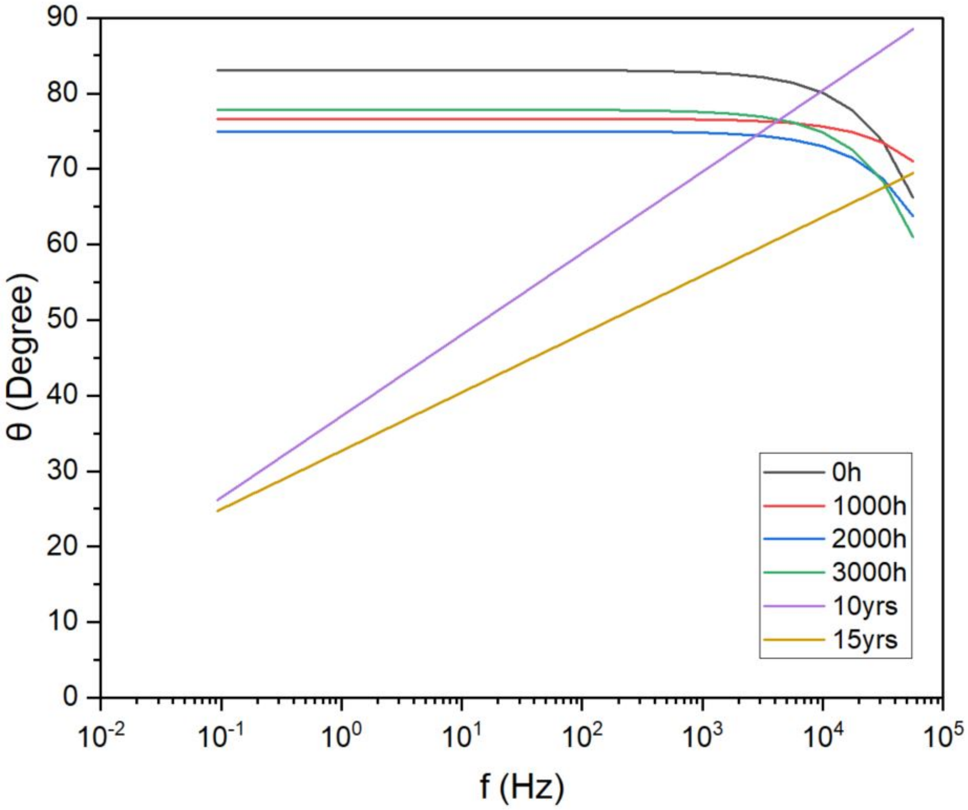

Figure 3.16: Phase angle comparison between different exposure conditions with increase in exposure time. The top four phase angle curves represent the accelerated exposure and the bottom two curves represent the natural exposure.

When the penetration of the electrolyte reaches a saturation point, it stabilizes the coating capacitance while decreasing the coating resistance. When such a situation is implemented in equation 3.1, there is a reduction of phase angle with increase in detoriation of the coating. It can seen from figure 3.16 that there is a steady decrease in the phase angle with exposure time. Before exposure the phase angles were close to 80°. According to [102], phase angle at 10 Hz is used for evaluating the performance of the coating. As can be seen in figure 3.16, there is a steady decrease in phase angle at 10 Hz with increase in exposure time. According to [102], if phase angle at 10 Hz is close to or below 40°, it indicates the initiation of corrosion. This scenario can be seen in figure 3.16 as well for the phase angles of the 15 years old ship. No visible corrosion was seen during testing of the ship. This can be interpreted in two ways. Firstly it is a good indication to perform more periodic checks on the ship to prevent any adverse effects. Secondly, the phase angle graph is a mean curve from multiple measurements. Therefore, it is a possibility that individual phase angle measurements is not be close to 40° at 10Hz. But it is important to note the steady decrease in phase angle with increase in exposure time at 10 Hz.

3.3. Traditional Electrochemical Impedance Spectroscopy (EIS)

3.3.1. Traditional EIS before exposure

The bode plot of the traditional EIS measurement can be seen in figure 3.17. The magnitude of impedance at 10^{-1} Hz is 7.21x10^{10} Ω cm^2. It can seen that the magnitude of impedance at low frequency of 10^{-1} Hz is lower compared to the CQM device. This is due to the way in which the measurements are taken using these two instruments. In traditional EIS, a three electrode setup is used with the working electrode connected using a copper tape to the bare metal of the test sample. The reference electrode used is the Ag/AgCl and the counter electrode is the platinum mesh electrode.The impedance plot in figure 3.17 has a lot of scatter and the profile is not as smooth as in the case of CQM, especially in the low frequency region.

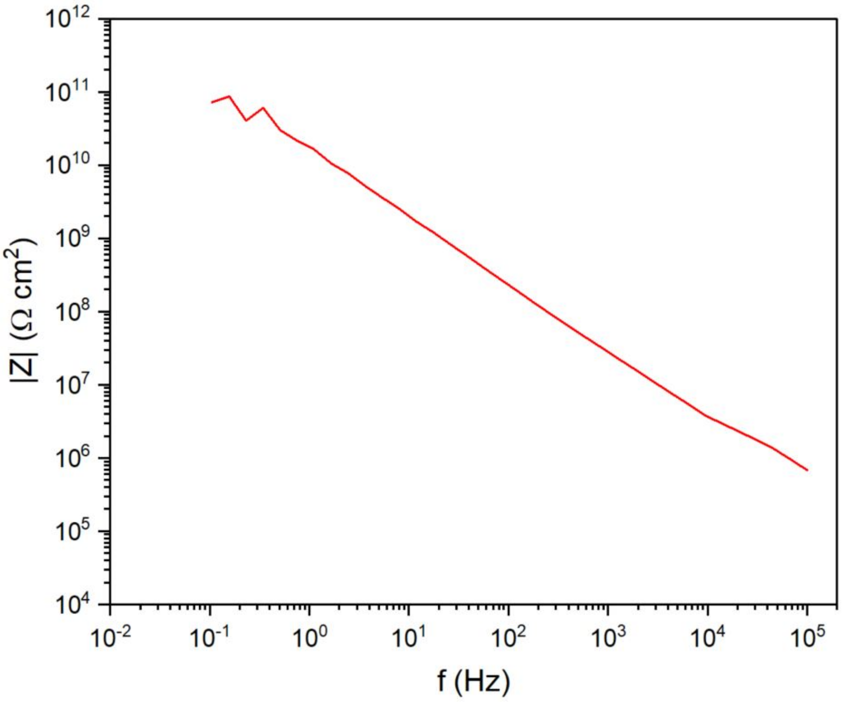

Figure 3.17: Traditional EIS : Before exposure

3.3.2. Traditional EIS after 2000 hours of exposure

The traditional EIS measurement was also done after 2000 hours of accelerated exposure. This was done using three different setups, which includes the classical three electrode setup and the other two setups can be explained with the images in figure 2.7 and figure 2.8. In figure 3.18, the impedance curve can be seen which is obtained from the three electrode setup. The impedance curve in figure 3.19 is obtained using the setup in figure 2.7. Even though both these measurements were taken after 2000 hours of measurements, there is a difference of one decade between the two results. In figure 3.20, the result obtained from traditional EIS setup before exposure is compared with the result obtained from the setup in figure 2.7 after 2000 hours of exposure. This was done to indicate the clear difference between the before and after exposure of the test panel. But when the results obtained from traditional EIS before exposure is compared with after exposure, it was quite surprising to observe the similarity in impedance as can be seen in figure 3.21.

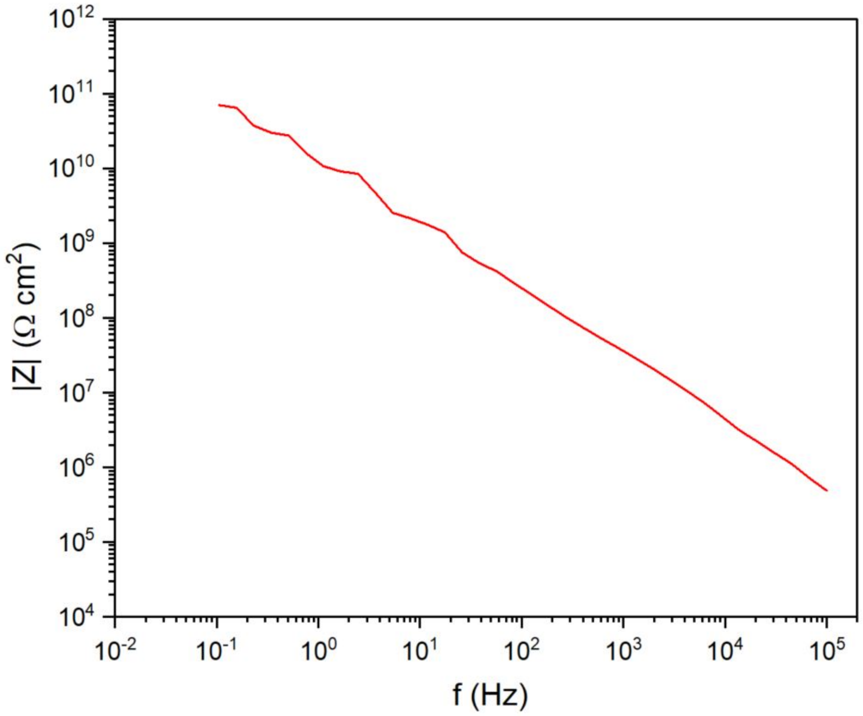

Figure 3.18: Traditional EIS : After 2000 hours of accelerated exposure

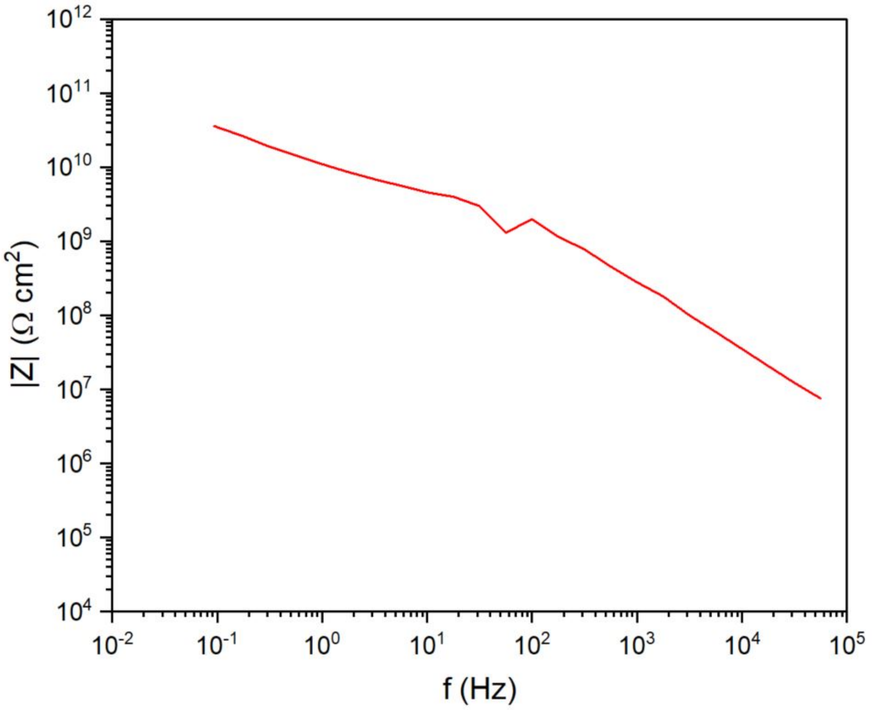

Figure 3.19: Traditional EIS : After 2000 hours of accelerated exposure(CQM - Glass tube setup)

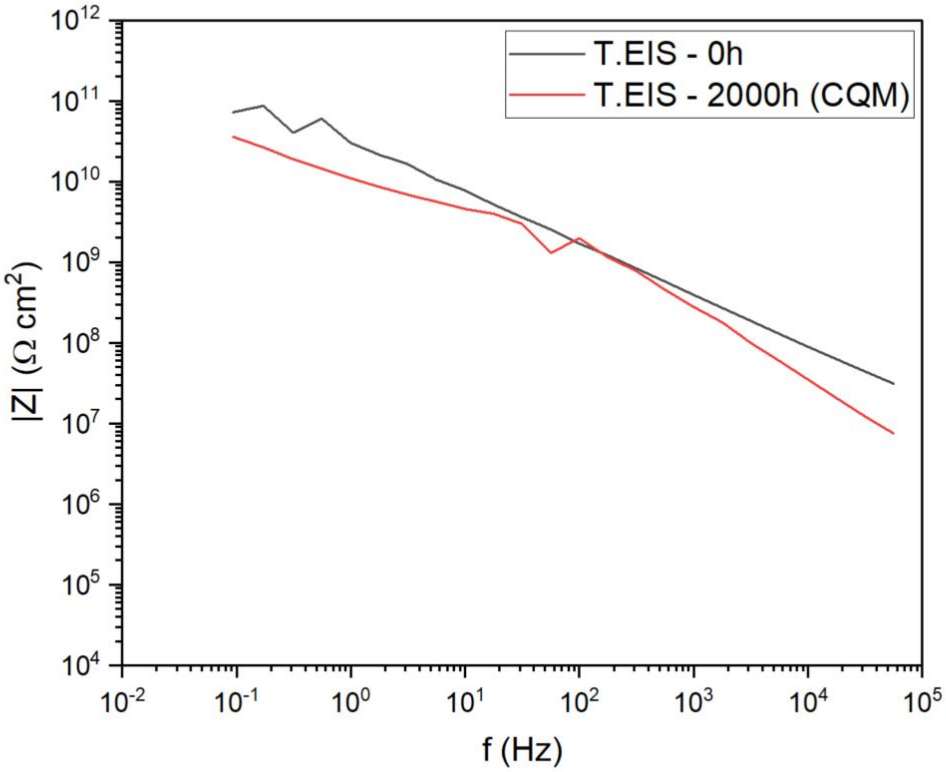

Figure 3.20: Traditional EIS : Comparing before and after exposure for 2000 hours(EIS and CQM (Glass tube setup)

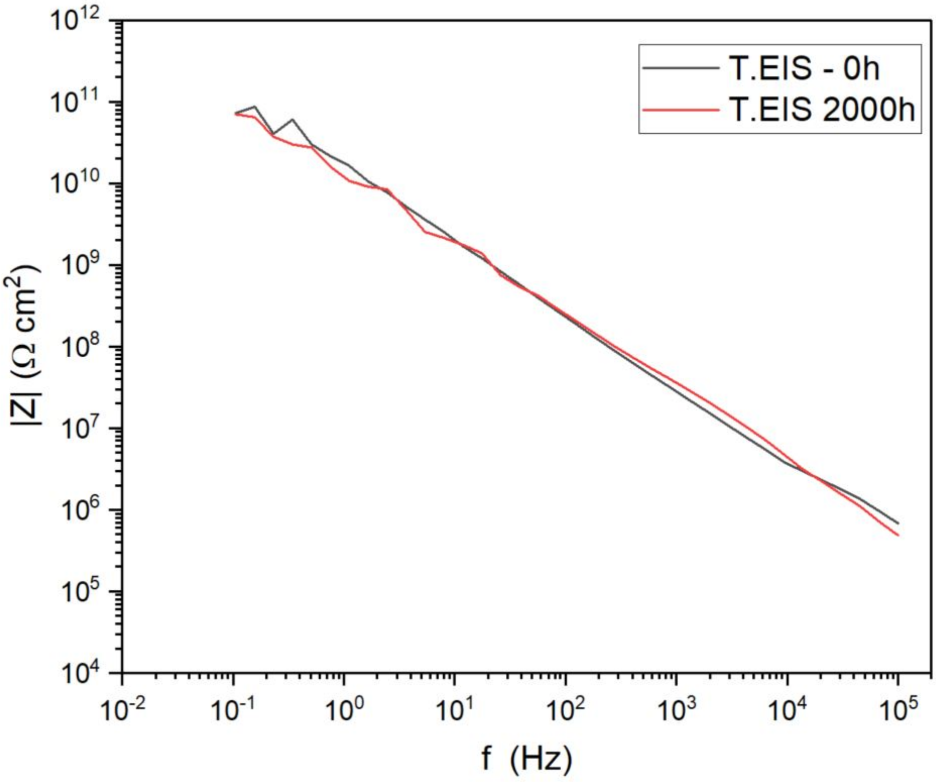

Figure 3.21: Traditional EIS:Comparing before and after exposure for 2000 hours

3.4. Equivalent circuit(EC)

The equivalent electrical circuit used in our case is the simple randles circuit and a modified randles circuit for samples that have undergone varied exposure. The two types of circuit used in this study can be seen below. The EIS data obtained has been fitted into equivalent circuits using Zview4 software.

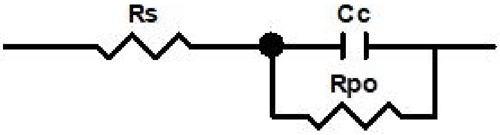

Figure 3.22: Simple Randles circuit

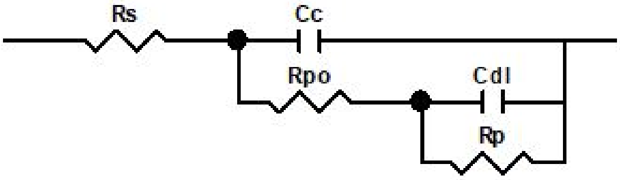

Figure 3.23: Modified randles circuit [98] [58] [22]

In the above equivalent electrical circuits, R$_s$ represents the uncompensated resistance between the working electrode and the reference electrode. C$_c$ is the capacitance of the coating being tested and it is dependent on the dielectric constant of the polymer, dielectric constant of free space which is equal to 8.85x10^{-14} F/cm , A is the exposed area and d is the thickness of the coating as can be seen in the equation below.[22]

$$C_c = \varepsilon\varepsilon_0 A/d[62] \tag{3.2}$$

3.4.1. EC before exposure

The equivalent electrical circuit for the coating system is illustrated below. The equivalent circuit chosen for the coating before exposure is a simple randles circuit. This choice was made based on literature, and the high impedance values in EIS measurements. As the system did not undergo any changes, the simple parallel circuit (randles circuit) is an ideal circuit to model the behaviour of the coating system. In the equivalent circuit, the R_s represents the solution resistance,C_c [58]and R_{po}, which are the coating capacitance and the pore resistance of the coating. The values of the parameters in the equivalent circuit can be seen below.

Table 3.1: Equivalent circuit parameter values of before exposure

Element	Value	Error %
R_s	88401	3.22%
C_c	2.03E-11	7.4123
R_{po}	7.01E+10	58.952

3.4.2. EC 1000 hours

The equivalent circuit chosen after the coating has been exposed to 1000 hours of exposure is a modified equivalent circuit. As the coating is been exposed to ISO 12944-9, the magnitude of impedance at 10^{-1} Hz reduces, thereby indicating the deteriorating nature of the coating.The value of the impedance did reduce, but not to a significant extent. This lead to the introduction of new elements in the equivalent circuit that could account for the electrochemical reactions taking place. This modified equivalent circuit consists of some new elements compared to the simple parallel randles circuit. This includes capacitance of the electrical double layer C_{dl}[58], polarisation resistance R_p and pore resistance represented by R_{po}. Their values can be seen in the table below.

Table 3.2: Equivalent circuit parameter values for 1000 hours of exposure

Element	Value	Error %
R_s	6.28E+04	33.378%
C_c	2.71E-11	8.3354
R_{po}	2.04E+08	40.224
C_{dl}	3.81E-11	19.7
R_p	1.43E+10	35.409

3.4.3. EC 2000 hours

The modified randles circuit has been used for the test sample exposed for 2000 hours of accelerated exposure. As compared to the test sample before exposure, there is noticeable reduction in the the magnitude of impedance after 1000 hours and 2000 hours of exposure. This is due to electrochemcial reactions taking place, which calls for the inclusion of additional elements to the simple randles circuit. The additional elements included to the simple randles circuit can be seen in the modified randles circuit in figure3.23. The representative values of the fit with the equivalent circuit can be seen in the table 3.3.

Table 3.3: Equivalent circuit parameter values for 2000 hours of exposure

Element	Value	Error %
R_s	54950	31.945%
C_c	3.51E-11	9.7664
R_{po}	4.28E+07	48.836
C_{dl}	3.99E-11	20.549
R_p	6.64E+09	24.321

3.4.4. EC 3000 hours

The modified randles circuit in figure 3.23 was used for the 3000 hours equivalent circuit as well.By using the modified randles circuit, the reduction in the various parameters can be seen as compared to the lower exposure times in figure 3.4. The individual comparisons of these parameters can be further sections of this chapter.

Table 3.4: Equivalent circuit parameter values for 3000 hours of exposure

Element	Value	Error %
R_s	42578	31.246%
C_c	4.95E-11	12.217
R_{po}	4.19E+06	33.836
C_{dl}	1.02E-10	14.139
R_p	8.35E+09	47.998

3.4.5. EC 10 years

The modified equivalent circuit was used for the EIS measurements obtained from the 10 years old ship. This was done to take into consideration the magnitude of impedance at low frequency and how they compared to the 1000 hours of the accelerated exposure. In the earlier section it was seen that the 1000 hours of accelerated exposure and the 10 years of field exposure were comparable with the impedance curves in the bode plot. As the modified randles circuit was used for fitting the data from 1000 hours of accelerated exposure, the same circuit was used for 10 years of field exposure as well. The parameters of the electrical equivalent circuit can be seen in table3.5

Table 3.5: Equivalent circuit parameter values for 10years of field exposure

Element	Value	Error %
R_s	1.06E+05	37.397%
C_c	1.35E-11	10.215
R_{po}	3.94E+07	52.023
C_{dl}	1.28E-11	23.79
R_p	2.62E+09	12.507

3.4.6. EC 15 years

In the earlier section, the impedance curve of 15 years of field exposure was compared with 2000 hours of accelerated impedance data. The impedance curves were very close to each other. Also, the magnitude of impedance obtained from the EIS measurements in this ship is lowest in comparison to the other cases in this study. Even they are low compared to the rest, the magnitude of impedance obtained at low frequency still does qualify as a good coating even after 15 years of exposure. Keeping in mind the above mentioned factors, the equivalent circuit chosen was the modified randles circuit. The parameters of the electrical equivalent circuit can be seen in table3.6

Table 3.6: Equivalent circuit parameter values for 15 years of field exposure

Element	Value	Error %
R_s	1.60E+05	39.36%
C_c	1.74E-11	15.278
R_{po}	6.47E+07	34.9
C_{dl}	6.70E-11	27.952
R_p	1.20E+09	21.388

3.5. Time dependence of Equivalent circuit Parameters

3.5.1. Coating Capacitance

As can be seen in figure 3.24, there is a sudden increase in the coating capacitance from 0 hours of exposure to 1000 hours and 2000 hours of exposure. The 1st data point in figure 3.25, refers to the coating capacitance on the 10 years of field exposure and the 2nd data point refers to the 15 years of field exposure ship. This type of behaviour is very much comparable to other coated metals from literature as can be seen in figure 3.26 [63]. The coating capacitance values are also lower compared to the 5 different marine coatings. This indicates that the glass flake vinyl ester coating is entirely resistant in comparison to other 5 coatings due to the presence of glass flakes.

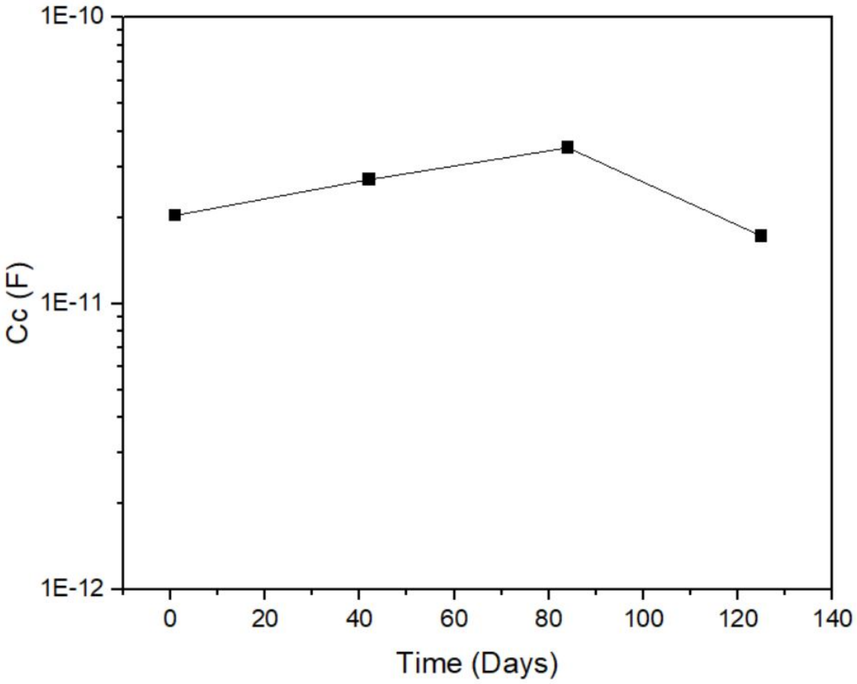

Figure 3.24: Coating Capacitance of the glass flake vinyl ester coating in accelerated exposure

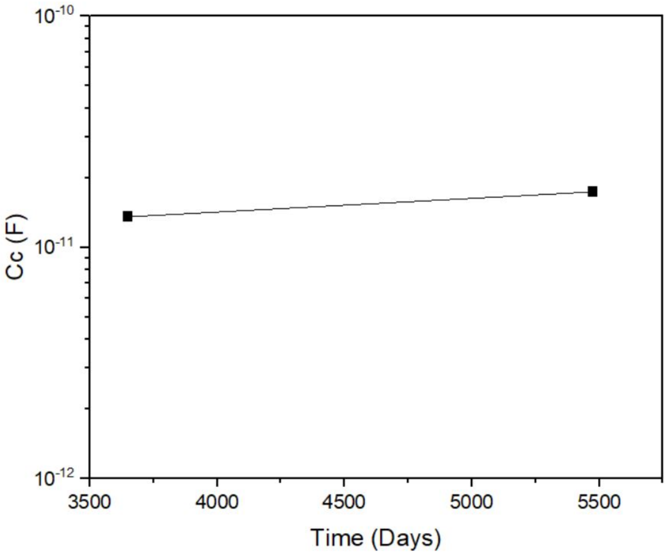

Figure 3.25: Coating capacitance of the glass flake vinyl ester coating in field exposure

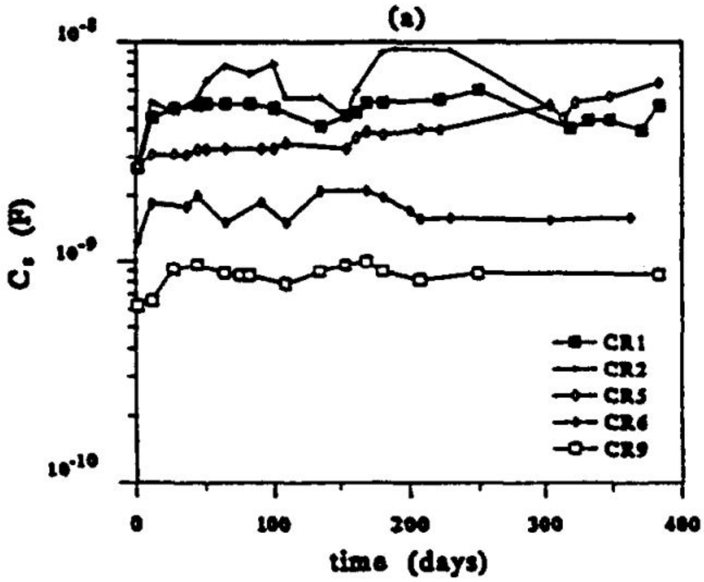

Figure 3.26: Coating capacitance of 5 different coatings [63]

3.5.2. Double layer capacitance (Cdl)

Double layer capacitance aids in estimating the corroding area at the coating/metal interface [22]. If there is an increase in the double layer capacitance (Cdl) with increase in exposure time, it directly relates to the increase in corroding area at the interface. In figure 3.27, it can be seen that there is marginal increase and then decrease in Cdl values in the accelerated exposure. In figure 3.28 as well a marginal increase can be seen. It can also be seen that all the Cdl values are within the same order of magnitude in both the accelerated and field exposure as compared to the other coatings in figure 3.29. In figure 3.29, a similar trend is seen, where the Cdl values increase with increase in exposure time. There is a big difference between these five coatings and the glass flake vinyl ester coating. The order of magnitude increase seen in figure 3.29 is very high compared to the glass flake vinyl ester coating in figure 3.27 an figure 3.28. Though there is an increasing pattern seen in both the graphs due to the magnitude of the Cdl values, the corroding area on the samples corresponding to figure 3.29 is much higher than in figure 3.27 and figure 3.28. From figure 3.27 and figure 3.28, it can be inferred that corroding area is very less in comparison or negligible.

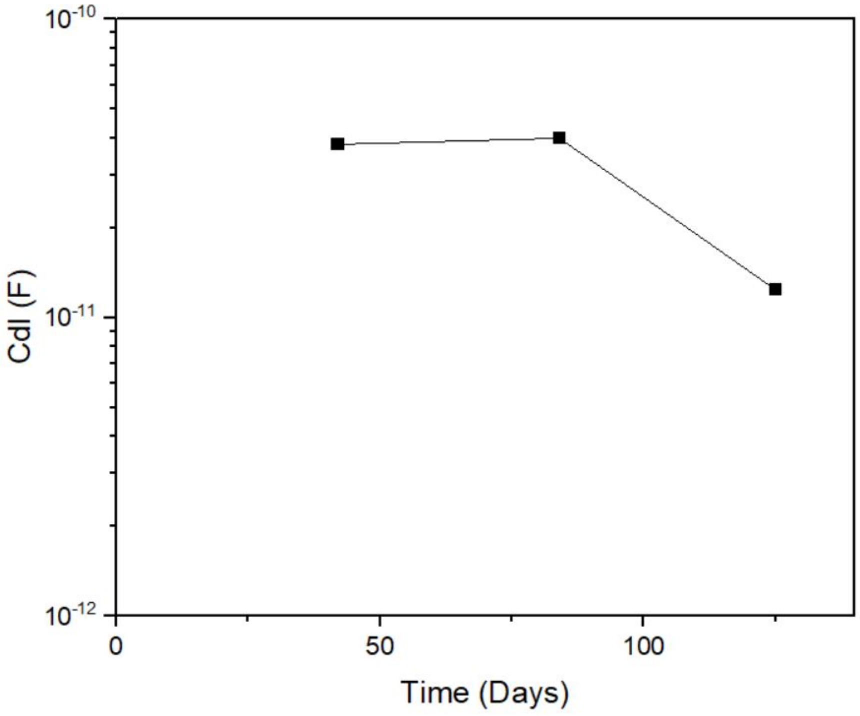

Figure 3.27: Cdl of the glass flake vinyl ester coating in accelerated exposure

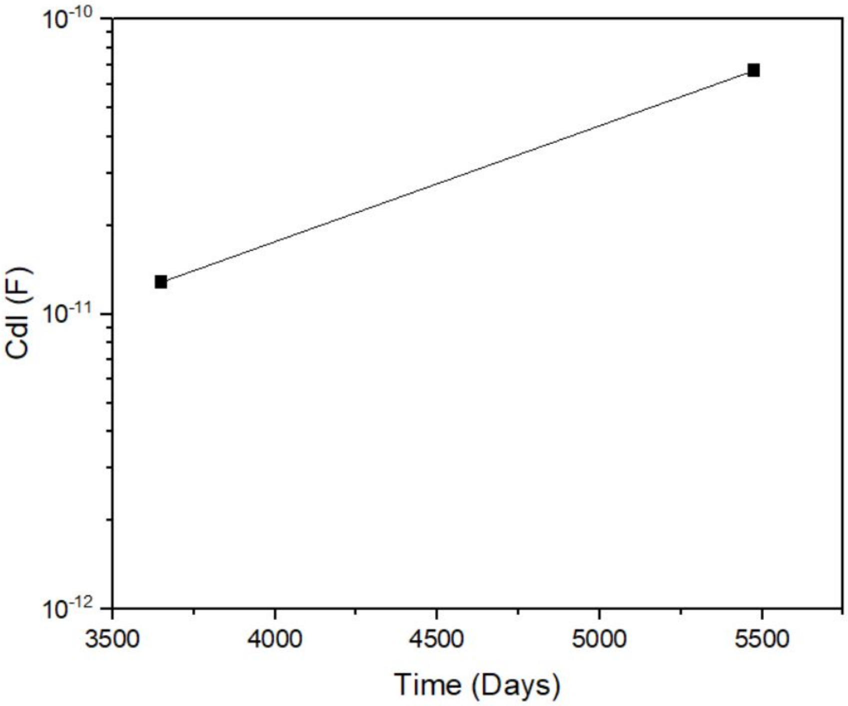

Figure 3.28: Cdl of the glass flake vinyl ester coating in field exposure

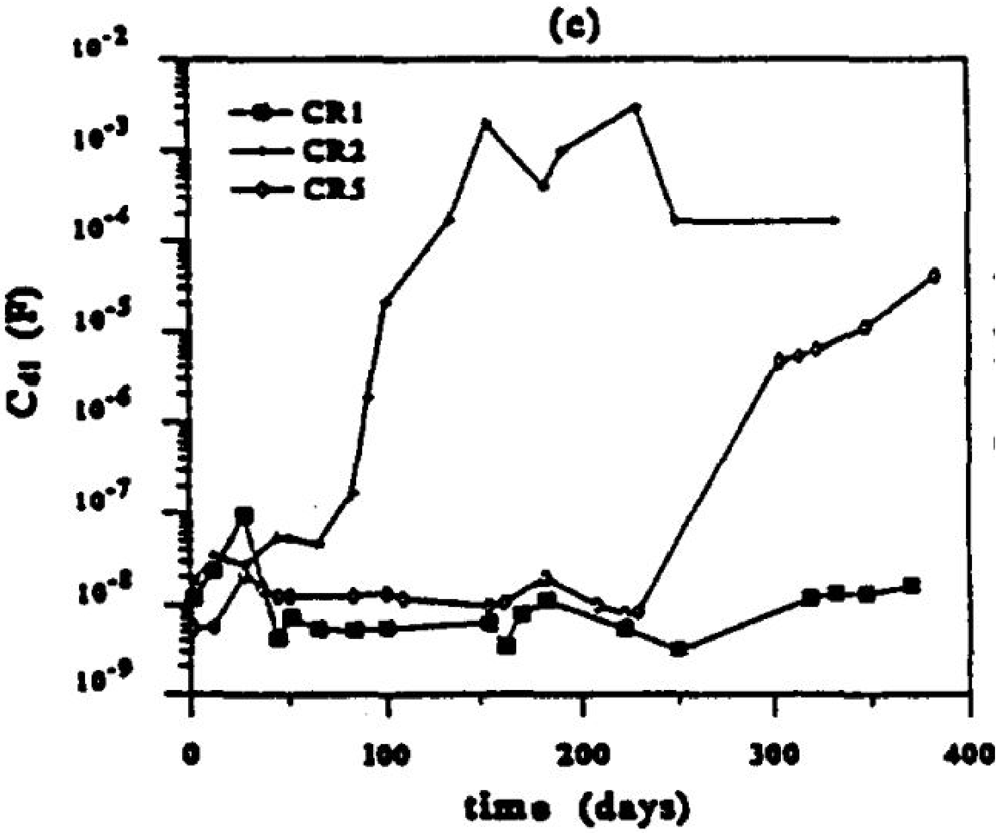

Figure 3.29: Cdl of 5 different marine coatings [63]

3.5.3. Polarisation Resistance (Rp)

Another parameter which aids in the estimating the corroding area is the polarisation resistance (Rp). It is known that as the polarisation resistance decreases with exposure time, there is an increase in the corroding area. As it is the polarisation resistance of the area at the interface between the coating and the metal. A decreasing trend can be seen in figure 3.30 and figure 3.31. A similar trend is expected with increased exposure times and can be seen for different marine coatings in figure 3.32. As seen for Cdl, there is a huge disparity in the order of magnitude. In figure 3.30, it can be seen that even though there is reduction in the polarisation resistance until 2000 hours of exposure, it almost regains its initial value after 3000 hours of exposure. In figure 3.31, it can be seen that there is only marginal reduction in the resistance. In figure 3.32, the difference in the order of magnitude is huge and in the case of CR2 in figure 3.32, the difference is almost four orders of magnitude. From these two graphs it can be inferred that, though the decreasing pattern is similar, the difference in the Rp values is huge. Therefore, corrosion is more likely to occur for coatings in figure 3.32 than for Ecopeed. Despite the decreasing trend, even after 15 years of exposure as seen in the second data point of figure 3.31 the reduction in values is not high as compared to the coatings in figure 3.32. This decrease in Rp values can also be compared to the impedance measurements from the bode plot. Where a similar reduction in magnitude of impedance was seen with increase in exposure time.

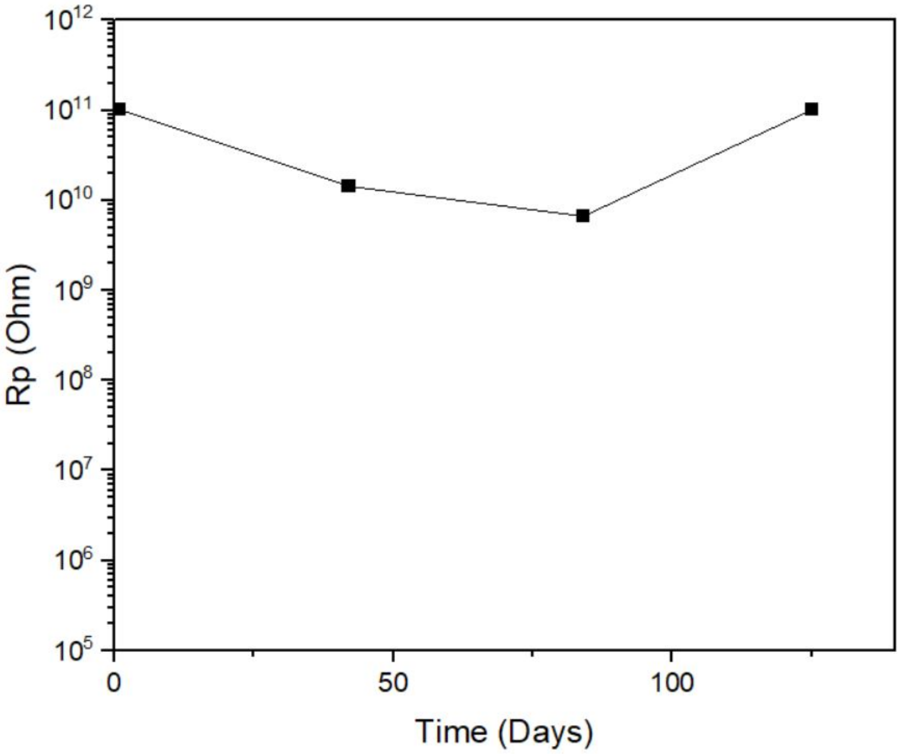

Figure 3.30: Rp of the glass flake vinyl ester coating in accelerated exposure

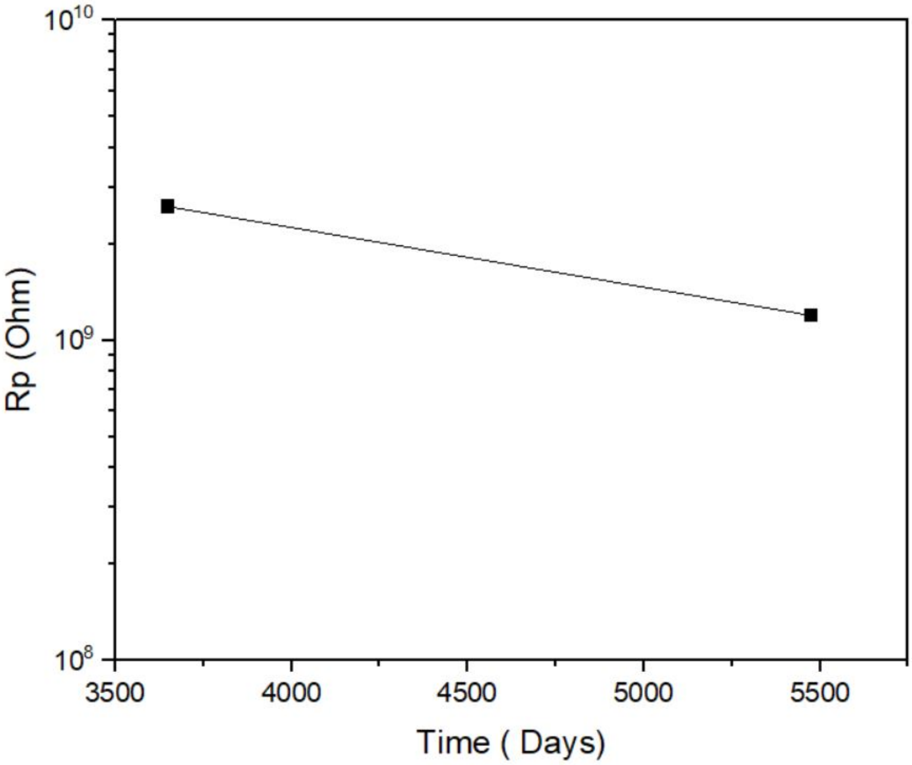

Figure 3.31: Rp of the glass flake vinyl ester coating in field exposure

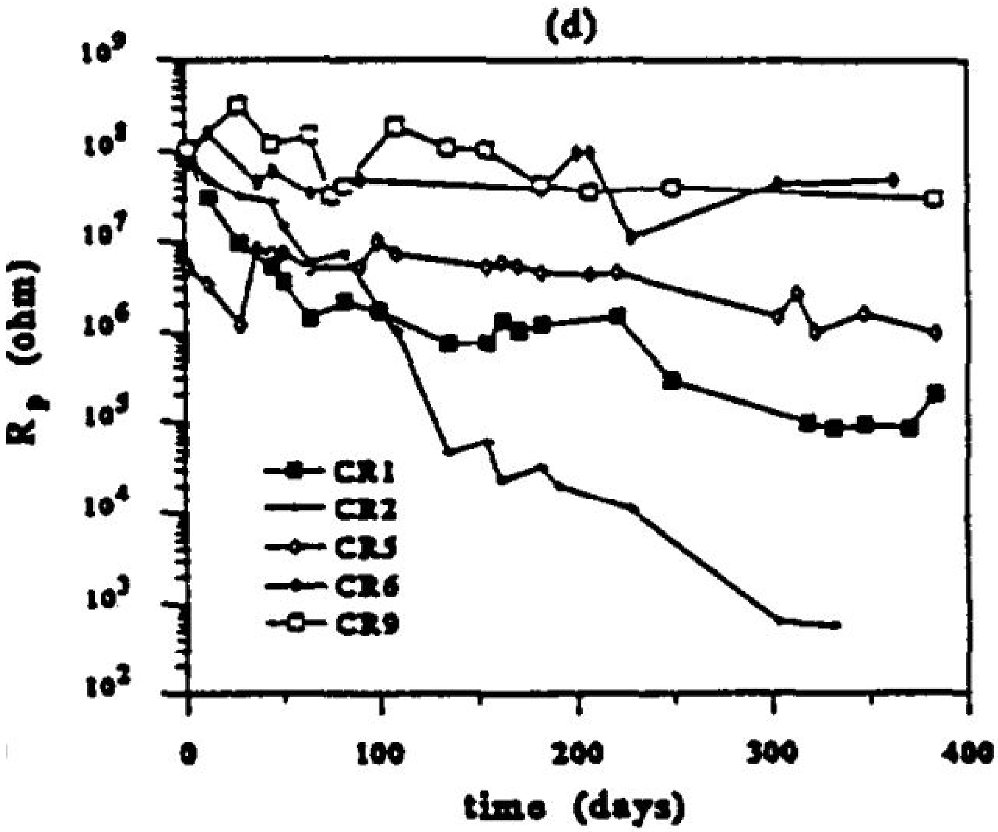

Figure 3.32: Rp of 5 different coatings [63]

In figure 3.26, it can be seen that the coating capacitance of these different marine coatings is between the range of 10^{-9} and 10^{-8} F. Which indicates higher coating capacitance values in comparison to figure 3.24 and 3.25, where the coating capacitance values are in the range of 10^{-11} F for the glass flake vinyl ester coating. Even though there is an increase in the coating capacitance with increased exposure time in the glass flake vinyl ester coating, the increase is marginal when compared to the coating capacitance in figure 3.26. With increase in coating capacitance, the usual scenario is the visible delamination and corrosion. In the case of the glass flake vinyl ester coating, the marginal increase in coating capacitance did not give rise to any visible delamination and corrosion in both the accelerated and field exposure. This is due to the presence of glass platelets in the the glass flake vinyl ester coating, which obstruct the ionic pathways to the underlying substrate.

4

Conclusion

Corrosion protection has been an interesting area of research for many decades, and finding an appropriate solution for different applications is a crucial task. Several types of coatings have been tested in literature for applications in different industries, which include ceramic, metallic and polymer coatings. Every coating designed to provide corrosion protection has its own working mechanism and durability depending on its exposure environment. This thesis focuses mainly on coatings that have been designed to withstand the harsh conditions of the marine environment.

The distinguishing factor among the corrosion protective coatings is their working mechanism which either aids or hampers their durability in the harsh conditions. To understand how long the working mechanism of a coating can provide corrosion protection can be found by the traditional method of exposing it to application conditions for years on end. This is a very time-consuming and expensive process; it could take years of development before the product enters the market. In order to circumvent the time constraint, accelerated tests were introduced, which can accelerate the exposure conditions in a relatively short duration of time. From the previous literature it was found that the accelerated tests increase the intensity of the factors that influence corrosion in natural environment. Intensifying the factors was expected to increase the rate of corrosion in a short duration in the accelerated environment.

The failure modes in the case of accelerated environment with intensified parameters did not match with the failure seen in the field test. The intensifying factors may also delay the onset of corrosion. It is important to take into consideration that there a lot of different accelerated tests, and each of their correlations with the natural exposure also differs significantly according to the literature. Besides, there is a lack of information available in the correlation of all the accelerated tests with the natural exposure. Therefore, to test a coating for its performance and durability, it was suggested to do the field and accelerated test simultaneously.

A vinylester reinforced with glass platelet has been in commercial use for almost two decades. This means that the coating has been on certain ships for years in its natural environment. This opportunity was used to test the glass flake vinyl ester coating, which has been on ships for duration of 10 and 15 years. At the same time, test panels were exposed to the accelerated environment of ISO 12944-9.

In order to predict the durability of the coating, one of the major tests conducted on the coatings is the electrochemical impedance spectroscopy (EIS), which is the primarily used test in this thesis. This test enables measuring the barrier properties of the coating. EIS measurements were done on the test panels at various intervals of the accelerated exposure. This includes the before exposure, 1000 hours, 2000 hours and 3000 hours of exposure. EIS measurements were also performed on the two ships mentioned above.

The base line for the data was taken as the results obtained from the panels prior to exposing them to the harsh conditions of the accelerated ISO 12944-9. A decreasing pattern was seen in the comparisons between the impedance curves with increasing exposure times. This was expected considering the long duration of exposure to the harsh conditions. This was seen both in the accelerated exposure and in the field exposure with increased exposure time. An attempt was made to check the correlations between the accelerated and the field exposure with the use of impedance curves. It was observed that the impedance curve of the 1000 hours of accelerated exposure had good correlation with the 10 years of field exposure. Therefore, it can be said that the 1000 hours of accelerated exposure in ISO 12944-9 had the same effect on the coating as the natural exposure after 10 years. An other attempt was made to compare the impedance curve of 15 years of natural exposure to 2000 and 3000 hours of accelerated exposure. The magnitude of impedance in the low frequency region for 15 years of natural exposure was lower than the magnitude of impedance for the accelerated exposure of 2000 and 3000 hours. This entails that further exposure in the accelerated cabinet is needed to match the impedance seen in the case of 15 years of natural exposure. At the same time, it can also be interpreted that the magnitude of impedance of 4.27x 10^9 Ω cm^2 for the 15 year old ship was still higher than the minimum industry standard requirement, which is $10^7 \Omega$ cm^2. Also there was no visible corrosion on the ship after 15 years of natural exposure.

The EIS results were fitted into equivalent electrical circuits with appropriately chosen equivalent circuit depending upon their exposure. Each equivalent circuit parameter follows a certain pattern with increased exposure time as was inferred from literature. Each of these parameters were plotted individually and the pattern they followed was observed. The pattern observed with the equivalent circuit parameters for a coating undergoing degradation is an increasing pattern for the coating capacitance and the capacitance double layer with increase in exposure time.

When comparing the equivalent circuit parameters of the glass flake vinyl ester coating with other marine coatings, the magnitude of coating capacitance and capacitance double layer were two orders of magnitude higher compared to other marine coatings that are used for comparison in this study. In the case of polarisation resistance, they were an order of magnitude higher in comparison to the other marine coatings. The difference in the magnitude of values of the equivalent circuit compared to the other marine coatings is attributed to the presence of glass platelets which obstruct the ionic pathways. All the patterns explained above were seen both in the accelerated and in the field exposure.

Conducting experiments using the accelerated test and the field test helped in understanding the performance of the coating in both these environments. For the case of impedance measurements performed on both the accelerated samples and field structures, the results indicate the coating is still performing really well and the impedance is above the minimum requirement of corrosion protection which is above $10^7 \Omega$ cm^2.

5

Recommendations

Recommendations for future research can be summarised as:

- Multiple coatings could be tested in both the accelerated and the field exposure, as different coatings behave differently in different environments and in different acceleration tests. Therefore, having a database that includes data on other marine coatings is essential in predicting the end of its functional life.
- Different tests can be conducted that estimates cracking, rusting, blistering using the ISO 4628 test. This can be added parameters used to correlate between the accelerated and the field test in a more quantitative manner.
- Although cyclic ageing has been the standard test for testing coating systems that undergo extreme exposure in marine conditions, it can always be improved further to better replicate the natural exposure conditions. In the cyclic ageing test, the different cycles and their time period is predefined. Rather, it can be programmed to randomly choose between the different exposure conditions and its time duration. Incorporation of randomness might aid in closing the gap further between artificial and natural exposure.
- The minimum industry standard requirement for a coating to provide corrosion protection is for the magnitude of impedance to be greater than $10^7 \Omega\ \mathrm{cm}^2$. Accelerated ISO 12944-9 test can be conducted to evaluate the number of hours required in accelerated exposure for the impedance to degrade to values lower than $10^7 \Omega\ \mathrm{cm}^2$ to predict the lifetime of a coating.
- EIS measurements were performed on a plate after exposure to 2000 hours of accelerated exposure and 2 months of drying in room temperature. Prior to EIS measurements, the test plate was conditioned using conditioning pads for a duration of 2 days. In this case the impedance was marginally above $10^7 \Omega\ \mathrm{cm}^2$, the minimum industry standard. This can be investigated further using EIS to verify the reproducability of the result with other test samples of the same coating.

Bibliography

[1] ISO 12944: 1-8. Paints and varnishes—corrosion protection of steel structures by protective paint systems, 2018.

[2] ASCOTT ISO 7253. Corrosion testing standards - iso 7253. URL `https://www.ascott-analytical.com/test-standards/iso-7253/`.

[3] E Alibakhshi, M Akbarian, M Ramezanzadeh, B Ramezanzadeh, and M Mahdavian. Evaluation of the corrosion protection performance of mild steel coated with hybrid sol-gel silane coating in 3.5 wt.% nacl solution. *Progress in Organic Coatings*, 123:190–200, 2018.

[4] A Amirudin and D Thieny. Application of electrochemical impedance spectroscopy to study the degradation of polymer-coated metals. *Progress in organic coatings*, 26(1): 1–28, 1995.

[5] Jeff Andrews, Freidun Anwari, Ben J Carlozzo, Mark DiLorenzo, Roy Glover, Steven Grossman, Carl J Knauss, Joseph McCarthy, Brian Mysza, Rene Patterson, et al. Correlation of accelerated exposure testing and exterior exposure sites. *JCT, Journal of coatings technology*, 66(837):49–67, 1994.

[6] ASCOTT. Corrosion testing standards - bs3900 part f12. URL `https://www.ascott-analytical.com/test-standards/bs-3900-part-f12/`.

[7] PK Satheesh Babu, A Mathiazhagan, and CG Nandakumar. Corrosion health monitoring system for steel ship structures. *International Journal of Environmental Science and Development*, 5(5):491, 2014.

[8] R Charles Bacon, Joseph J Smith, and Frank M Rugg. Electrolytic resistance in evaluating protective merit of coatings on metals. *Industrial & Engineering Chemistry*, 40(1): 161–167, 1948.

[9] KR Baldwin and CJE Smith. Accelerated corrosion tests for aerospace materials: current limitations and future trends. *Aircraft Engineering and Aerospace Technology*, 1999.

[10] David R Bauer. Interpreting weathering acceleration factors for automotive coatings using exposure models. *Polymer Degradation and Stability*, 69(3):307–316, 2000.

[11] AJ Betts and LH Boulton. Crevice corrosion: review of mechanisms, modelling, and mitigation. *British corrosion journal*, 28(4):279–296, 1993.

[12] Gordon P Bierwagen, L He, J Li, L Ellingson, and DE Tallman. Studies of a new accelerated evaluation method for coating corrosion resistance—thermal cycling testing. *Progress in organic coatings*, 39(1):67–78, 2000.

[13] N Bonanos, BCH Steele, EP Butler, J Ross Macdonald, William B Johnson, Wayne L Worrell, Gunnar A Niklasson, Sara Malmgren, Maria Strømme, SK Sundaram, et al. Applications of impedance spectroscopy. *Impedance spectroscopy: Theory, experiment, and applications*, pages 175–478, 2018.

[14] SK Boocock. Meeting industry needs for improved testing. *Journal of Protective Coatings and Linings*, 12:70–70, 1995.

[15] Petroleum Books. Corrosion definition and cost - chapter 1, oct 2019. URL `https://oilprocessing.net/oil/viewtopic.php?f=6&t=40`.

[16] Tom Bos. Cyclic laboratory tests for evaluating coatings: A brief review of literature. *Journal of Protective Coatings and Linings*, (25):73–79, 2008.

[17] Tom Bos. Prediction of coating durability. *Early detection using electrochemical methods, WM Bos*, 2008.

[18] Simon J Brigham and Charles Watkinson. Understanding and use of glass flake. *Paint Coat. Ind*, 25:22–24, 2009.

[19] Ben J Carlozzo, Jeff Andrews, F Anwari, M DiLorenzo, R Glover, S Grossman, C Harding, J McCarthy, and B Mysza. Correlation of accelerated exposure testing and exterior exposure sites. ii. one-year results. *Journal of Coatings Technology(USA)*, 68(858): 47–61, 1996.

[20] Shuang-Ling Chong. A comparison of accelerated tests for steel bridge coatings in marine environments. *Journal of Protective Coatings & Linings*, 14(3), 1997.

[21] David A Claydon. Performance testing of anti-corrosive coatings. In *Proceedings of the SSPC 2002 Conference Proceedings (SSPC: The Society for Protective Coatings), Tampa, FL, USA*, pages 1–9, 2002.

[22] ND Cogger and NJ Evans. An introduction to electrochemical impedance measurement. *Solarton Ltd., Farnborough, UK*, 1999.

[23] Corrosion Costs. Preventive strategies in the united states. *Supplement to Materials Performance*, 2002.

[24] N.D Cremer. Federation of societies for coatings technology. In *Federation of Societies for Coatings Technology 1989 Paint Show*, 1989.

[25] GD Davis, LA Krebs, and CM Dacres. Coating evaluation and validation of accelerated test conditions using an in-situ corrosion sensor. *Journal of Coatings Technology*, 74 (935):69–74, 2002.

[26] Joseph R Davis. *Corrosion: Understanding the basics*. Asm International, 2000.

[27] Adriaan Jan De Jong. Characterization of coatings inside food and beverage cans. *Delft University Press*, 2000.

[28] F Deflorian, S Rossi, and M Fedel. Organic coatings degradation: Comparison between natural and artificial weathering. *Corrosion Science*, 50(8):2360–2366, 2008.

[29] ASCOTT BS3900 Part F4. Corrosion testing standards - bs3900 part f4. URL `https://www.ascott-analytical.com/test-standards/bs-3900-part-f4/`.

[30] GS Frankel. Pitting corrosion of metals: a review of the critical factors. *Journal of the Electrochemical society*, 145(6):2186, 1998.

[31] Ting Fu, Xiaobo Tang, Zekai Cai, Yu Zuo, Yuming Tang, and Xuhui Zhao. Correlation research of phase angle variation and coating performance by means of pearson's correlation coefficient. *Progress in Organic Coatings*, 139:105459, 2020.

[32] J.D. Garber and J.H. Lin. Corrosion 92, paper 336. In *NACE*, 1989.

[33] G Gardner. Astm's new coating test method addresses interactive effects of weathering and corrosion. *Journal of protective coatings & linings*, 15(9), 1998.

[34] FM Geenen. Characterization of organic coatings with impedance measurements. *F. M. Geenen, PhD Thesis, Delft Univ. of Technology 1991, 190*, page 181, 1991.

[35] Stefanos Gkatzogiannis, Joscha Weinert, Imke Engelhardt, Peter Knoedel, and Thomas Ummenhofer. Correlation of laboratory and real marine corrosion for the investigation of corrosion fatigue behaviour of steel components. *International Journal of Fatigue*, 126: 90–102, 2019.

[36] Paul Heffer and Bill Lee. Braving the elements: Analyzing the weathering performance of chromate-free coating systems. *Metal finishing*, 103(7-8):33–60, 2005.

[37] A Heyer, F D'Souza, CF Leon Morales, G Ferrari, JMC Mol, and JHW De Wit. Ship ballast tanks a review from microbial corrosion and electrochemical point of view. *Ocean Engineering*, 70:188–200, 2013.

[38] Marinus Hoeflaak, B de Ruiter, and Joost H Maas. Calibrating the climate: Ii: Correlations between different weathering tests. 2006.

[39] J Hubrecht, AF Skenazi, J Vereecken, and D Coutsouradis. Corrosion resistance of galfan and coil coated galfan in chloride containing atmospheres. *ATB Métallurgie*, 25 (3):243–252, 1985.

[40] Paul Iannarelli, Douglas Beaumont, Yanwen Liu, Xiaorong Zhou, Timothy L Burnett, Michele Curioni, Stuart B Lyon, Simon R Gibbon, Suzanne Morsh, Seyedgholamreza Emad, et al. The degradation mechanism of a marine coating under service conditions of water ballast tank. *Progress in Organic Coatings*, 162:106588, 2022.

[41] FP Ijsseling. General guidelines for corrosion testing of materials for marine applications: Literature review on sea water as test environment. *British Corrosion Journal*, 24 (1):53–78, 1989.

[42] ASTM INTERNATIONAL, mar 2018.

[43] LFE Jacques. Accelerated and outdoor/natural exposure testing of coatings. *Progress in polymer science*, 25(9):1337–1362, 2000.

[44] James R Johnson. Phorgotten phenomena: A primary cause of coating failure. *Materials performance*, 38(6):48–49, 1999.

[45] Martin Kendig and J Scully. Basic aspects of electrochemical impedance application for the life prediction of organic coatings on metals. *Corrosion*, 46(1):22–29, 1990.

[46] Ole O Knudsen, Unni STEINSMO, Marit BJORDAL, and Sarbjyot NIJJER. Accelerated testing: correlation between four accelerated tests and five years of offshore field testing. *Journal of protective coatings & linings*, 18(12):52–56, 2001.

[47] Ole Øystein Knudsen and Amy Forsgren. *Corrosion control through organic coatings*. CRC Press, 2017.

[48] Gerhardus H Koch, Michiel PH Brongers, Neil G Thompson, Y Paul Virmani, Joe H Payer, et al. Corrosion cost and preventive strategies in the united states. Technical report, United States. Federal Highway Administration, 2002.

[49] Hee-Baek Lee, Chung-Seo Park, Seong-Mo Son, Kyung-Jin Park, Sang-Sik Park, and Hyundai Heavy. Combatting rudder erosion with cavitation-resistant coating. *Journal of Protective Coatings & Linings*, 32(3):38–41, 2015.

[50] Henry Leidheiser Jr and Martin W Kendig. The mechanism of corrosion of poly butadiene-coated steel in aerated sodium chloride. *Corrosion*, 32(2):69–76, 1976.

[51] Herem Jan Willem Lenderink. *Filiform Corrosion of coated Aluminium Alloys*. PhD thesis, Delft University of Technology, 1995.

[52] Herem Jan Willem Lenderink. *Filiform Corrosion of coated Aluminium Alloys*. PhD thesis, Delft University of Technology, 1995.

[53] Jie Liu, Zhonghai Lu, Lunwu Zhang, Chuanpeng Li, Rui Ding, Xiaodong Zhao, Peiqing Zhang, Bin Wang, and Hongtao Cui. Studies of corrosion behaviors of a carbon steel/copper-nickel alloy couple under epoxy coating with artificial defect in 3.5 wt.% nacl solution using the wbe and eis techniques. *Progress in Organic Coatings*, 148: 105909, 2020.

[54] Shenglin Liu, Xueping Zheng, and Gangqiang Geng. Dry sliding wear behavior and corrosion resistance of nicrbsi coating deposited by activated combustion-high velocity air fuel spray process. *Materials & design*, 31(2):913–917, 2010.

[55] Zhe Liu, Yanchun Dong, Zhenhua Chu, Yong Yang, Yingzhen Li, and Dianran Yan. Corrosion behavior of plasma sprayed ceramic and metallic coatings on carbon steel in simulated seawater. *Materials & Design (1980-2015)*, 52:630–637, 2013.

[56] Digby D Macdonald. Reflections on the history of electrochemical impedance spectroscopy. *Electrochimica Acta*, 51(8-9):1376–1388, 2006.

[57] James Ross Macdonald. Impedance spectroscopy: old problems and new developments. *Electrochimica Acta*, 35(10):1483–1492, 1990.

[58] MMAM Mahdavian and MM Attar. Another approach in analysis of paint coatings with eis measurement: phase angle at high frequencies. *Corrosion Science*, 48(12):4152–4157, 2006.

[59] AU Malik, PC Mayan Kutty, Nadeem A Siddiqi, Ismaeel N Andijani, and Shahreer Ahmed. The influence of ph and chloride concentration on the corrosion behaviour of aisi 316l steel in aqueous solutions. *Corrosion science*, 33(11):1809–1827, 1992.

[60] K Mallon, B Rutherford, and P Connors. Accelerated test program utilizing a cyclical test method and analysis of methods to correlate with field testing. *K. Mallon, B. Rutherford, and P. Connors, Paper*, (331), 1992.

[61] PE Mallon, Y Li, R Zhang, H Chen, Y Wu, TC Sandreczki, YC Jean, R Suzuki, and T Ohdaira. Durability of polymeric coatings: effects of natural and artificial weathering. *Applied surface science*, 194(1-4):176–181, 2002.

[62] Florian Mansfeld. Electrochemical impedance spectroscopy (eis) as a new tool for investigating methods of corrosion protection. *Electrochimica Acta*, 35(10):1533–1544, 1990.

[63] Florian Mansfeld. Models for the impedance behavior of protective coatings and cases of localized corrosion. *Electrochimica Acta*, 38(14):1891–1897, 1993.

[64] Florian Mansfeld. Use of electrochemical impedance spectroscopy for the study of corrosion protection by polymer coatings. *Journal of applied electrochemistry*, 25(3):187–202, 1995.

[65] Tim Marchant. The cost of corrosion-tim marchant, principal naval architect at bmt defence services, explains how design-based solutions to maritime corrosion could provide cost savings to the defence sector. *DMJ. Defence management journal*, 14(47): 74, 2009.

[66] R Martin. The new supertanker plague. *Wired Digital*, 10, 2002.

[67] William Q Meeker and Luis A Escobar. Pitfalls of accelerated testing. *IEEE transactions on reliability*, 47(2):114–118, 1998.

[68] Bobbi Jo Merten, Allen Skaja, David Tordonato, and Daryl Little. *Re-Evaluating Electrochemical Impedance Spectroscopy (EIS) for the Field Inspector's Toolbox: A First Approach*. US [Department of the Interior], Bureau of Reclamation, 2014.

[69] Y. Montle, J. F.; Korobov. American paint & coatings. *American Paint & Coatings Journal 76*, pages 36–44, 1991.

[70] Manuel Morcillo, Jenifer Alcántara, Iván Díaz, Belén Chico, Joaquín Simancas Peco, et al. Marine atmospheric corrosion of carbon steels. 2015.

[71] JN Murray and HP Hack. Testing organic architectural coatings in astm synthetic seawater immersion conditions using eis. *Corrosion*, 48(8):671–685, 1992.

[72] Tatsuro Nakai, Hisao Matsushita, and Norio Yamamoto. Pitting corrosion and its influence on local strength of hull structural members. In *International Conference on Offshore Mechanics and Arctic Engineering*, volume 41960, pages 25–35, 2005.

[73] Wayne B Nelson. *Accelerated testing: statistical models, test plans, and data analysis*. John Wiley & Sons, 2009.

[74] A Della Pergola, Federica Lollini, Elena Redaelli, and Luca Bertolini. Numerical modeling of initiation and propagation of corrosion in hollow submerged marine concrete structures. *Corrosion*, 69(12):1158–1170, 2013.

[75] J Pospíšil, J Pilař, NC Billingham, A Marek, Z Horak, and S Nešprek. Factors affecting accelerated testing of polymer photostability. *Polymer Degradation and Stability*, 91(3): 417–422, 2006.

[76] SS Rajahram, TJ Harvey, and RJK Wood. Erosion–corrosion resistance of engineering materials in various test conditions. *Wear*, 267(1-4):244–254, 2009.

[77] Abhishek Rajput, Meral Ak, Sang Jin Kim, Sung Hwan Noh, Jae Hyeong Park, and Jeom Kee Paik. Effects of the surface preparation on the life of epoxy coating in steel ship plates: an experimental study. *Ships and Offshore Structures*, 14(sup1):199–206, 2019.

[78] CM Rizzo, JK Paik, F Brennan, CA Carlsen, C Daley, Y Garbatov, L Ivanov, BC Simonsen, N Yamamoto, and HZ Zhuang. Current practices and recent advances in condition assessment of aged ships. *Ships and Offshore Structures*, 2(3):261–271, 2007.

[79] Blanca M Rosales, Alejandro R Di Sarli, Oladis De Rincón, Alvaro Rincón, Cecilia I Elsner, and Bettina Marchisio. An evaluation of coil coating formulations in marine environments. *Progress in Organic Coatings*, 50(2):105–114, 2004.

[80] BM Rosales, AR Di Sarli, F Fragata, F Corvo, MS De Villalaz, S Flores, E Almeida, J Simancas, S Rivero, and OT De Rincón. Patina network-performance of coil coating in natural atmospheres of ibero-america. *Revista de metalurgia*, pages 201–205, 2003.

[81] DP Schmidt, BA Shaw, E Sikora, WW Shaw, and LH Laliberte. Corrosion protection assessment of sacrificial coating systems as a function of exposure time in a marine environment. *Progress in Organic Coatings*, 57(4):352–364, 2006.

[82] U Schulz, P Trubiroha, U Schernau, and H Baumgart. The effects of acid rain on the appearance of automotive paint systems studied outdoors and in a new artificial weathering test. *Progress in organic coatings*, 40(1-4):151–165, 2000.

[83] AJ Sedriks. Marine corrosion. Technical report, NAVAL RESEARCH LAB WASHINGTON DC, 1985.

[84] Aaishwarika Raj Sharma and Rakesh Goyal. Study of corrosion behaviour of al2o3-13% tio2 and cr2o3 coated ship hull steel in 3.5% nacl solution. In *Journal of Physics: Conference Series*, volume 1969, page 012021. IOP Publishing, 2021.

[85] Sidney Siegel. Nonparametric statisticsfor the behavioral sciences. Technical report, 1956.

[86] CH Simpson, CJ Ray, and BS Skerry. Accelerated corrosion testing of industrial maintenance paints using a cyclic corrosion weathering method. *Journal of Protective Coatings & Linings*, 8(5), 1991.

[87] Z Stoynov. Impedance modelling and data processing: structural and parametrical estimation. *Electrochimica acta*, 35(10):1493–1499, 1990.

[88] Kenneth B Tator. Risk assessment and economic considerations when coating ballast tanks. In *Workshop: coatings for corrosion protection: offshore oil and gas operation facilities, marine pipeline and ship structures, Mississippi, USA*, 2004.

[89] ELEMENT MATERIALS TECHNOLOGY. Q&a: Astm b117 salt fog testing, may 2022. URL `https://www.element.com/nucleus/2016/astm-b117-salt-fog-testing-q-and-a`.

[90] Tahsin Tezdogan and Yigit Kemal Demirel. An overview of marine corrosion protection with a focus on cathodic protection and coatings. *Brodogradnja: Teorija i praksa brodogradnje i pomorske tehnike*, 65(2):49–59, 2014.

[91] HJ Tiemens and M Hoeflaak. Improved prediction of durability of coated metal sheet by artificial testing. In *ECCA Autumn Congress*, 2001.

[92] B Van Rompay. Is the much sought-after, better alternative underwater hull coating system already here? In *Proceedings of the RINA, Royal Institution of Naval Architects—International Conference on Marine Coatings, London, UK*, pages 38–43, 2013.

[93] Boud van Rompay. Hull coating degradation - the hidden cost. *Ship Hull Performance*, 2012.

[94] Boud van Rompay. Conquering corrosion in offshore vessels. *Ship Hull Performance*, 2013.

[95] Everhardus Petrus Maria van Westing. Determination of coating performance with impedance measurements. 1992.

[96] Lucien Veleva. Protective coatings and inorganic anti-corrosion pigments. *Paint and Coating Testing Manual*, pages 282–299, 2012.

[97] GW Walter. A review of impedance plot methods used for corrosion performance analysis of painted metals. *Corrosion Science*, 26(9):681–703, 1986.

[98] Fei Wang, Jinxia Xu, Yi Xu, Linhua Jiang, and Guoxu Ma. A comparative investigation on cathodic protections of three sacrificial anodes on chloride-contaminated reinforced concrete. *Construction and Building Materials*, 246:118476, 2020.

[99] Chao Wei, George Wang, Marcus Cridland, David L Olson, and Stephen Liu. Corrosion protection of ships. In *Handbook of Environmental Degradation of Materials*, pages 533–557. Elsevier, 2018.

[100] Hamer W.J. *Polypyrrole electrochemistry: Environmentally friendly corrosion protection of steel: (im)possibilities*. PhD thesis, Technical Universtiy of Delft, 2005.

[101] Xiaolong Zhang. Cr (vi) and cr (iii)-based conversion coatings on zinc. 2005.

[102] Yu Zuo, R Pang, W Li, JP Xiong, and YM Tang. The evaluation of coating performance by the variations of phase angles in middle and high frequency domains of eis. *Corrosion Science*, 50(12):3322–3328, 2008.